

EUROPEAN SPACE AGENCY
CONTRACT REPORT

The work described in this report was done under ESA contract.
Responsibility for the contents resides in the author or organisation that prepared it.

Survey of Total Ionising Dose Tolerance of Power Bipolar Transistors and Silicon Carbide Devices for JUICE

TN6.6
SEE Test Report for
SiC JFET
IJW120R100T1

Manufacturer:
Infineon

Date code/Lot code: HAA547

Report no.	Version	Date	NEO no.
071/2018	2.0	2019-06-07	NEO-14-086
Author	Coauthors	Checked by	Project
Michael Steffens +49 2251 18-222 michael.steffens@int.fraunhofer.de	--	Stefan Höffgen	Survey of Total Ionising Dose Tolerance of Power Bipolar Transistors and Silicon Carbide Devices for JUICE (AO/1-7859/14/NL/SW)
Customer	Project management		
European Space Agency (ESA), contract number 4000113976/15/NL/RA	Project Coordinator: Stefan Höffgen (INT) ESA Technical Project Officer: Marc Poizat (ESA/ESTEC)		



Document Approval

Project	AO/1-8148/14/NL/SFe
Project Title	Survey of total ionising dose tolerance of power bipolar transistors and Silicon Carbide devices for JUICE
Doc ID	D6.6
Document Title	TN6.6 SEE Test Report for SiC JFET IJW120RT100T1
Issue.Revision	2.0
Date	2019-06-07

Prepared by	
	Name: Michael Steffens, INT

Approved by	
	Name: Stefan Höffgen, INT

Accepted by	
	Name: Marc Poizat, ESTEC

Version history

Table 1: Revision history

Version	Date	Changed by	Changes
0.1	2019-03-15	Steffens	Initial draft, Sections 1-5, Appendices A+B
1.0	2019-05-10	Steffens	Initial Release
2.0	2019-06-07	Steffens	Fixed header in Appendices, Added remark on total fluences in tests at CERN (Section 2.2 and 8.5)

Table of contents

Document Approval	2
1 Introduction	9
2 Summary	11
3 Sample preparations	15
4 Setup and Measurements	20
5 Tests at UCL.....	30
6 Tests at JULIC	36
7 Tests at GANIL.....	42
8 Tests at CERN	45
A Fraunhofer INT.....	49
B Appendix: Tests at UCL.....	52
C Appendix: Tests at JULIC	66
D Appendix: Tests at GANIL.....	77
E Appendix: Tests at CERN	80

List of figures

Figure 1: Safe operating voltage across the campaigns	12
Figure 2: Cross sections at $V_{GS} = 0$ V for each campaign.	13
Figure 3: The ESD package with the samples	15
Figure 4: Sample marking	16
Figure 5: DUT decapsulation.	17
Figure 6: Functional tests after parylene coating	18
Figure 7: Die pictures.....	18
Figure 8: SEB / SEGR Detection Circuit.....	21
Figure 9: Test board layout	22
Figure 10: UCL: Measurement equipment/setup	24
Figure 11: GANIL: Measurement equipment/setup.....	26
Figure 12: CERN: Measurement equipment/setup.....	27
Figure 13: JULIC: Measurement equipment/setup	28
Figure 14: UCL vacuum chamber with electrical feedthroughs.	30
Figure 15: Plot of LETs and Ranges in Silicon Carbide at UCL.	32
Figure 16: Overview of results: Heavy Ions at UCL.....	33
Figure 17: Beam line and irradiation site at the JULIC injector cyclotron, FZ Jülich	36
Figure 18: Schematic setup of the beam exit window at JULIC and the ionization chamber.....	37
Figure 19: The initial proton energy	37
Figure 20: Overview of results: Protons at JULIC	40
Figure 21: Test setup at GANIL.....	42
Figure 22: Results: Heavy Ions at GANIL.	44
Figure 23: Beam line and irradiation site at the H8 beam line, CERN.	45
Figure 24: Results: Heavy Ions at CERN.....	48
Figure 25: Run# 035, IJW120R100T1, Al-250, $2.7e+05$ ions/cm ² , DUT 11, VDS= 600.0 V, VGS= -14.5 V	53
Figure 26: Run# 036, IJW120R100T1, Al-250, $1.5e+04$ ions/cm ² , DUT 12, VDS= 600.0 V, VGS= -14.5 V	53
Figure 27: Run# 037, IJW120R100T1, Al-250, $5.9e+03$ ions/cm ² , DUT 13, VDS= 600.0 V, VGS= -14.5 V	54
Figure 28: Run# 038, IJW120R100T1, C-131, $3.0e+05$ ions/cm ² , DUT 14, VDS= 600.0 V, VGS= -14.5 V	54
Figure 29: Run# 039, IJW120R100T1, C-131, $3.0e+05$ ions/cm ² , DUT 14, VDS= 750.0 V, VGS= -14.5 V	55
Figure 30: Run# 040, IJW120R100T1, C-131, $3.0e+05$ ions/cm ² , DUT 14, VDS= 900.0 V, VGS= -14.5 V	55
Figure 31: Run# 041, IJW120R100T1, C-131, $5.5e+04$ ions/cm ² , DUT 14, VDS= 1050.0 V, VGS= -14.5 V	56
Figure 32: Run# 042, IJW120R100T1, C-131, $3.0e+05$ ions/cm ² , DUT 15, VDS= 900.0 V, VGS= -14.5 V	56
Figure 33: Run# 043, IJW120R100T1, C-131, $3.0e+05$ ions/cm ² , DUT 15, VDS= 900.0 V, VGS= -19.5 V	57
Figure 34: Run# 044, IJW120R100T1, C-131, $3.0e+05$ ions/cm ² , DUT 16, VDS= 900.0 V, VGS= -19.5 V	57
Figure 35: Run# 045, IJW120R100T1, Ne-238, $3.0e+05$ ions/cm ² , DUT 17, VDS= 400.0 V, VGS= -14.5 V	58
Figure 36: Run# 046, IJW120R100T1, Ne-238, $3.0e+05$ ions/cm ² , DUT 17, VDS= 600.0 V, VGS= -14.5 V	58

Figure 37: Run# 047, IJW120R100T1, Ne-238, 1.3e+04 ions/cm ² , DUT 17, VDS= 750.0 V, VGS= -14.5 V	59
Figure 38: Run# 048, IJW120R100T1, Ne-238, 9.6e+04 ions/cm ² , DUT 15, VDS= 600.0 V, VGS= -14.5 V	59
Figure 39: Run# 049, IJW120R100T1, Ne-238, 3.0e+05 ions/cm ² , DUT 16, VDS= 500.0 V, VGS= -14.5 V	60
Figure 40: Run# 050, IJW120R100T1, Ne-238, 3.0e+05 ions/cm ² , DUT 16, VDS= 550.0 V, VGS= -14.5 V	60
Figure 41: Run# 051, IJW120R100T1, Ne-238, 3.0e+05 ions/cm ² , DUT 16, VDS= 550.0 V, VGS= -19.5 V	61
Figure 42: Run# 052, IJW120R100T1, Ne-238, 9.2e+04 ions/cm ² , DUT 16, VDS= 600.0 V, VGS= -14.5 V	61
Figure 43: Run# 053, IJW120R100T1, Al-250, 3.0e+05 ions/cm ² , DUT 18, VDS= 400.0 V, VGS= -14.5 V	62
Figure 44: Run# 054, IJW120R100T1, Al-250, 3.0e+05 ions/cm ² , DUT 20, VDS= 500.0 V, VGS= -14.5 V	62
Figure 45: Run# 055, IJW120R100T1, Al-250, 1.3e+05 ions/cm ² , DUT 18, VDS= 500.0 V, VGS= -14.5 V	63
Figure 46: Run# 056, IJW120R100T1, Al-250, 3.0e+05 ions/cm ² , DUT 22, VDS= 400.0 V, VGS= -14.5 V	63
Figure 47: Run# 057, IJW120R100T1, Al-250, 3.0e+05 ions/cm ² , DUT 20, VDS= 400.0 V, VGS= -14.5 V	64
Figure 48: Run# 058, IJW120R100T1, Al-250, 3.0e+05 ions/cm ² , DUT 22, VDS= 400.0 V, VGS= -19.5 V	64
Figure 49: Run# 059, IJW120R100T1, Al-250, 3.0e+05 ions/cm ² , DUT 22, VDS= 450.0 V, VGS= -14.5 V	65
Figure 50: Run# 060, IJW120R100T1, Al-250, 3.0e+05 ions/cm ² , DUT 22, VDS= 450.0 V, VGS= -19.5 V	65
Figure 51: Run# 018, IJW120R100T1, p, 2.0e+10 ions/cm ² , DUT 1, VDS= 600.0 V, VGS= -14.5 V	69
Figure 52: Run# 019, IJW120R100T1, p, 2.0e+10 ions/cm ² , DUT 1, VDS= 750.0 V, VGS= -14.5 V	69
Figure 53: Run# 020, IJW120R100T1, p, 2.0e+10 ions/cm ² , DUT 1, VDS= 900.0 V, VGS= -14.5 V	70
Figure 54: Run# 021, IJW120R100T1, p, 2.0e+10 ions/cm ² , DUT 1, VDS= 1050.0 V, VGS= -14.5 V	70
Figure 55: Run# 022, IJW120R100T1, p, 2.0e+10 ions/cm ² , DUT 1, VDS= 1200.0 V, VGS= -14.5 V	71
Figure 56: Run# 023, IJW120R100T1, p, 2.0e+10 ions/cm ² , DUT 1, VDS= 600.0 V, VGS= -17.0 V	71
Figure 57: Run# 024, IJW120R100T1, p, 2.0e+10 ions/cm ² , DUT 1, VDS= 900.0 V, VGS= -17.0 V	72
Figure 58: Run# 025, IJW120R100T1, p, 2.0e+10 ions/cm ² , DUT 1, VDS= 1200.0 V, VGS= -17.0 V	72
Figure 59: Run# 026, IJW120R100T1, p, 2.0e+10 ions/cm ² , DUT 1, VDS= 600.0 V, VGS= -19.5 V	73
Figure 60: Run# 027, IJW120R100T1, p, 2.0e+10 ions/cm ² , DUT 1, VDS= 900.0 V, VGS= -19.5 V	73
Figure 61: Run# 028, IJW120R100T1, p, 2.0e+10 ions/cm ² , DUT 2, VDS= 1200.0 V, VGS= -19.5 V	74
Figure 62: Run# 029, IJW120R100T1, p, 2.0e+10 ions/cm ² , DUT 2, VDS= 1200.0 V, VGS= -14.5 V	74

Figure 63: Run# 030, IJW120R100T1, p, 1.9e+10 ions/cm ² , DUT 2, VDS= 1200.0 V, VGS= -17.0 V	75
Figure 64: Run# 031, IJW120R100T1, p, 6.3e+10 ions/cm ² , DUT 2, VDS= 1200.0 V, VGS= -19.5 V	75
Figure 65: Run# 032, IJW120R100T1, p, 2.0e+10 ions/cm ² , DUT 3, VDS= 1200.0 V, VGS= -14.5 V	76
Figure 66: SRIM2013 simulations of the Ganil Xenon tests on SiC	77
Figure 67: Run# 147, IJW120R100T1, Xe 0 mmAl, 150 mm Air, 6.0e+05 ions/cm ² , DUT 25, VDS= 300.0 V, VGS= -14.5 V	79
Figure 68: Run# 148, IJW120R100T1, Xe 0 mmAl, 150 mm Air, 6.0e+05 ions/cm ² , DUT 25, VDS= 400.0 V, VGS= -14.5 V	79
Figure 69: SRIM2013 simulations of Xenon ions of 10 GeV/n energy on Si and SiC	80
Figure 70: Run# 012, IJW120R100T1, Xe 0 °, 1.8e+03 ions/cm ² , DUT 1, VDS= 1200.0 V, VGS= -14.5 V	82
Figure 71: Run# 013, IJW120R100T1, Xe 0 °, 5.6e+03 ions/cm ² , DUT 1, VDS= 1200.0 V, VGS= -19.5 V	82
Figure 72: Run# 014, IJW120R100T1, Xe 0 °, 1.2e+05 ions/cm ² , DUT 1, VDS= 1200.0 V, VGS= -19.5 V	83
Figure 73: Run# 015, IJW120R100T1, Xe 0 °, 2.0e+04 ions/cm ² , DUT 1, VDS= 1250.0 V, VGS= -19.5 V	83
Figure 74: Run# 016, IJW120R100T1, Xe 0 °, 1.4e+03 ions/cm ² , DUT 1, VDS= 1300.0 V, VGS= -19.5 V	84

List of tables

Table 1: Revision history	2
Table 2: Summary	11
Table 3: Sample shipment	15
Table 4: Sample marking:	16
Table 5: Initial test program	20
Table 6: Measurement parameters.	23
Table 7: UCL: Measurement equipment and instrumentation	23
Table 8: GANIL: Measurement equipment and instrumentation	24
Table 9: CERN: Measurement equipment and instrumentation	26
Table 10: JULIC: Measurement equipment and instrumentation	28
Table 11: UCL: Ion energies, LETs and ranges in Silicon Carbide covered by 10 µm Parylene: ...	31
Table 12: UCL: Irradiation steps of SiC JFET IJW120R100T1.	32
Table 13: Results: Heavy Ions at UCL - Calculated cross sections Calculated with the formulae in ESCC25100 with CL=0.95 and flux uncertainty of 10% (approx. worst case)	34
Table 14: Results of simulations of the LET with package thickness.	38
Table 15: JULIC: Irradiation steps of SiC JFET IJW120R100T1.	39
Table 16: Results: Heavy Ions at UCL - Calculated cross sections Calculated with the formulae in ESCC25100 with CL=0.95 and flux uncertainty of 10% (approx. worst case)	40
Table 17: GANIL: Beam characteristics.	43
Table 18: GANIL: Irradiation steps of SiC JFET IJW120R100T1.	43
Table 19: Results: Heavy Ions at GANIL - Calculated cross sections	44
Table 20: CERN: Irradiation steps of SiC JFET IJW120R100T1.	47
Table 21: Results: Heavy Ions at CERN - Calculated cross sections	48

Table 22: Mold material of example C2M0080120D. Values indicated with * are estimates.....	67
Table 23: Results of GRAS simulations of the LET with package thickness.....	67
Table 24: Intermediate results of MULASSIS simulations of the proton energy with package thickness.	67
Table 25: Results of SRIM simulations of the LET with package thickness.....	68
Table 26: GANIL: Beam characteristics.....	77

1 Introduction

1.1 Scope

The Fraunhofer Institute for Technological Trend Analysis (INT) carried out a series of Single Event Effects tests with protons and heavy ions on SiC JFET IJW120R100T1 from Infineon for the ESA project "Survey of Total Ionizing Dose Tolerance of Power Bipolar Transistors and Silicon Carbide Devices for JUICE" (ESA-TOPSIDE, AO/1-8148/14/NL/SFe) under contract number 4000113976/15/NL/RA.

This reports documents the preparation, execution and the results of these tests.

1.2 Applicable Documents

- [AD1] ITT/AO/1-8148/14/NL/SFe "Statement of work: Survey of Total Ionizing Dose Tolerance of Power Bipolar Transistors and Silicon Carbide Devices for JUICE"
- [AD2] Proposal for ITT/AO/1-8148/14/NL/SFe, Fraunhofer INT

1.3 Reference Documents

- [1] Website of Fraunhofer INT: <http://www.int.fraunhofer.de>
- [2] Guidelines for Evaluating and Expressing the Uncertainty of NIST Measurement Results, B.N. Taylor and C.E. Kuyatt, NIST Technical Note 1297, 1994, <http://www.nist.gov/pml/pubs/tn1297/index.cfm>.
- [3] ESCC Basic Specification No. 25100, issue 2, October 2014
- [4] Datasheet of SiC JFET IJW120R100T1, "SiC- JFET Silicon Carbide- Junction Field Effect Transistor 1200 V CoolSiC™ Power Transistor IJW120R100T1", Infineon, Final Datasheet Rev. 2.0, <2013-09-11>
- [5] TN3.6 "SEE (HI) Test Plan IJW120R100T1 (SiC JFET)", Issue 1, Revision 4, 2018-04-15
- [6] TN3.12 "SEE (p) Test Plan IJW120R100T1 (SiC JFET)" Issue 1 Revision 0, 2017-06-14
- [7] MIL-STD-750-1 w/CHANGE 5, Method 1080.1, "Single-Event Burnout and Single-Event Gate Rupture", 2015
- [8] P. Oser et. al., "Effectiveness Analysis of a Non-Destructive Single Event Burnout Test Methodology", IEEE TNS, vol. 61, no. 4, pp. 1865-1873 (2014).
- [9] Website of the HIF Facility at UCL: <http://www.cyc.ucl.ac.be/HIF/HIF.php> , last accessed: 2019-01-17
- [10] SRIM 2013, www.srim.org, detailed in Ziegler et. Al., "SRIM - The stopping and range of ions in matter (2010)", Nuclear Instruments and Methods in Physics Research Section B, Volume 268, Issue 11-12, p. 1818-1823.016-12-08)
- [11] Website of SPENVIS, <https://www.spenvis.oma.be/>
- [12] Website of the PSTAR database at NIST, <https://physics.nist.gov/PhysRefData/Star/Text/PSTAR.html>
- [13] Website of the GANIL facility for irradiation of electronic components: <https://www.ganil-spiral2.eu/en/industrial-users-2/applications-industrielles/irradiation-of-electronic-components>

- [14] Website of the H8 beam line at CERN:
sba.web.cern.ch/sba/BeamsAndAreas/resultbeam.asp?beamline=H8
- [15] García Alía et al., “Ultraenergetic Heavy-Ion Beams in the CERN Accelerator Complex for Radiation Effects Testing”, IEEE TNS, vol. 66, No. 1, p. 458, 2018. DOI:
10.1109/TNS.2018.2883501
- [16] Fernández-Martínez et al., “Characterization of the Ultra-High Energy Xe beam of the CERN NAH8 line”, Report for users – ongoing analysis

2 Summary

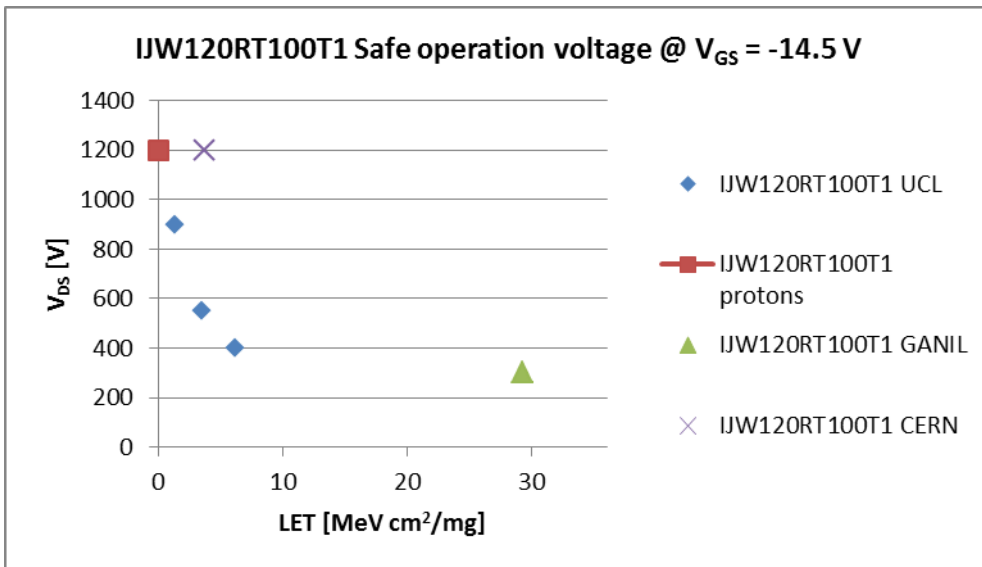
Table 2: Summary

Test Report Number	071/2018
Project (INT)	NEO-14-086
Customer	European Space Agency (ESA), contract number 4000113976/15/NL/RA
Contact	Project Coordinator: Stefan Höffgen (INT) ESA Technical Project Officer: Marc Poizat (ESA/ESTEC)
ESA project / contract number	AO/1-8148/14/NL/SFe 4000113976/15/NL/RA
Device under test	IJW120R100T1
Family	SiC JFET
Technology	Silicon Carbide- Junction Field Effect Transistor
Package	TO247-3
Date code / Wafer lot	HAA547
SN	UCL: #11, #12, #13, #14, #15, #16, #17, #18, #20, #22 GANIL: #25 CERN: #1 (delivery #2) JULIC: #1, #2, #3 (previously Gamma irradiated)
Manufacturer	Infineon
Irradiation test house	Fraunhofer INT
Radiation source	UCL, CERN and GANIL: Heavy Ions, JULIC: Protons
Irradiation facility	UCL, CERN, GANIL, JULIC
Generic specification	ESCC 25100 Iss. 2
Detail specification	MIL-STD-750-1 w/CHANGE 5, Method 1080.1
Test plan	TN3.6 "SEE (HI) Test Plan IJW120R100T1 (SiC JFET)", Issue 1, Revision 4, 201 TN3.12 "SEE (p) Test Plan IJW120R100T1 (SiC JFET)" Issue 1 Revision 0, 2017-06-14
Single/Multiple Exposure	Multiple
Parameters tested	SEB, SEGR
Dates	UCL: 2018-04-16 – 2018-04-17 CERN: 2017-11-30 – 2017-12-01

	GANIL: 2018-06-06 – 2018-06-07 JULIC: 2017-09-19 – 2017-09-20
--	--

2.1 Overview of results

Figure 1: Safe operating voltage across the campaigns



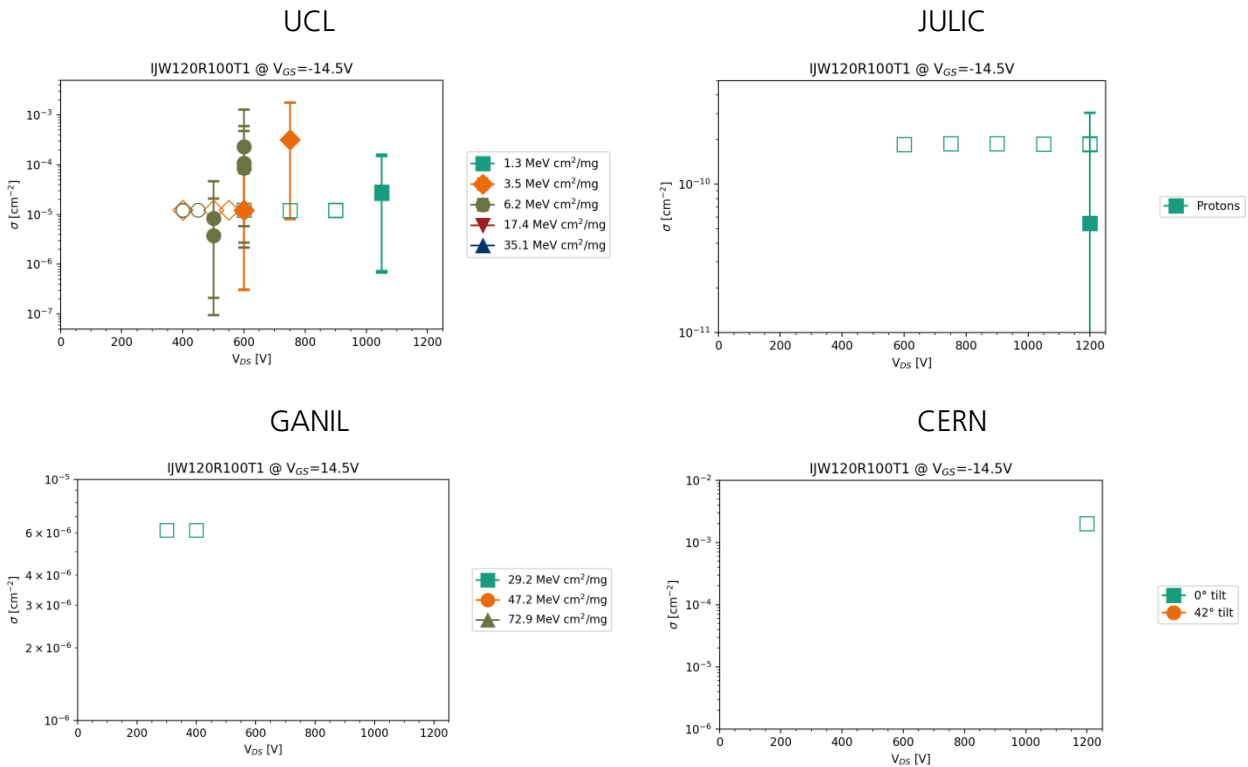
The heavy ion tests at UCL with the SiC JFET IJW120R100T1 were performed with 3 different LETs at a reduced target fluence of 3E5 ions/cm². The voltage achievable for a safe operation up to the target fluence decreases from 900 V with carbon ions (LET = 1.3 MeV cm²/mg) down to 400 V with Aluminium (LET = 6.2 MeV cm²/mg). LETs are given in SiC according to Table 11.

Test with protons of 45 MeV initial energy (approx. 33 MeV at the DUT) passed up to 1200 V.

The voltage achievable for a safe operation with the GANIL Xenon ions decrease down to 300 V at these larger LETs. These results are inline with the other SiC results across the campaigns.

Tests at CERN were performed only with a single DUT from the same code. The voltage of safe operation found at CERN is similar to the proton tests but much higher than found in the heavy ion tests at UCL. However when looking at all devices tested at CERN, all of them passed tests at larger voltages than at UCL.

Figure 2: Cross sections at $V_{GS} = 0$ V for each campaign. Filled symbols mark the cross section in case of device failures and error bars mark the upper lower limits. Open symbols mark the cross section upper limit in case no failure was observed during a run.



2.2 Comments

- **All campaigns:**
 - Huge sensitivity in conjunction with a limited number of devices led to major deviations from the intended test plan.
 - Destructive events could not be mitigated.
- **Tests at UCL:**
 - We can distinguish only in one case that the gate breaks approx. 2 secs before the drain breaks. In any other instance they fail within data sampling accuracy simultaneously.
- **Tests at JULIC:**
 - Tests were performed with packaged DUTs.
 - Test device were previously tested with Co-60 to 1 Mrad(Si).
- **Tests at CERN:**
 - Tests were performed with packaged DUTs.
 - The effective fluences across the tests were $< 1.2E5$ ions/cm². The low fluence might be an explanation for the increased "safe operation" levels observed in these tests compared to the other test campaigns.

- Most device failures occurred at the first spill of beam. Properly deducing the fluence of failure and thus the cross sections of the devices is not possible in these cases, so the cross sections in case of failures given for the CERN results should only be seen as a rough order of magnitude.

3 Sample preparations

3.1 Sample shipment

A total of 30 Samples were procured by INT at a commercial supplier (Mouser Electronics) for the conduction of these tests for ESA. The parcel contained devices with one identification code (HAA547) and was used for the campaigns at UCL, GANIL and JULIC. For the campaign at CERN 20 additional samples were procured which, in contrast to all other devices procured for that campaign, showed the same identification code. Due to the devices being so-called “commercial-off-the-shelf” (COTS) devices, it is not clear whether this identifies the wafer or just the packaging).

Table 3: Sample shipment

Samples ordered	Samples received	Samples sent back
January 2016	February 2016	still at INT (partially used for other tests in this project)
November 2017	November 2017	still at INT

Figure 3: The ESD package with the samples



3.2 Sample identification/ marking

The samples were soldered to adapter pins, to ease the mounting to the board, exchanging, plugging and storage of the samples.

The samples were colour marked to differentiate the samples between each other and to separate the samples of the different campaigns or types.

Figure 4: Sample marking



3.3 Sample safekeeping

The samples were stored in an Electro-Static Discharge (ESD) box (Figure 4) to handle them safely during the test, the interim storage after the last measurement and the final shipment.

Table 4: Sample marking: Due to a limited number of samples, the DUTs tested with protons were previously used for a 1 Mrad(Si) TID campaign. Only DUTs used in the tests of this report are shown. While the lotcode of the second delivery is identical to the device of the first delivery, sample marking of individual samples was reset.

Condition	S/N	Color Code	Comment
UCL	11	[Red]	decap, coated
	12	[Red]	decap, coated
	13	[Red]	decap, coated
	14	[Red]	decap, coated
	15	[Red]	decap, coated
	16	[Red]	decap, coated
	17	[Red]	decap, coated
	18	[Red]	decap, coated
	20	[Red]	decap, coated
	22	[Red]	decap, coated
GANIL	25	[Red]	decap, coated

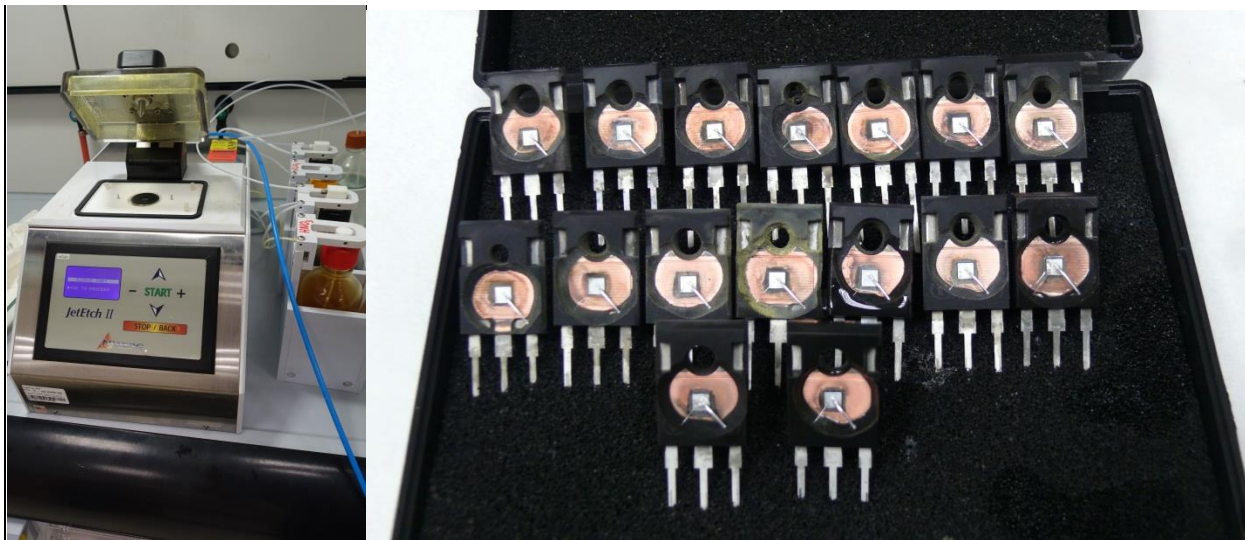
CERN	1 (delivery #2)		non-decap
JULIC	1		non-decap, previously used for TID
	2		non-decap, previously used for TID
	3		non-decap, previously used for TID

3.4 Sample decapsulation and preparation

In preparation for the heavy ion test campaign at UCL and GANIL, the DUTs were decapsulated and parylene coated.

DUT decapsulation was performed at INT using a Nisene JetEtchII (Figure 5). The JetEtch II uses sprays of acid, in our case a 2:1 mixture of sulfuric to nitric acid, to remove the capping layers covering the dye and the active region of the device without inducing mechanical stress on the device. Decapsulation was performed with the device already soldered onto their respective socket adapters.

Figure 5: DUT decapsulation. Left side: Nisene JetEtch II at INT. Right side: batch of decapsulated IJW120R100T1



For etching, sulfuric acid at a flow of 5 ml/min was applied for 360 s at a temperature of 90°C.

After decapsulation the functionality of all DUTs was checked. Due to the missing insulation provided by the package material, only tests at low voltage to prevent corona discharges were performed. 16 decapsulated devices passed these functional tests. 12 were considered for the coating process.

Parylene coating was performed by the "Advanced Chip & Wire Bonding" group, department "System Integration and Interconnection Technologies (SIIT)", at Fraunhofer IZM in Berlin.

Tests of the drain and gate threshold voltages performed at INT after receiving the coated samples, are shown in Figure 6. All decapsulated and coated samples qualified for the heavy ion tests.

Figure 6: Functional tests after parylene coating

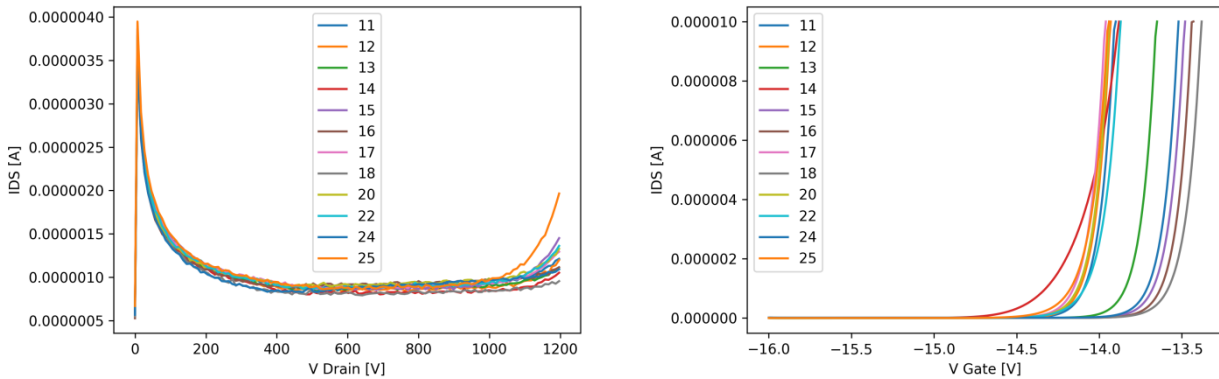
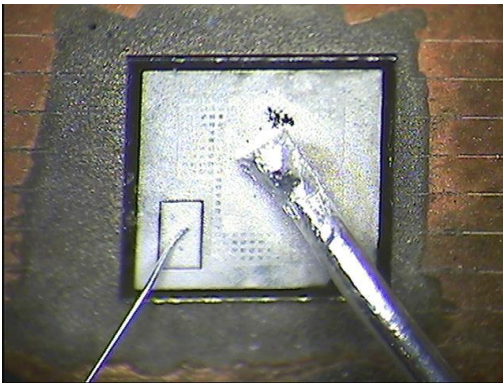
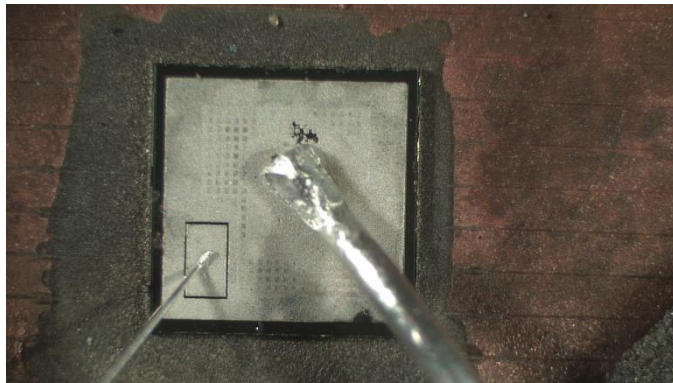


Figure 7: Die pictures. Images were taken with different optical microscopes. The camera used before the tests has a lower quality and resolution.



DUT #11 before tests at UCL



DUT #11 after tests at UCL

Figure 7 shows microscopic images of one DUT (#11) after parylene coating and after the tests at UCL wherein this DUT showed destructive failure. The surface of the DUT does not show signs indicating this destructive failure.

3.5 Sample safekeeping

The samples were stored in an Electro-Static Discharge (ESD) box (Figure 4) to handle them safely during the test, the interim storage after the last measurement and the final shipment.

4 Setup and Measurements

The test approach and setup covered in this section is mostly independent of the facility.

The tests performed with Heavy ions or protons aimed primarily at determining the safe operating area (applicable range of V_{DS} and V_{GS} for safe operation) rather than getting detailed cross sections for each setting and LET. This is mostly due to the high sensitivity of most of the SiC devices studied in this project to even moderate LETs.

Due to a limited number of devices and having destructive failures which could not be mitigated, the required number of 3 samples to check the pass compliance of each test is not reached in any case.

4.1 Intended test program

The methodology of the test and the capture of Single-Event-Burnout (SEB) and Single-Event-Gate-Rupture (SEGR) follows the tests of the MOSFETs.

The tests of the SiC JFETIJW120R100T1 differ slightly, as that device is normally-on. To operate it in off-mode requires a voltage of minimum -14.5 V at the gate.

Starting at 50% of the rated V_{DS} , the drain source voltage would be increased in steps of 150 V due to beam time limitation. Afterwards the Single-Event gate rupture (SEGR) susceptibility would be tested for some VDS settings starting at lower V_{DS} to cover any dependence on V_{DS} .

Due to increased sensitivity of the devices to even moderate LETs and V_{DS} , the actual tests did not follow this plan.

Table 5: Initial test program

#	V_{DS} [V]	V_{GS} [V]	#	V_{DS} [V]	V_{GS} [V]	#	V_{DS} [V]	V_{GS} [V]
1	600	-14.5	6	600	-17	7	600	-19.5
2	750	-14.5						
3	900	-14.5	8	900	-17	9	900	-19.5
4	1050	-14.5						
5	1200	-14.5	10	1200	-17	11	1200	-19.5

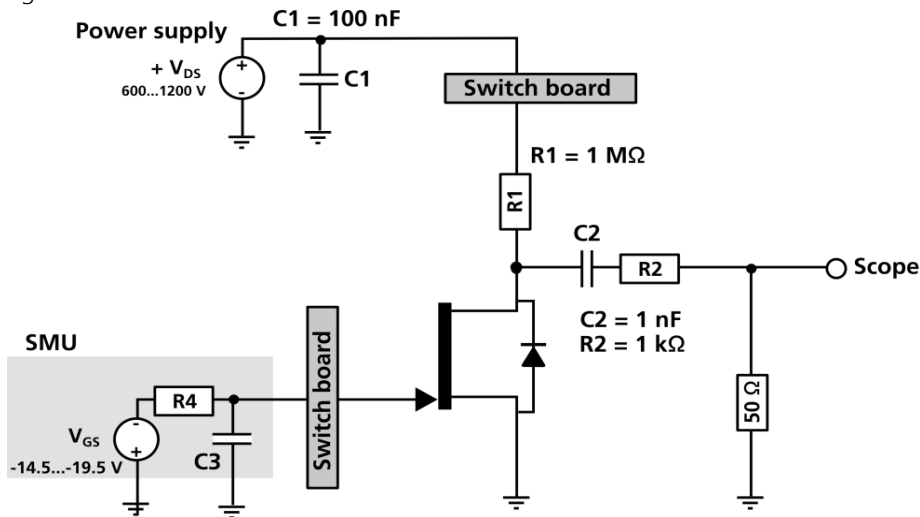
In addition, as the JFET does not have a gate oxide, we don't expect SEGR to occur and thus the PIGS tests after the runs might not be necessary. Still, after each test step, a post-irradiation-gate-stress-(PIGS) test is planned with the drain at maximum rated voltage and the gate swept to its maximum rating.

4.2 Test Board and Detection Circuit

A custom-build printed-circuit board (Figure 9) was manufactured to

- bias the samples according to the circuit-layout of the irradiation test plan [5]
- fix the samples at the radiation source
- switch between the samples and connect the respectively active sample to the external setup
- detect and mitigate destructive SEB by using the voltage drop across a resistor in case of a SEB.

Figure 8: SEB / SEGR Detection Circuit



In Figure 8, the SEB circumvention should be governed by Resistor R1. Increased current will lead to an immediate voltage drop over R1 and consequently a decrease of the voltage on the MOSFET. This should set the voltage below the SEB threshold voltage and thus act like a power shutdown on the device.

Capacitor C2 is used for DC decoupling of scope. C2 and R2 set the transient characteristics of signal due to SEB charge. The dimension of C2 should be small enough so that in case of a SEB and immediate voltage drop on MOSFET, the charge provided by C2 could not further damage the device.

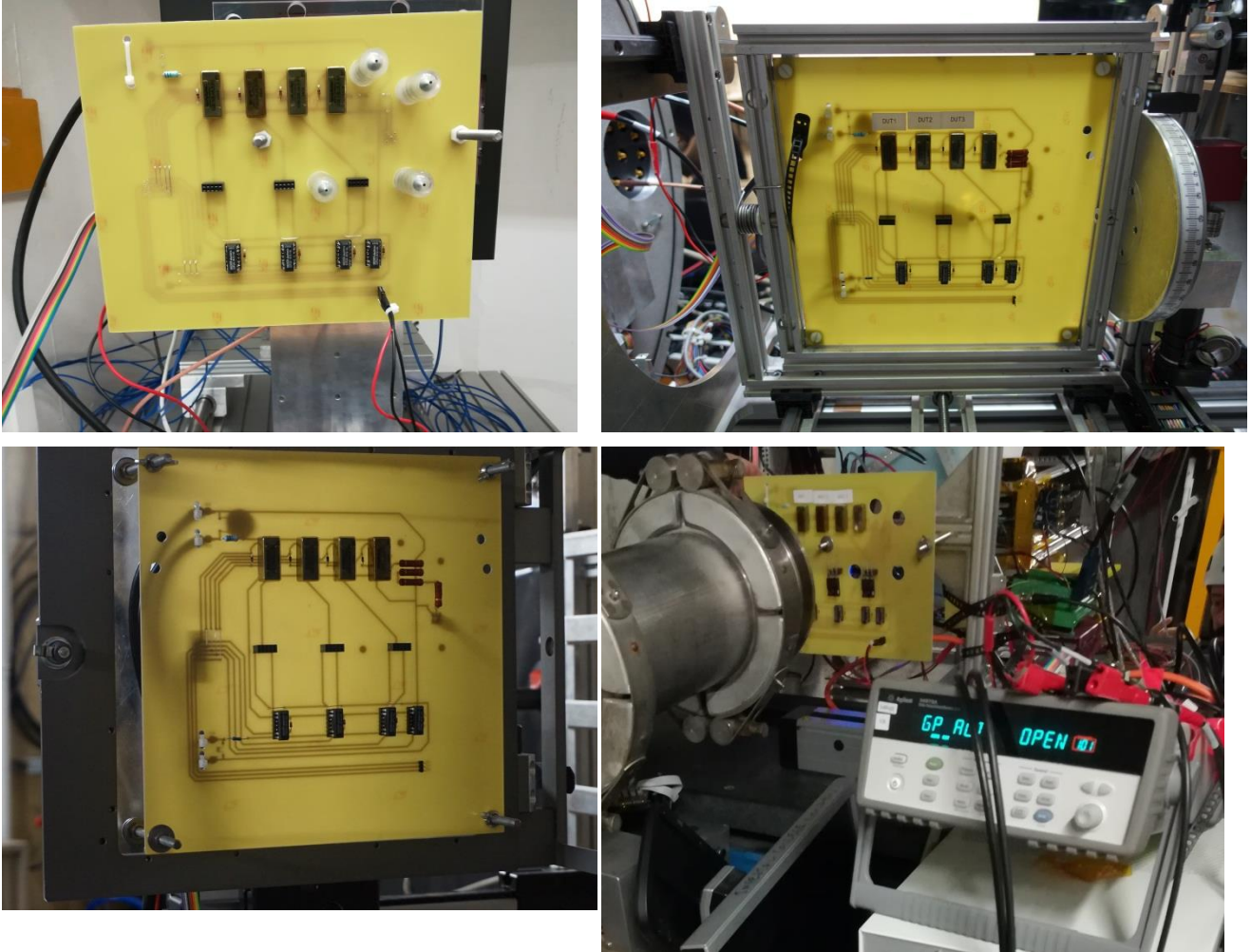
No circumvention or protection was included on the gate, as "SEGR"¹ cannot be circumvented and the DUT would be destroyed anyway.

This setup expanded on the setup proposed by P. Oser et. al. [8].

However, in the actual tests this design did neither circumvent nor mitigate destructive SEB, thus the devices were destroyed on each SEB event.

¹ The term SEGR would correctly apply to a gate with a gateoxide which the JFET does not have.

Figure 9: Test board layout Top left side: proton tests at JULIC, Top right side: Heavy ion tests at UCL, bottom left: Heavy ion tests at GANIL, bottom right side: Heavy ion tests at CERN



The boards used for the Heavy Ion and proton tests are functionally identical, but the proton board featured additional holes for four ionization chambers. The DUT was then positioned off-center from the beam, such that all ionization chambers and the DUT position are at the same distance from the center, thus allowing to calculate the proton flux at the DUT position without a fixed installation at the facility which would allow to do that. As a drawback, only one DUT position on the board could be used.

For protons the board was at a distance of 1.8 m from the beam line exit window. Due to interaction in air and the exit window, the proton beam with initial energy 45 MeV was then broadened and reduced in energy to approx. 39 MeV.

The DUTs were exposed to the protons non-delidded, thus when passing the package and hitting the sensitive volume of the devices, the proton energy is further reduced.

Calculations of the LETs in SiC are shown in the respective sections of the campaigns.

At CERN the beam was shared with other experiments, but the INT setup was the first in line after the beam exit window. The installation at the beam line did not feature a moveable table, so a ISEL linear guide and step motor was used to achieve sample and board movement along one axis. With this, the samples were moved away from the beam to perform the PIGS tests.

4.3 Measurement parameters

Parameters are continuously monitored during the runs. V_{DS} and V_{GS} are only indicated at the respective runs, I_{DS} and I_{GS} are shown.

Table 6: Measurement parameters. Based on [4], taken from [5]

No.	Characteristics	Symbol	Remark
1	Drain-Source Voltage	V_{DS}	Set
2	Drain-Source Current	I_{DS}	Monitored for SEB
3	Gate-Source Voltage	V_{GS}	Set
4	Gate-Source Current	I_{GS}	Monitored for SEGR

4.4 Measurement equipment

The test equipment is shown in Table 7 - Table 10 and Figure 10 - Figure 13.

The due date of the calibration can change from campaign to campaign if a new calibration was performed in the time between.

Table 7: UCL: Measurement equipment and instrumentation

Equipment	Manufacturer	Model	INT-Code	Calibr. due	Measurement
High Power System Source Meter	Keithley	2657A	E-SMU-012	03/2018	V_{DS} , I_{DS}
System Source Meter	Keithley	2400	E-SMU-002	10/2019	V_{GS} , I_{GS}
Data Acquisition/Switch unit	Agilent	34970A	E-SMF-002	n/a	Switch matrix for V_{DS} and V_{GS} relais
Triple Output Power Supply	Agilent	E3631A	E-PS3-002	n/a	Power supply of of relais
Triple Output Power Supply	Agilent	E3631A	E-PS3-003	n/a	Power supply for Line driver (SEB)

Equipment	Manufacturer	Model	INT-Code	Calibr. due	Measurement
Line driver	INT	--	--	--	transients to oscilloscope) Amplification of device output to transport signal over long cables
Digital Oscilloscope	Rohde & Schwarz	RTO2044	E-DSO-004	VB	intended for capturing of SEB transients, no results

Figure 10: UCL: Measurement equipment/setup

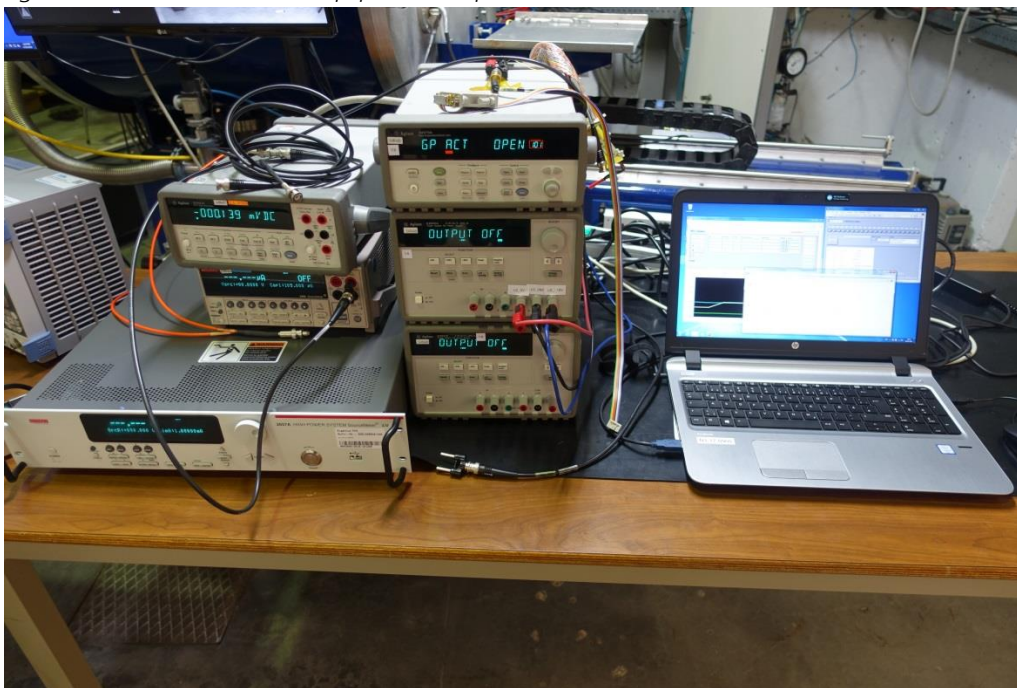


Table 8: GANIL: Measurement equipment and instrumentation

Equipment	Manufacturer	Model	INT-Code	Calibr. due	Measurement
High Power System Source Meter	Keithley	2657A	E-SMU-012	03/2020	V_{bs} , I_{bs}

Equipment	Manufacturer	Model	INT-Code	Calibr. due	Measurement
System Source Meter	Keithley	2400	E-SMU-002	10/2019	V_{GS} , I_{GS}
Data Acquisition/Switch unit	Agilent	34970A	E-SMF-002	n/a	Switch matrix for V_{DS} and V_{GS} relais
Triple Output Power Supply	Agilent	E3631A	E-PS3-001	n/a	Power supply of of relais
Triple Output Power Supply	Agilent	E3631A	E-PS3-002	n/a	Power supply for Line driver (SEB transients to oscilloscope)
Line driver	INT	--	--	--	Amplification of device output to transport signal over long cables
Digital Oscilloscope	Rohde & Schwarz	RTO2044	E-DSO-004	VB	intended for capturing of SEB transients, no results

Figure 11: GANIL: Measurement equipment/setup

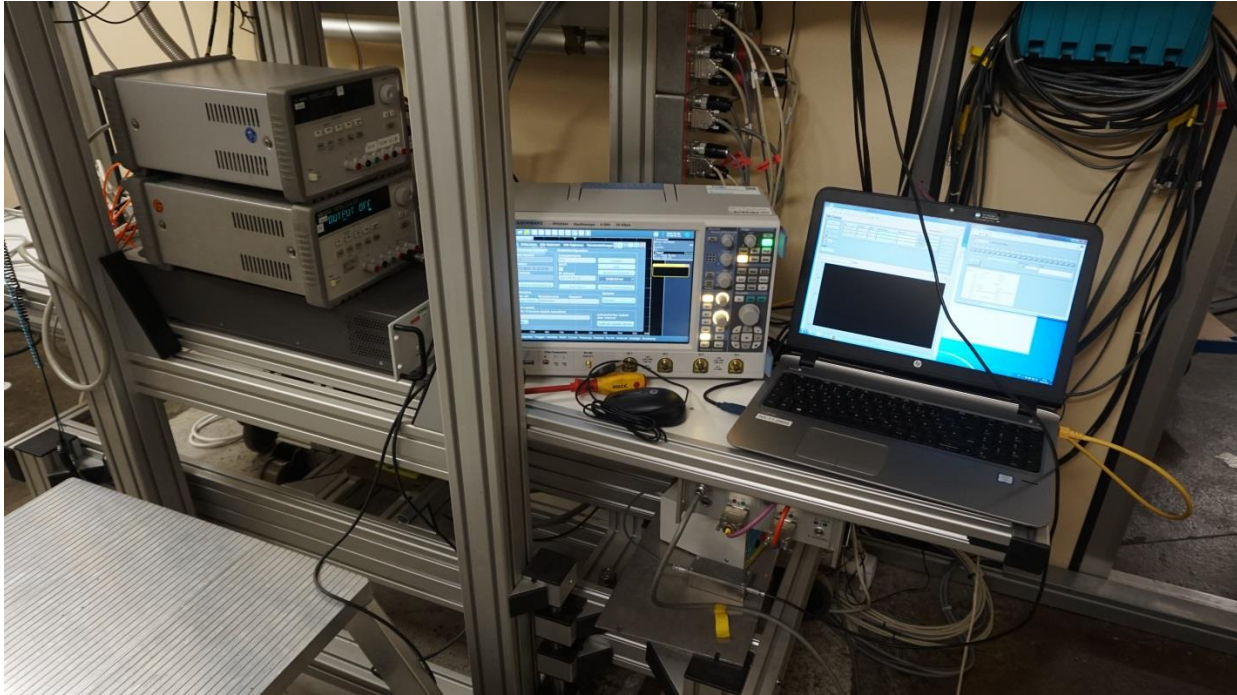


Table 9: CERN: Measurement equipment and instrumentation

Equipment	Manufacturer	Model	INT-Code	Calibr. due	Measurement
High Power System Source Meter	Keithley	2657A	E-SMU-012	03/2020	V_{DS} , I_{DS}
System Source Meter	Keithley	2400	E-SMU-002	10/2019	V_{GS} , I_{GS}
Data Acquisition/Switch unit	Agilent	34970A	E-SMF-002	n/a	Switch matrix for V_{DS} and V_{GS} relais
Triple Output Power Supply	Agilent	E3631A	E-PS3-001	n/a	Power supply of of relais
Triple Output Power Supply	Agilent	E3631A	E-PS3-002	n/a	Power supply for Line driver (SEB transients to oscilloscope)
Line driver	INT	--	--	n/a	Amplification of device output to transport signal

Equipment	Manufacturer	Model	INT-Code	Calibr. due	Measurement
Digital Oscilloscope	Rohde & Schwarz	RTO2044	E-DSO-004	VB	over long cables intended for capturing of SEB transients, no results
Step motor	ISEL	LES4	--	n/a	Moving samples along 1 direction
Linear guide	ISEL	IT116 G	--	n/a	Moving samples along 1 direction

Figure 12: CERN: Measurement equipment/setup.

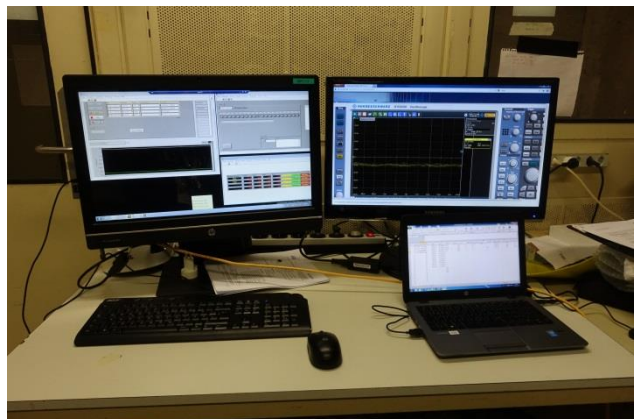
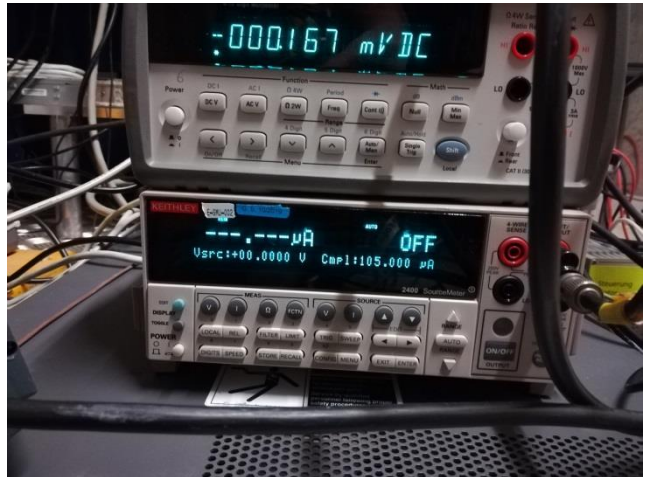
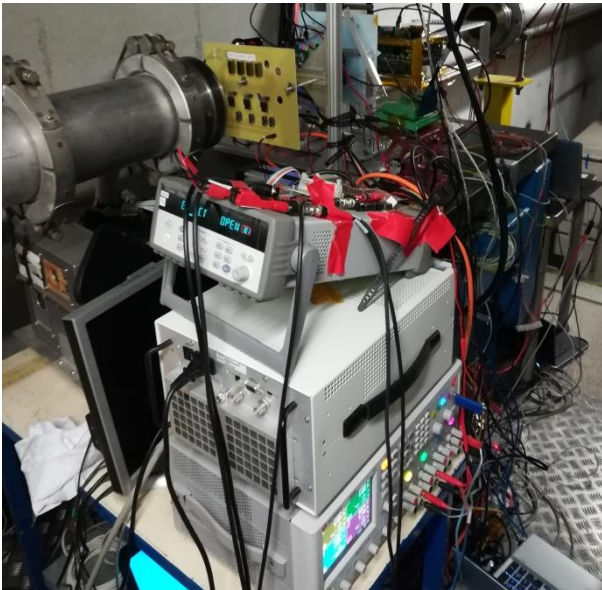
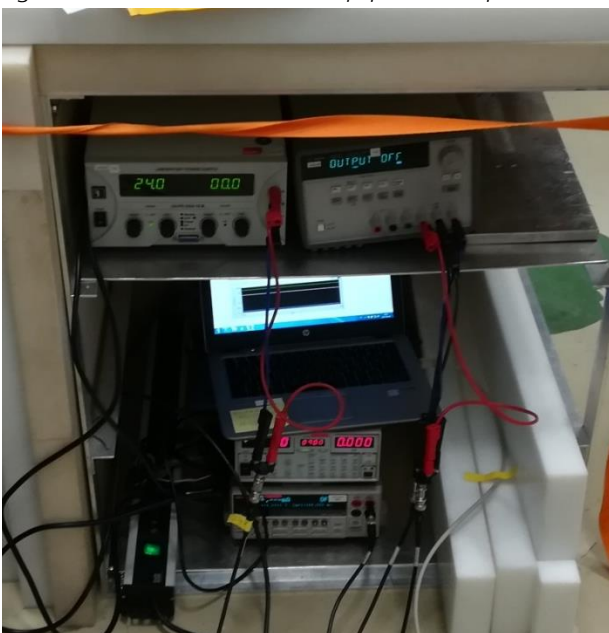


Table 10: JULIC: Measurement equipment and instrumentation

Equipment	Manufacturer	Model	INT-Code	Calibr. due	Measurement
5 kV Power supply	Keithley	2290E-5	E-PS1-030	10/2017	V_{DS}, I_{DS}
System Source Meter	Keithley	2400	E-SMU-002	10/2017	V_{GS}, I_{GS}
Laboratory Power Supply	EA	EA-PS-3032-10B	E-PS1-001	n/a	Control of relais for switching V_{GS}
Triple Output Power Supply	Agilent	E3631A	E-PS3-001-	n/a	Power supply for Line driver (SEB transients to oscilloscope)
Line driver	INT	--	--	--	Amplification of device output to transport signal over long cables
6 GHz Oscilloscope	Agilent	infiniium 54855A DSO	E-DSO-001	VB	intended for capturing of SEB transients, no results

As only one DUT was on the board, no switch matrix was included in the setup, and the power supplies were only used to power the relais, not for switching between DUTs.

Figure 13: JULIC: Measurement equipment/setup



4.5 Measurement procedures

Bias conditions of the drain and gate were fixed for each step. When no destructive events occurred during a run, a PIGS test was scheduled. In some instances across the campaigns, that PIGS test might not have been performed. These instances are commented in the respective sections.

For the CERN campaign, the samples were moved out of the beam to perform the PIGS tests. At the other campaigns the beam was stopped for the PIGS tests.

5 Tests at UCL

5.1 Facility

The main heavy ion test was performed at the HIF facility of the CYCLONE cyclotron of the Université catholique de Louvain (UCL) in Louvain-la-Neuve.

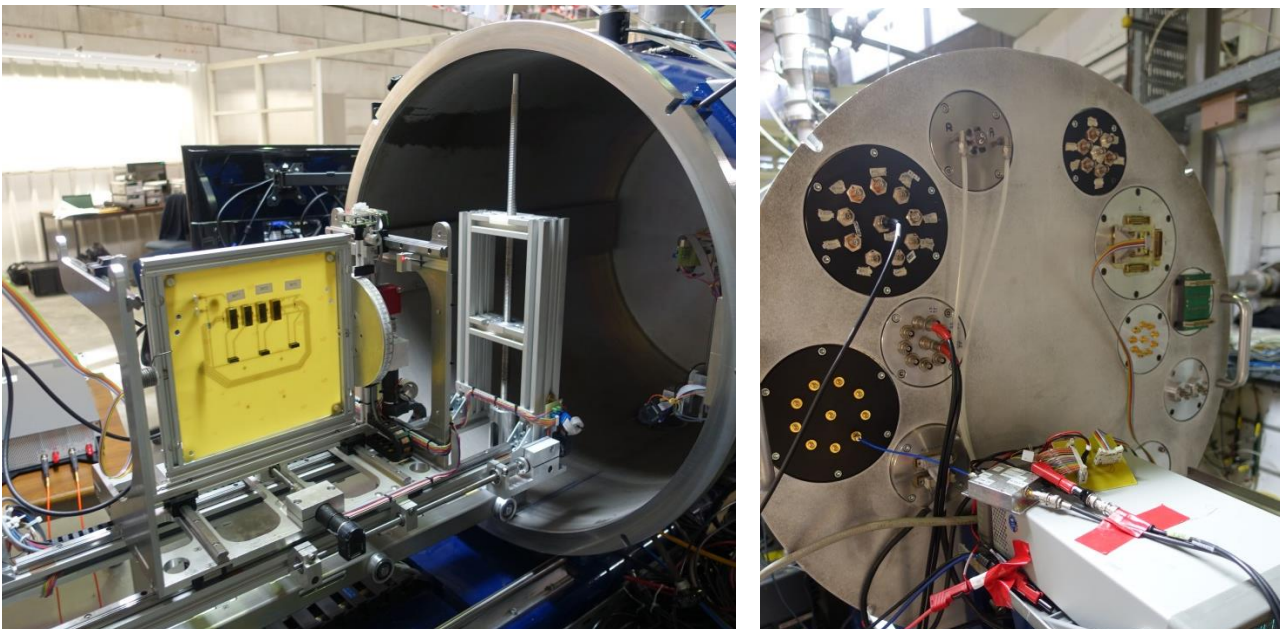
The facility can provide selected heavy ion beams from Carbon to Xenon in a particle cocktail with mass/charge ratio of approx. $M/Q=3.3$, allowing to switch from ion species to ion species quickly within the cocktail.

The experimental setup at the facility consists of the main vacuum chamber with a sample holder, which is moveable in x- and y-direction and can be tilted along one axis.

Feedthroughs can be used to connect boards within the enclosure with outside instrumentation (Figure 14).

Users can start and stop the irradiation from the user station next to the test chamber, other beam parameters like the particle flux can only be set by an operator.

Figure 14: UCL vacuum chamber with electrical feedthroughs. Two SHV cable feedthroughs, one DB9 feedthrough and one SMA feedthrough were used to connect the board with the outside instrumentation.



5.2 Beam parameters

The resulting total energies of the respective ions, as well as their LET and range in Silicon is provided by UCL [9]. However this data is not valid for Silicon Carbide.

SRIM 2013 [10] simulations by Fraunhofer INT show the respective values for the heavy ion beams provided by UCL under normal incidence in Silicon Carbide covered by a 10 μm Parylene layer. Detailed data and a comparison to the data in blank Silicon Carbide is included in the test plan [5].

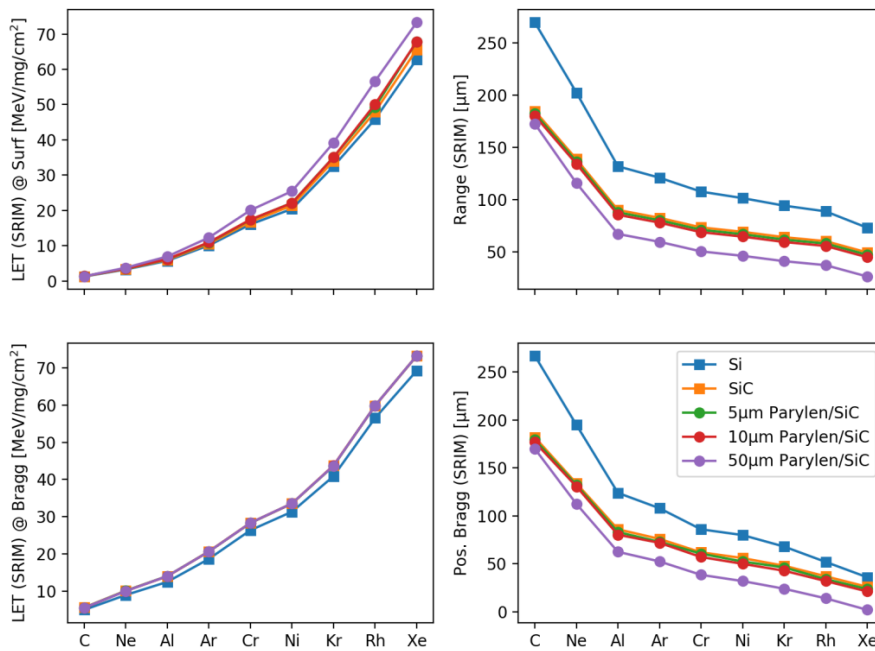
Tests with the IJW120R100T1 were only performed with ions marked in bold letters in Table 11.

Table 11: UCL: Ion energies, LETs and ranges in Silicon Carbide covered by 10 μm Parylene: Shown are the ions available at UCL [9]. LETs highlighted in bold font were actually used. LET and range data are based on SRIM2013 [10] simulations done at Fraunhofer INT.

Ion	Energy [MeV]	LET ^{SRIM} @ Surface [MeV cm ² /mg]	Range ^{SRIM*} [μm]	LET ^{SRIM} @ Bragg Peak [MeV cm ² /mg]	Depth of Bragg Peak* [μm]
C	131	1.33	180.22	5.49	176.90
Ne	238	3.49	134.13	10.02	130.70
Al	250	6.20	85.42	13.99	80.30
Ar	379	10.95	77.91	20.63	71.90
Cr	513	17.41	68.74	28.34	57.10
Ni	582	22.09	64.53	33.55	50.00
Kr	769	35.06	59.36	43.77	42.80
Rh	972	50.14	55.57	59.84	32.00
Xe	995	67.81	44.79	73.27	21.20

* Range and position of Bragg peak is given within the Silicon Carbide layer.

Figure 15: Plot of LETs and Ranges in Silicon Carbide at UCL. Additional data with Parylene layers and data for Silicon are included. Thin Parylene layers have limited impact.



5.3 Geometry

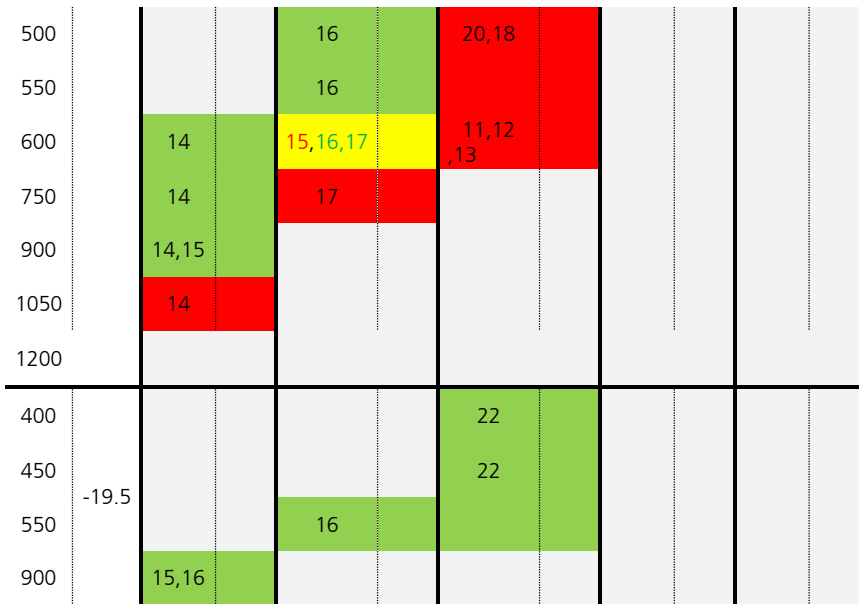
The board is attached to the moveable board holder (Figure 14) which can be fully retracted from the chamber for ease of access. Tests are then performed with the chamber sealed and evacuated.

5.4 Irradiation steps

The log file of the tests performed at UCL can be found in Appendix B. Table 12 shows an overview over the test indicating pass and fail results. A detailed evaluation of the results is shown in Section 5.5.

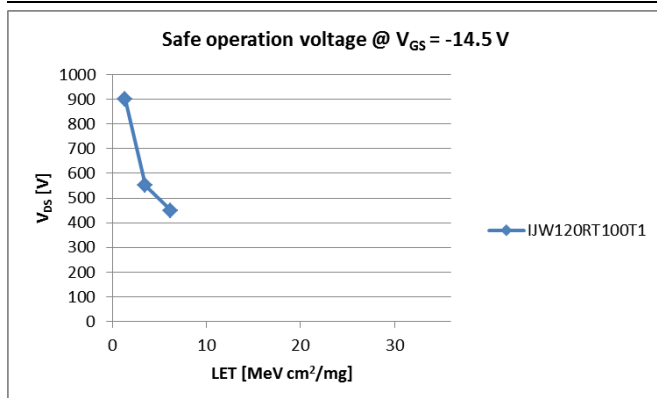
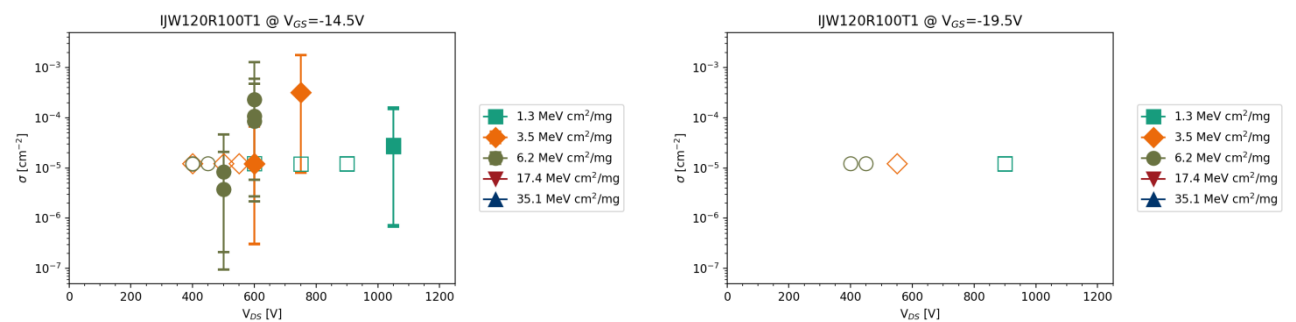
Table 12: UCL: Irradiation steps of SiC JFET IJW120R100T1. Numbers indicate the DUT serial number from Table 4. Table cells without numbers indicate that no run was performed under these conditions. Green or red background color indicate PASS or FAIL respectively. If a DUT fails at some voltage, all higher voltages are also indicated as fail. Yellow color (if applicable) indicates mixed results (e.g. 1 DUT passing, 1 DUT failing at the same level) or non-conclusive results with the device showing some damage not clearly attributable to a fail.

		C		Ne		Al		Cr		Kr	
V_DS [V]	V_GS [V]	1.3		3.5		6.2		17.4		35.1	
		in-situ	PIGS	in-situ	PIGS	in-situ	PIGS	in-situ	PIGS	in-situ	PIGS
400	-14.5			17		18,22,20					
450				16		22					



5.5 Results

Figure 16: Overview of results: Heavy Ions at UCL. The top two images show the cross section results for various settings of V_{GS} . Filled symbols mark the cross section in case of device failures and error bars mark the upper lower limits. Open symbols mark the cross section upper limit in case no failure was observed during a run. The bottom image shows the safe operating voltage at $V_{GS} = -14.5$ V.



The SiC JFET IJW120R100T1 showed high vulnerability with respect to the heavy ions even at low LETs and a reduced target fluence of 3E5 ions/cm². A device which passes a run up to 3E5 ions/cm² without errors has an upper limit of the cross section of $\sigma \leq 1.23E-5 \text{ cm}^2$ assuming 95%CL and 10% flux uncertainty.

In these tests this cross section can be attributed to the 450 V level with Aluminium ions and the 900 V level of Carbon atoms. Higher LET ions were not used, as the necessary derating to safely operate the DUTs and the fluence until failure were already fairly low at Aluminium.

We can distinguish only in one case that the gate breaks approx. 2 secs before the drain breaks. In any other instance they are within data sampling accuracy simultaneously.

Table 13: Results: Heavy Ions at UCL - Calculated cross sections Calculated with the formulae in ESCC25100 with CL=0.95 and flux uncertainty of 10% (approx. worst case)

#	Ion	DUT #	V_DS, V	V_GS	Failure fluence [cm-2]	σ lower [cm2]	σ [cm2]	σ upper [cm2]	Effect	Comment
35	Al	11	600	-14.5	9.25E+03	2.74E-06	1.08E-04	6.03E-04	SEB, SEGR	Destructive event at indicated fluence, within data sampling accuracy simultaneously in both Gate and Drain
36	Al	12	600	-14.5	1.17E+04	2.17E-06	8.56E-05	4.77E-04	SEB, SEGR	Destructive event at indicated fluence, within data sampling accuracy simultaneously in both Gate and Drain
37	Al	13	600	-14.5	4.35E+03	5.83E-06	2.30E-04	1.28E-03	SEB, SEGR	Destructive event at indicated fluence, within data sampling accuracy simultaneously in both Gate and Drain
38	C	14	600	-14.5	3.02E+05	0	0	1.22E-05	--	--
39	C	14	750	-14.5	3.04E+05	0	0	1.21E-05	--	--
40	C	14	900	-14.5	3.04E+05	0	0	1.21E-05	--	--
41	C	14	1050	-14.5	3.50E+04	7.24E-07	2.86E-05	1.59E-04	SEGR, SEB	Destructive SEGR at indicated fluence, within data sampling accuracy drain follows 2 secs later
42	C	15	900	-14.5	3.03E+05	0	0	1.22E-05	--	--
43	C	15	900	-19.5	3.03E+05	0	0	1.22E-05	--	--
44	C	16	900	-19.5	3.04E+05	0	0	1.21E-05	--	--
45	Ne	17	400	-14.5	3.04E+05	0	0	1.22E-05	--	--
46	Ne	17	600	-14.5	3.03E+05	0	0	1.22E-05	--	--
47	Ne	17	750	-14.5	3.15E+03	8.03E-06	3.17E-04	1.77E-03	SEB, SEGR	Destructive event at indicated fluence, within data sampling accuracy simultaneously in both Gate and Drain
48	Ne	15	600	-14.5	8.31E+04	3.05E-07	1.20E-05	6.70E-05	SEB, SEGR	Destructive event at indicated fluence, within data sampling accuracy simultaneously in both Gate and Drain
49	Ne	16	500	-14.5	3.03E+05	0	0	1.22E-05	--	--
50	Ne	16	550	-14.5	3.04E+05	0	0	1.22E-05	--	--

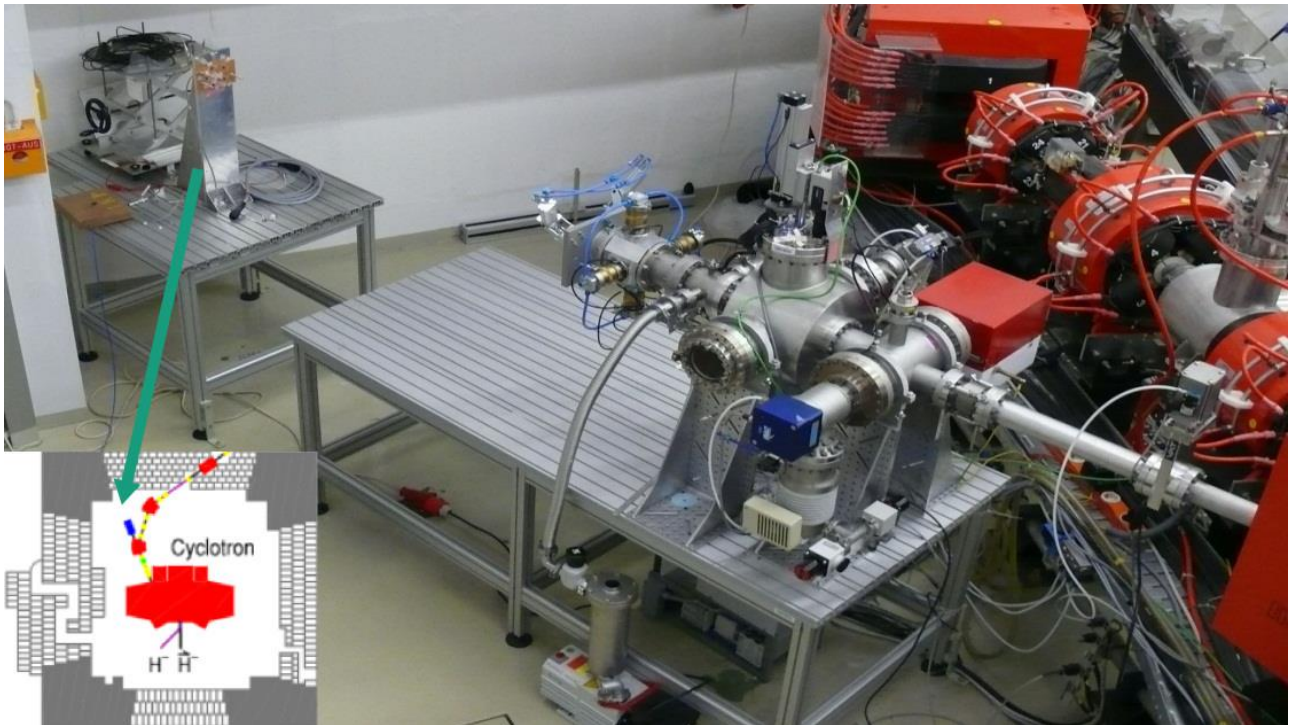
51	Ne	16	550	-19.5	3.02E+05	0	0	1.22E-05	--	--	
52	Ne	16	600	-14.5	8.23E+04	3.08E-07	1.22E-05	6.77E-05	SEB, SEGR		Destructive event at indicated fluence, within data sampling accuracy simultaneously in both Gate and Drain
53	Al	18	400	-14.5	3.01E+05	0	0	1.22E-05	--	--	
54	Al	20	500	-14.5	2.68E+05	9.45E-08	3.73E-06	2.08E-05	SEB, SEGR		Destructive event at indicated fluence, within data sampling accuracy simultaneously in both Gate and Drain
55	Al	18	500	-14.5	1.20E+05	2.11E-07	8.34E-06	4.65E-05	SEB, SEGR		Destructive event at indicated fluence, within data sampling accuracy simultaneously in both Gate and Drain
56	Al	22	400	-14.5	3.04E+05	0	0	1.21E-05	--	--	
58	Al	22	400	-19.5	3.02E+05	0	0	1.22E-05	--	--	
59	Al	22	450	-14.5	3.01E+05	0	0	1.22E-05	--	--	
60	Al	22	450	-19.5	3.02E+05	0	0	1.22E-05	--	--	

6 Tests at JULIC

6.1 Facility

Proton tests were performed at the JULIC injector cyclotron of the Forschungszentrum Jülich (FZJ, Research Centre Jülich). JULIC is the injector cyclotron of the Cooler Synchrotron COSY.

Figure 17: Beam line and irradiation site at the JULIC injector cyclotron, FZ Jülich



The initial energy of the proton beam is fixed to 45.0 MeV inside the cyclotron (vacuum). Usually the device under test (DUT) is placed at 1.8 m distance from the exit window of the beam. After passing the exit window of 1 mm aluminium and the air the mean proton energy is reduced to 39.3 MeV at the surface of DUT (Figure 18 and Figure 19). The maximum current of the beam is 10 μA (i.e. $6.24 \cdot 10^{13}$ p+/s). The beam has a Gaussian profile with a FWHM of about 7 cm at the surface of the DUTs.

The dose is measured online with Farmer Ionisation Chambers 30010 (measurement volume of 0.6 cm³) from PTW and an electrometer Multidos T10004 from PTW. Typically this type of ionisation chamber (IC) is used as an absolute dose-meter in high energy photon, electron, or proton-radiation therapy. The ionisation chambers are calibrated with a Co-60 gamma reference field against national standards by the manufacturer. The PMMA cap of the chamber further reduces the energy to 30.5 MeV inside the chamber.

The dose D given by the IC is related to the particle fluence Φ by the linear energy transfer (LET):

$$D = \frac{1}{\rho} \cdot \underbrace{\frac{dE}{dx}}_{LET} \cdot \Phi$$

The conversion factor is obtained by a numerical simulation by MULASSIS (Geant4). For the experimental setup a fluence $\Phi = 10^{10} \text{ p}^+/\text{cm}^2$ at the exit window produces a dose $D = 24.38(15) \text{ Gy}(\text{air})$ in the ionization chamber. Alternatively, the LET (also called stopping power) of protons in different materials can be looked up at [12].

Figure 18: Schematic setup of the beam exit window at JULIC and the ionization chamber. The DUT is placed in same distance as the IC.

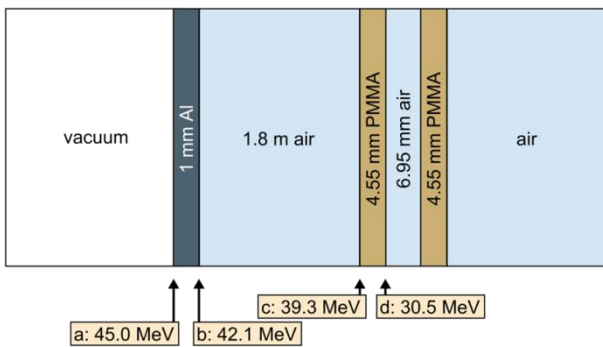
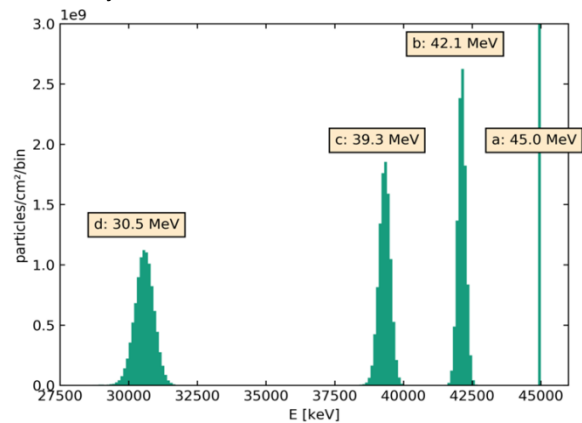


Figure 19: The initial proton energy of 45.0 MeV gets reduced to 39.3 MeV at the position of the IC/DUT. The PMMA cap of the chamber further reduces the energy to 30.5 MeV, calculation by MULASSIS (Geant4) on SPENVIS[11].



For the current tests, packaged Silicon Carbide devices were irradiated with the protons. Thus to calculate the LET on the die, additional simulations were performed with GRAS (Geant4).

6.2 Beam parameters

To receive the impact in terms of proton energy and LET on the Silicon Carbide die with packaged DUTs, radiation transport simulations have to be made. Simulation were performed with GRAS and a combination of MULASSIS and SRIM. Details on the approach and intermediate results are given in Appendix C.1. We see more of an impact on package thickness and nearly no impact of the package material. Thus here we will give a summary of the results just by thickness of the package.

Table 14: Results of simulations of the LET with package thickness. Details on the approach and intermediate results are given in Appendix C.1

Thickness	0.5 mm		1 mm		2 mm		3 mm	
LET _{GRAS} [MeV cm ² /mg]	0.012		0.008		0.005		0.003	
LET _{SRIM} [MeV cm ² /mg]	0.013		--		--		0.016	
Atomic recoil	Silicon	Carbon	Silicon	Carbon	Silicon	Carbon	Silicon	Carbon
Peak LET _{SRIM} [MeV cm ² /mg] at max. recoil	12.30	5.81	12.16	5.81	11.86	5.80	11.31	5.80
Range [μm]	2.01	6.6	1.96	6.3	1.84	5.7	1.72	5.1

While the results from GRAS and SRIM are not identical, the proton induced LET is well below 0.02 MeV cm²/mg in any case. The LETs of the recoil nuclei in SiC vary strongly with the LET of Si at or below 12.3 MeV cm²/mg and the LET of C around 5.8 MeV cm²/mg. For the overall data evaluation we identify the proton data with an LET of 0.01 MeV cm²/mg.

The thickness of the actual package of the DUTs is around 2 mm.

6.3 Geometry

The DUT was positioned off-center from the beam, such that all ionization chambers and the DUT position are at the same distance from the center, thus allowing to calculate the proton flux at the DUT position without a fixed installation at the facility which would allow to do that. As a drawback, only one DUT position on the board could be used at a time. The beam still was incident normally (90°) to the surface of the DUT.

6.4 Irradiation steps

The log file of the tests performed at JULIC can be found in Appendix C. Table 15 shows an overview over the test indicating pass and fail results. A detailed evaluation of the results is shown in Section 6.5

No PIGS tests were performed with these devices.

Table 15: JULIC: Irradiation steps of SiC JFET IJW120R100T1. Numbers indicate the DUT serial number from Table 4. Table cells without numbers indicate that no run was performed under these conditions. Green or red background colour indicate PASS or FAIL respectively. If a DUT fails at some voltage, all higher voltages are also indicated as fail. Yellow colour (if applicable) indicates mixed results (e.g. 1 DUT passing, 1 DUT failing at the same level) or non-conclusive results with the device showing some damage not clearly attributable to a fail.

		Protons	
V_DS [V]	V_GS [V]	E _{init} = 45 MeV	
		in-situ	PIGS
600	-14.5	1	
750		1	
900		1	
1050		1	
1200		1,2,3	
600	-17.0	1	
900		1	
1200		1,2	
600	-19.5	1	
900		1	
1200		1,2	

6.5 Results

With the first two devices and tests up to approx. 2×10^{10} p/cm², no effects were observed at all. One of these DUTs also passed a test up to 6.3×10^{10} p/cm² at maximum drain and gate voltage.

However when trying to confirm this with a third device, we saw a simultaneous occurrence (within timing accuracies, which were 1 data point each approx. 100 ms in this campaign) of SEB and SEGR. No previous tests with this DUT, including the TID tests these devices were subjected to, indicated any other behaviour of this DUT compared to the other two.

Figure 20: Overview of results: Protons at JULIC. The images show the cross section results for various settings of V_{GS} . Circles mark the cross section in case of device failures and error bars mark the upper lower limits. Triangles mark the cross section upper limit in case no failure was observed during a run.

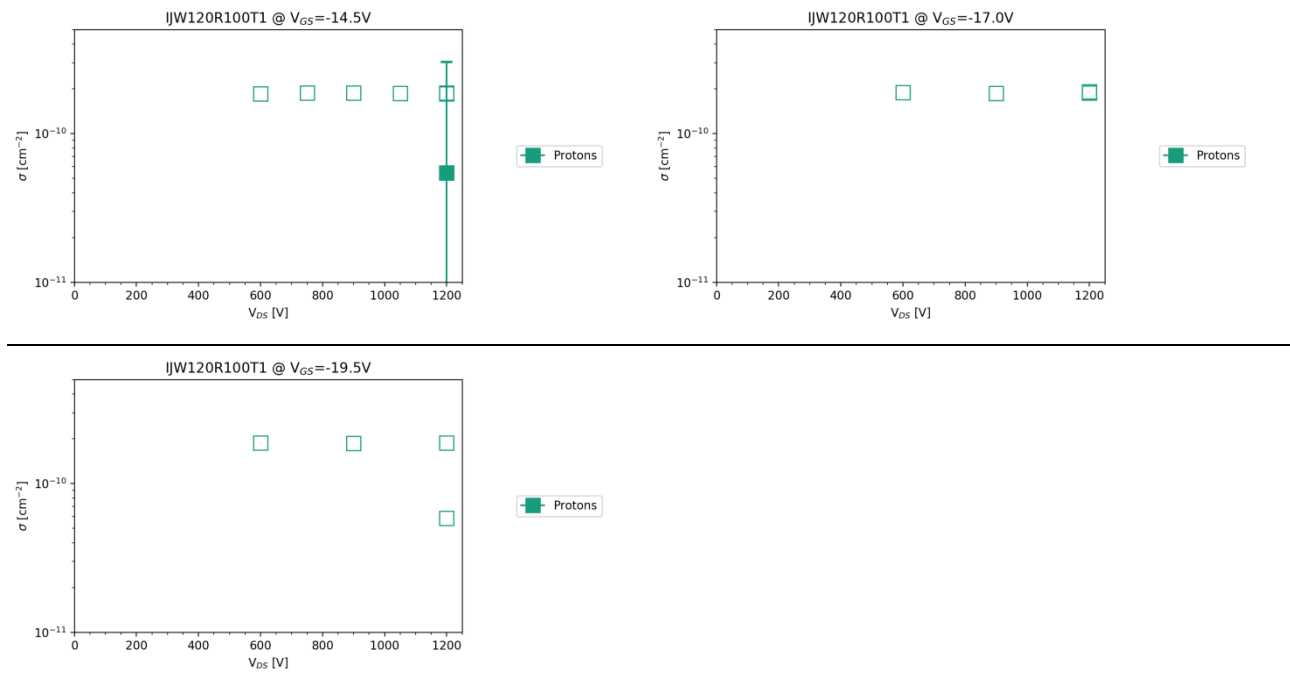


Table 16: Results: Heavy Ions at UCL - Calculated cross sections Calculated with the formulae in ESCC25100 with $CL=0.95$ and flux uncertainty of 10% (approx. worst case)

#	Ion	DUT #	V_{DS} , V	V_{GS}	Failure fluence [cm ⁻²]	σ lower [cm ²]	σ [cm ²]	σ upper [cm ²]	Effect	Comment
18	p	#1	600	-14.5	> 2E+10	0	0	1.85E-10	--	--
19	p	#1	750	-14.5	> 1.96E+10	0	0	1.88E-10	--	--
20	p	#1	900	-14.5	> 1.96E+10	0	0	1.88E-10	--	--
21	p	#1	1050	-14.5	> 1.98E+10	0	0	1.86E-10	--	--
22	p	#1	1200	-14.5	> 1.96E+10	0	0	1.88E-10	--	--
23	p	#1	600	-17	> 1.96E+10	0	0	1.89E-10	--	--
24	p	#1	900	-17	> 1.97E+10	0	0	1.87E-10	--	--
25	p	#1	1200	-17	> 1.97E+10	0	0	1.87E-10	--	--
26	p	#1	600	-19.5	> 1.96E+10	0	0	1.88E-10	--	--
27	p	#1	900	-19.5	> 1.97E+10	0	0	1.87E-10	--	--
28	p	#2	1200	-19.5	> 1.96E+10	0	0	1.88E-10	--	--
29	p	#2	1200	-14.5	> 2E+10	0	0	1.85E-10	--	--
30	p	#2	1200	-17	> 1.93E+10	0	0	1.91E-10	--	--
31	p	#2	1200	-19.5	> 6.3E+10	0	0	5.85E-11	--	--
32	p	#3	1200	-14.5	1.84E+10	1.38E-12	5.45E-11	3.03E-10	SEB/SEGR	within timing accuracy (0.1 s)



7 Tests at GANIL

7.1 Facility

GANIL offers the irradiation of electric components with heavy ions over a wide LET range.

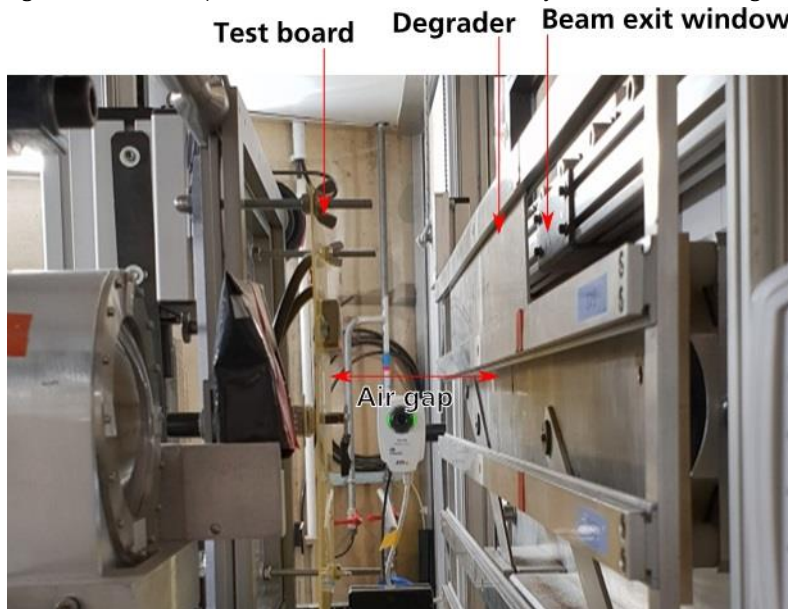
Additional heavy ion tests were performed at the G4 cave at GANIL, Caen, France.

The facility can provide selected heavy ion beams from Argon to Lead with a larger kinetic energy per nucleon than is available e.g. at UCL. The available ion at the time of our tests was Xenon.

The experimental tests at the facility take place in air and the setup consists of a sample holder, which is moveable in x-,y- and z-direction and variable degraders that can be put between the beam exit window and the DUT. By inclusion or variation of the degrader and by varying the air gap between exit window and DUT, the LET in Silicon can be tuned from approx. 26.5 MeV cm²/mg to 64.3 MeV cm²/mg and the corresponding ranges of the ions in Silicon go from 685 μm to 35 μm over that LET range.

DUT aligned is done with the help of a laser system.

Figure 21: Test setup at GANIL. Ion LETs can be set by variation of the degrader and the air gap.



7.2 Beam parameters

The resulting total energies of the respective ions, as well as their LET and range in Silicon are provided by GANIL [13]. However this data is not valid for Silicon Carbide.

SRIM 2013 [10] simulations by Fraunhofer INT in Table 17 show the respective values for the Xenon beam provided by GANIL under normal incidence in Silicon Carbide covered by a 10 μm Paralene layer with the air gap and degrader settings used in the experiments. For comparison, the values in Silicon provided by GANIL are included in the table. The devices used for these tests were de-lidded, so packages were not included in the simulations.

Table 17: GANIL: Beam characteristics. Values in Silicon are provided by GANIL [13], Values in SiC are calculated by INT

Degrader [mm Al]	Air gap [mm]	LET (Si) (MeV.cm ² /mg)	Range (Si) [μm]	LET _{SURF} (SiC) [MeV.cm ² /mg]	Range (SiC) [μm]
0	150	27.76	640.33	29.2	430
0.4	95	42.03	226.23	47.2	141
0.5	180	60.12	65.68	72.9	30

7.3 Geometry

The board is attached to the moveable board holder (Figure 21). Tests are then performed in air.

7.4 Irradiation steps

The tests at GANIL with the IJW120R100T1 were performed near the end of the beam time and only limited data could be taken.

Table 18: GANIL: Irradiation steps of SiC JFET IJW120R100T1. Numbers indicate the DUT serial number from Table 4. Table cells without numbers indicate that no run was performed under these conditions. Green or red background color indicate PASS or FAIL respectively. If a DUT fails at some voltage, all higher voltages are also indicated as fail. Yellow color (if applicable) indicates mixed results (e.g. 1 DUT passing, 1 DUT failing at the same level) or non-conclusive results with the device showing some damage not clearly attributable to a fail.

		Xe, 0 mm Al, 150 mm Air		Xe, 0.4 mm Al, 95 mm Air		Xe, 0.5 mm Al, 180 mm Air	
V_DS [V]	V_GS [V]	in-situ	PIGS	in-situ	PIGS	in-situ	PIGS
300	-14.5	25	25				
400		25	25				

The log file of the tests performed at GANIL can be found in Appendix D. Table 18 shows an overview over the test indicating pass and fail results. A detailed evaluation of the results is shown in Section 7.5.

7.5 Results

Only two tests at the minimal gate voltage to achieve an off-mode operation were performed. No effect was observed at $V_{DS} = 300$ V, but a very pronounced degradation over nearly two orders of magnitude was found at 400 V.

Figure 22: Results: Heavy Ions at GANIL. The cross section results for various settings of V_{DS} . Filled symbols mark the cross section in case of device failures and error bars mark the upper lower limits. Open symbols mark the cross section upper limit in case no failure was observed during a run.

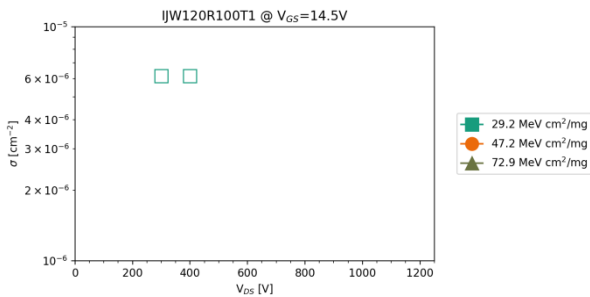


Table 19: Results: Heavy Ions at GANIL - Calculated cross sections Calculated with the formulae in ESCC25100 with $CL=0.95$ and flux uncertainty of 10% (approx. worst case)

#	Ion	Al [μm]	Air [mm]	DUT #	V_{DS} , V	V_{GS}	Failure fluence [cm^{-2}]	σ lower [cm^2]	σ [cm ²]	σ upper [cm ²]	Effect	Comment
147	Xe	0	150	25	300	-14.5	6.00E+05	0	0	6.15E-06	--	--
148	Xe	0	150	25	400	-14.5	6.00E+05	0	0	6.15E-06	Degr.	Pronounced degradation (nearly 2 orders of magnitude) counted as FAIL. No single destructive event. Clear failure at PIGS test.

8 Tests at CERN

8.1 Facility

Tests at CERN took place at the H8 beam line [14] from the T4 target of the SPS North Experimental Area with a Xenon beam of 30 or 40 GeV/n. The opportunity to test at this beam line was given in a joint effort from ESA and CERN [15].

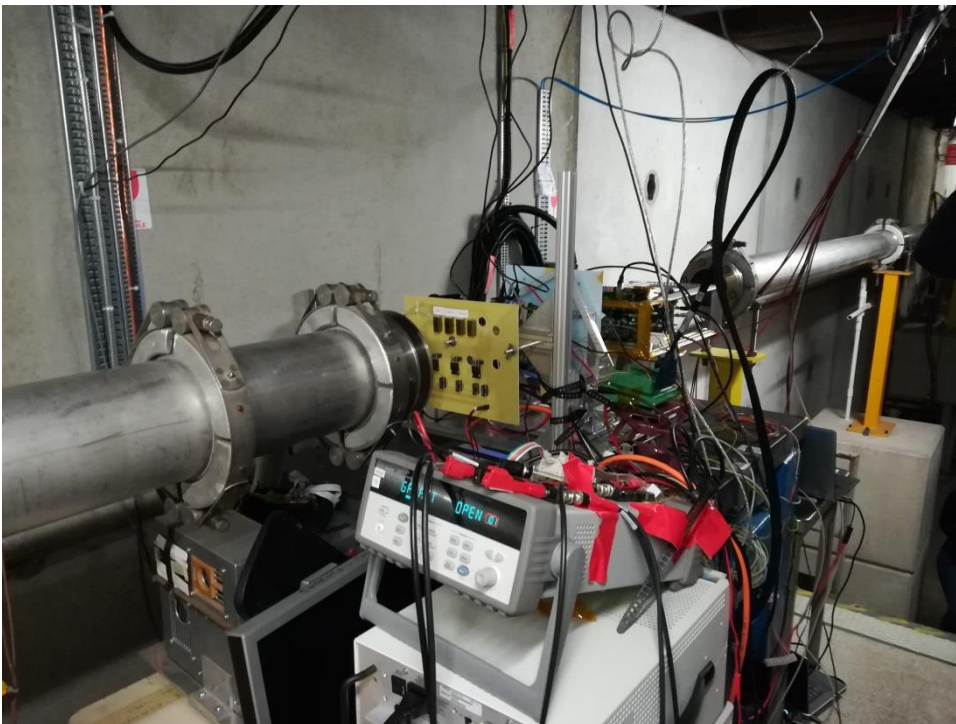
The ion beam is ultra-energetic and thus highly penetrating, which has several practical advantages for testing:

- The test can take place in air
- The DUTs do not need to be de-lidded
- Multiple test boards can be placed successively in the beam.

The INT test board was positioned first in line during all the tests, so energy reduction and thus LET modifications by other boards in the beam line does not occur.

The test site is not specifically intended for SEE tests of electronics, therefore additional infrastructure like a moveable frame holder are not installed.

Figure 23: Beam line and irradiation site at the H8 beam line, CERN.



8.2 Beam parameters

The beam was delivered in spills of approx. 8 s length at an interval of 30 – 50 s [15][16]. While the time-average flux is thus relatively low in the range of $1 - 2 \cdot 10^3$ ions/(cm²·s), the actual flux during the spill time is much higher.

The dosimetry on-site was recorded by CERN and preliminarily available during the campaign. The translation from the dosimeter readout to the actual particle flux and fluence was available after the campaign [16].

The total fluences given in Appendix E are based on the timestamps of the individual runs and the dosimetry information provided by CERN. Most device failures occurred at the first spill of beam. Properly deducing the fluence of failure and thus the cross sections of the devices is not possible in these cases, so the cross sections in case of failures given in Section 8.5 should only be seen as a rough order of magnitude.

The calculation of the LET for particles of these energies cannot be done easily e.g. with SRIM due to the interactions with matter at these energies. The LET values for silicon were simulated with FLUKA by Rubén García Alía et al. and reported [15]. There different LET values were considered, one unrestricted value taking into account all ionization caused by the beam (approx. 6.3 MeV cm²/mg) and a volume-restricted value covering the area of a 9.3 MeV/n Silicon particle track (approx. 3.7 MeV cm²/mg). Comparisons with the ESA SEU [15] indicate that the volume-restricted LET is a more proper expression for the particle LET in Silicon.

We adopt the LET value of 3.7 MeV cm²/mg for our tests although these were determined in Silicon and we would require the value in SiC. While we cannot show or prove this assumption here, indicative simulations with SRIM using 10 GeV/n Xenon ions (maximum possible energy) are shown in the Appendix E.1.

8.3 Geometry

The test board was attached to a frame holder on a motor unit, allowing to shift the board along one axis. Three DUTs could be installed on the board and irradiated separately. For the PIGS or POST tests, the DUTs were moved out of the beam, which ran continuously except when installing new DUTs.

The beam was incident normally on the DUTs.

8.4 Irradiation steps

Table 20: CERN: Irradiation steps of SiC JFET IJW120R100T1. Numbers indicate the DUT serial number from Table 4. Table cells without numbers indicate that no run was performed under these conditions. Green or red background color indicate PASS or FAIL respectively. If a DUT fails at some voltage, all higher voltages are also indicated as fail. Yellow color (if applicable) indicates mixed results (e.g. 1 DUT passing, 1 DUT failing at the same level) or non-conclusive results with the device showing some damage not clearly attributable to a fail.

V_DS [V]	V_GS [V]	Xe, 0°		Xe, 45°	
		in-situ	PIGS	in-situ	PIGS
1200	-14.5	1			
1200		1			
1250	-19.5	1			
1300		1			

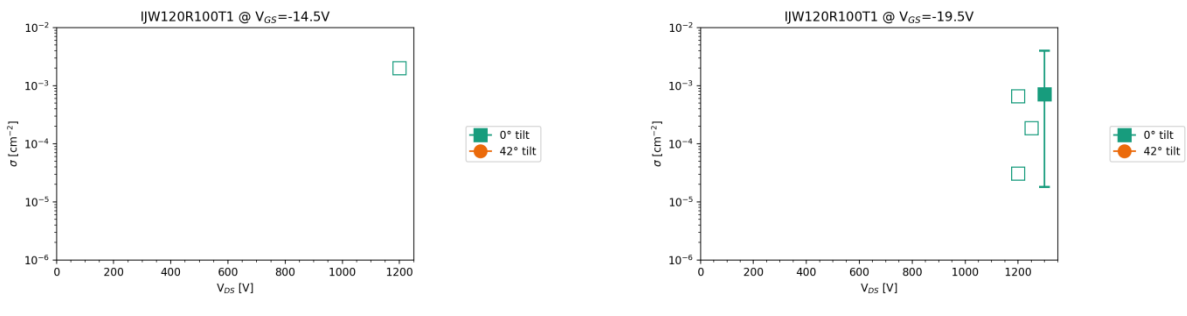
8.5 Results

The tests with the IJW120R100T1 at CERN did not show any destructive failures at the maximum rating of 1200 V. A destructive failure was only observed when the device was operated out of specs at 1300 V. As testing mostly took place at the maximum rated voltage, PIGS tests were not performed.

A striking difference to the previous tests is the increased voltage of safe operation of above 1200 V. This value was 900 V with the lowest LET at UCL and 1050 V with protons. With protons however, this attribution was made because 1 out of 3 DUTs failed at 1200 V.

Tests at CERN were performed with a DUT from the same lot as the previous tests, so lot-to-lot variability could not be an explanation for this difference, but when looking at the proton results, part-to-part variability could be an option, especially since this was not confirmed with a second device.

Figure 24: Results: Heavy Ions at CERN. The cross section results for various settings of V_{DS} . Filled symbols mark the cross section in case of device failures and error bars mark the upper lower limits. Open symbols mark the cross section upper limit in case no failure was observed during a run.



The effective fluences across the tests were $< 1.2E5$ ions/cm². The low fluence might be an explanation for the increased “safe operation” levels observed in these tests compared to the other test campaigns.

Table 21: Results: Heavy Ions at CERN - Calculated cross sections Calculated with the formulae in ESCC25100 with $CL=0.95$ and flux uncertainty of 10% (approx. worst case)

#	Ion	Tilt [°]	DUT #	V_DS, V	V_GS	Failure fluence [cm-2]	σ lower [cm2]	σ [cm2]	σ upper [cm2]	Effect	Comment
012	Xe	0	1	1200	-14.5	1.85E+03	0	0	2.00E-03	--	
013	Xe	0	1	1200	-19.5	5.64E+03	0	0	6.54E-04	--	
014	Xe	0	1	1200	-19.5	1.20E+05	0	0	3.07E-05	--	Settings and DUT identical to run #13
015	Xe	0	1	1250	-19.5	2.00E+04	0	0	1.84E-04	--	Gate current briefly goes from ~4E-6A to negative 0.5E-6A. Recovers after a few seconds.
016	Xe	0	1	1300	-19.5	1.40E+03	1.81E-05	7.14E-04	3.98E-03	SEGR / SEB	Destructive failure of the gate and drain simultaneously. Low test fluence.

A Fraunhofer INT

A.1. About the institute

The Fraunhofer Institute for Technological Trend Analysis INT provides scientifically sound assessments and counselling on the entire spectrum of technological developments. On this basis, the Institute conducts Technology Forecasting, making possible a long-term approach to strategic research planning. Fraunhofer INT constantly applies this competence in projects tailor-made for our clients.

Over and above these skills, we run our own experimental and theoretical research on the effects of ionizing and electromagnetic radiation on electronic components, as well as on radiation detection systems. To this end, INT is equipped with the latest measurement technology. Our main laboratory and large-scale appliances are radiation sources, electromagnetic simulation facilities and detector systems that cannot be found in this combination in any other civilian body in Germany.

For more than 40 years, INT has been a reliable partner for the Federal German Ministry of Defence, which it advises in close cooperation and for which it carries out research in technology analysis and strategic planning as well as radiation effects. INT also successfully advises and conducts research for domestic and international civilian clients: both public bodies and industry, from SMEs to DAX 30 companies.

Further information can be found on the website [1].

A.2. Business unit Nuclear Effects in Electronics and Optics

The Business Unit „Nuclear Effects in Electronic and Optics (NEO)“ at Fraunhofer INT investigates the effects of ionizing radiation on electronic, optoelectronic, and photonic components and systems. Its work is based on more than 40 years of experience in that field.

NEO performs irradiation tests based on international standards and advises companies regarding radiation qualification and hardening of components and systems. The knowledge obtained in years of radiation testing is also used for the development of new radiation sensor systems. These activities are performed either at irradiation facilities installed at INT or at partner institutions to which our scientists have regular access.

A multitude of modern equipment to measure electrical and optical parameters is available. Furthermore our institute runs a precision mechanical workshop and an electronic laboratory. This enables us to conduct most of the irradiation tests without help or equipment of the customer.

The activities within NEO are:

- Investigations of the effects in all kinds of radiation environments
- Performance, analysis, and evaluation of irradiation tests done at Fraunhofer INT and external facilities

- Ensuring the operability of components and systems in typical radiation environments, such as space, nuclear facilities, medicine, or accelerators
- Consulting users and manufacturers on the use of products in radiation environments by selecting, optimizing and hardening
- Measurement of the radiation effects on optical fibers and fiber Bragg gratings (FBG)
- Development of radiation sensors based on optical fibers, FBGs, oscillating crystals, UV-EPROMs, and SRAMs
- Participation in the development of international test procedures for IEC, IEEE, NATO, and IAEA
- Since 2013 all services of the business unit are certified according to ISO 9001

A.3. Irradiation facilities

Fraunhofer INT operates several irradiation facilities on site that are dedicated to perform irradiation tests. For that purpose the design and operation characteristics are highly optimised from many decades of experience and to comply with all relevant standards and test procedures.

Furthermore Fraunhofer INT accesses regularly external facilities, partly with dedicated irradiation spots for exclusive use to Fraunhofer INT.

These irradiation facilities are:

- Co-60 irradiation sources on site to simulate the effect of total dose
- Neutron generators on site to simulate the displacement damage of heavy particles
- 450 keV X-ray irradiation facility on site
- Laser induced single event test system on site
- Dedicated proton irradiation spot at the injector cyclotron of FZ Jülich to simulate the effects of solar and trapped protons
- External Co-60 irradiation sources for high dose and high dose rate irradiations

The facilities used in the context of this work will be described in detail in the following sections.

A.4. QM-Certificate



MANAGEMENT SYSTEM CERTIFICATE

Certificate No: 126306-2012-AQ-GER-DAKKS	Initial certification date: 13. February 2013	Valid: 14. February 2019 - 12. February 2022
---	--	---

This is to certify that the management system of



**Fraunhofer-Institut für
Naturwissenschaftlich-Technische
Trendanalysen INT**

Appelsgarten 2, 53879 Euskirchen, Germany

has been found to conform to the Quality Management System standard:

ISO 9001:2015


This certificate is valid for the following scope:

**Scientific research on the effects of nuclear and electromagnetic radiation
as well as application and development of methods for their characterization**

Place and date:
Essen, 14. February 2019



For the issuing office:
DNV GL - Business Assurance
Schnieringshof 14, 45329 Essen, Germany


Thomas Beck
Technical Manager

Lack of fulfillment of conditions as set out in the Certification Agreement may render this Certificate invalid.
ACCREDITED UNIT: DNV GL Business Assurance Zertifizierung und Umweltgutachter GmbH, Schnieringshof 14, 45329 Essen, Germany.
TEL: +49 201 7296-222. www.dnvgl.de/assurance

B Appendix: Tests at UCL

B.1. Logfile / Test steps

In case of device failure the fluences in this table indicate the fluence provided by the facility not the fluence until failure which may differ by some additional seconds of beam.

#	Run (UCL)	Date	Time	Ion	Device Type	Device	Position on board	DUT #	V_DS, V	V_GS	beam time [s]	fluence [cm-2]
35	45	16.4.	21:17	Al	MOSFET	IJW120R100T1	#1	11	600	-14.5	57	2.67E+05
36	46	16.4.	21:23	Al	MOSFET	IJW120R100T1	#2	12	600	-14.5	19	1.49E+04
37	47	16.4.	21:40	Al	MOSFET	IJW120R100T1	#3	13	600	-14.5	48	5.93E+03
38	48	16.4.	22:08	C	MOSFET	IJW120R100T1	#1	14	600	-14.5	381	3.02E+05
39	49	16.4.	22:18	C	MOSFET	IJW120R100T1	#1	14	750	-14.5	151	3.04E+05
40	50	16.4.	22:22	C	MOSFET	IJW120R100T1	#1	14	900	-14.5	151	3.04E+05
41	51	16.4	22:26	C	MOSFET	IJW120R100T1	#1	14	1050	-14.5	27	5.49E+04
42	52	16.4.	22:35	C	MOSFET	IJW120R100T1	#2	15	900	-14.5	153	3.03E+05
43	53	16.4.	22:40	C	MOSFET	IJW120R100T1	#2	15	900	-19.5	156	3.03E+05
44	54	16.4.	22:45	C	MOSFET	IJW120R100T1	#3	16	900	-19.5	157	3.04E+05
45	55	16.4.	23:04	Ne	MOSFET	IJW120R100T1	#1	17	400	-14.5	156	3.04E+05
46	56	16.4.	23:08	Ne	MOSFET	IJW120R100T1	#1	17	600	-14.5	156	3.03E+05
47	57	16.4.	23:12	Ne	MOSFET	IJW120R100T1	#1	17	750	-14.5	8	1.29E+04
48	58	16.4.	23:15	Ne	MOSFET	IJW120R100T1	#2	15	600	-14.5	47	9.60E+04
49	59	16.4.	23:24	Ne	MOSFET	IJW120R100T1	#3	16	500	-14.5	152	3.03E+05
50	60	16.4.	23:36	Ne	MOSFET	IJW120R100T1	#3	16	550	-14.5	152	3.04E+05
51	61	16.4.	23:41	Ne	MOSFET	IJW120R100T1	#3	16	550	-19.5	153	3.02E+05
52	62	16.4.	23:46	Ne	MOSFET	IJW120R100T1	#3	16	600	-14.5	173	9.24E+04
53	63	16.04.	0:20	Al	MOSFET	IJW120R100T1	#1	18	400	-14.5	296	3.01E+05
54	64	16.04.	0:29	Al	MOSFET	IJW120R100T1	#2	20	500	-14.5	311	3.02E+05
55	65	16.04.	0:38	Al	MOSFET	IJW120R100T1	#1	18	500	-14.5	122	1.27E+05
56	66	16.04.	0:43	Al	MOSFET	IJW120R100T1	#3	22	400	-14.5	152	3.04E+05
57	67	16.04.	0:50	Al	MOSFET	IJW120R100T1	#2	20	400	-14.5	149	3.02E+05
58	68	16.04.	0:58	Al	MOSFET	IJW120R100T1	#3	22	400	-19.5	150	3.02E+05
59	69	16.04.	1:05	Al	MOSFET	IJW120R100T1	#3	22	450	-14.5	279	3.01E+05
60	70	16.04.	1:12	Al	MOSFET	IJW120R100T1	#3	22	450	-19.5	301	3.02E+05

B.2. Measurements

Figure 25: Run# 035, IJW120R100T1, Al-250, $2.7e+05$ ions/cm², DUT 11, $V_{DS}= 600.0$ V, $V_{GS}= -14.5$ V

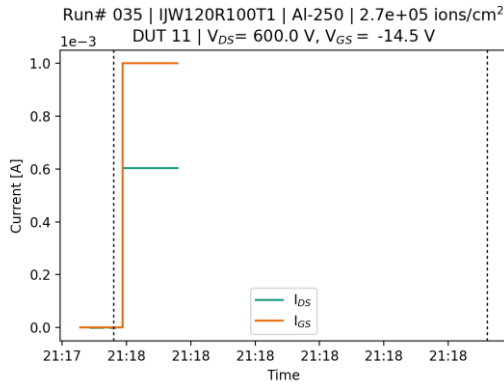


Figure 26: Run# 036, IJW120R100T1, Al-250, $1.5e+04$ ions/cm², DUT 12, $V_{DS}= 600.0$ V, $V_{GS}= -14.5$ V

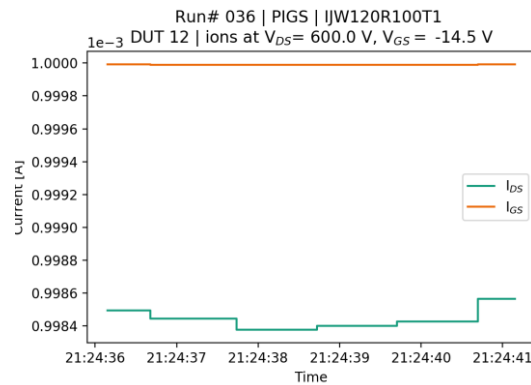
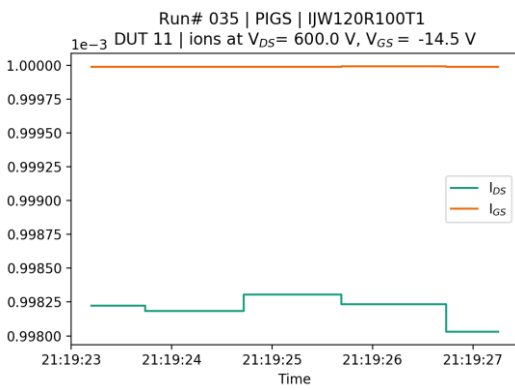
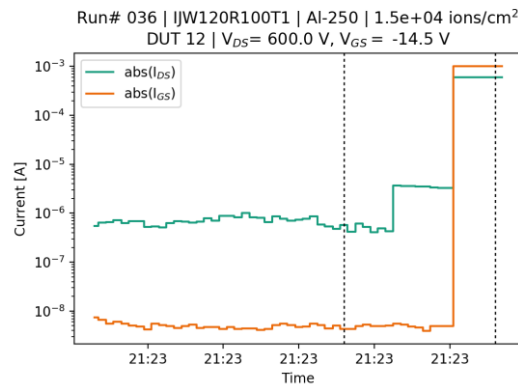
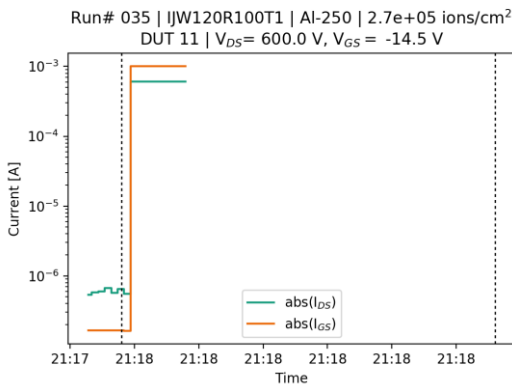
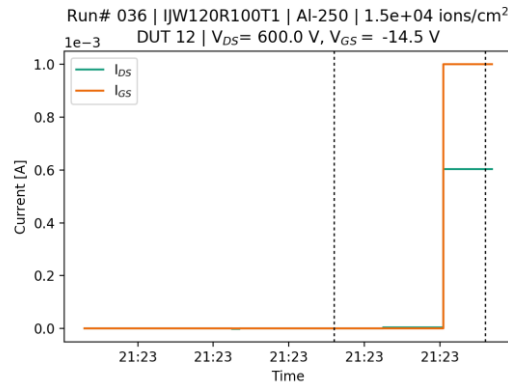


Figure 27: Run# 037, IJW120R100T1, Al-250, $5.9e+03$ ions/cm², DUT 13, VDS= 600.0 V, VGS= -14.5 V

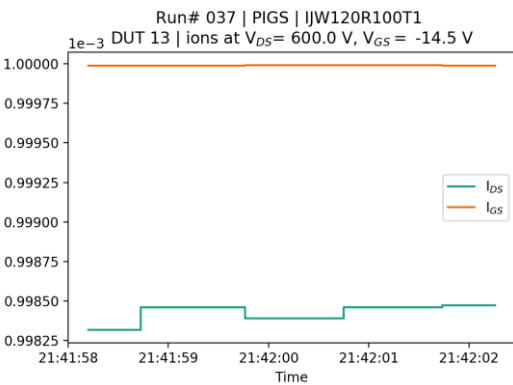
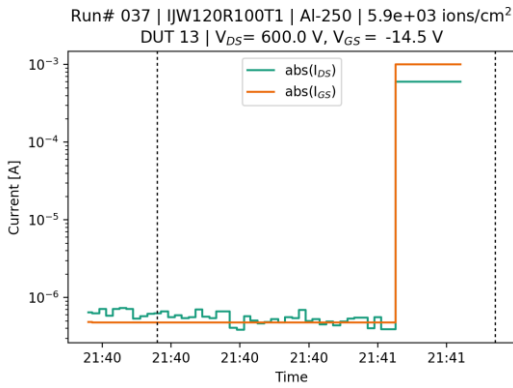
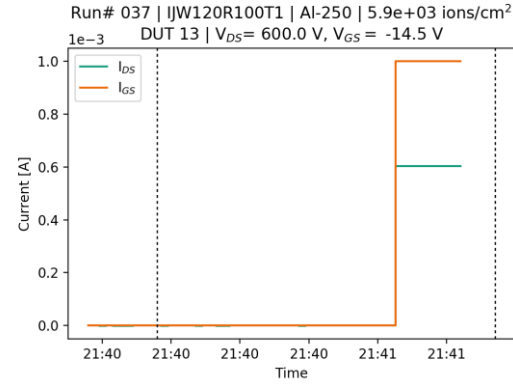


Figure 28: Run# 038, IJW120R100T1, C-131, $3.0e+05$ ions/cm², DUT 14, VDS= 600.0 V, VGS= -14.5 V

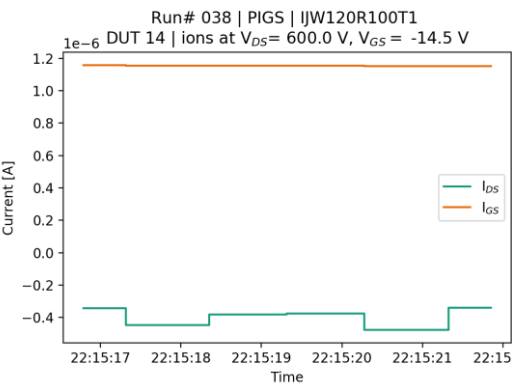
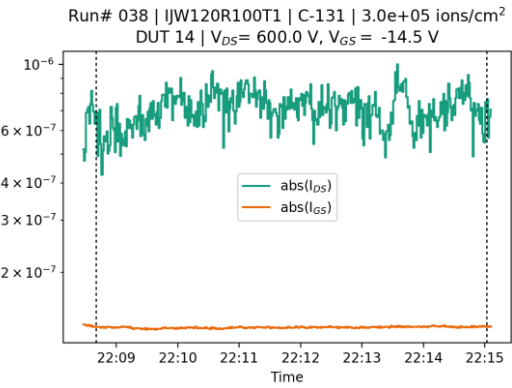
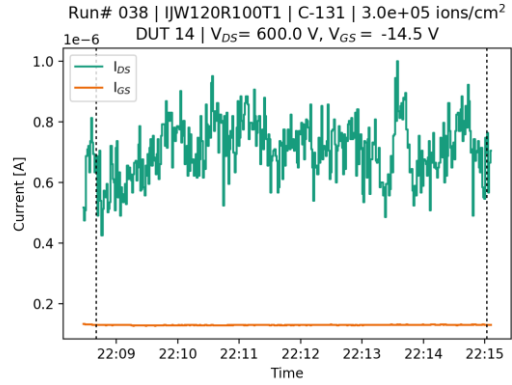


Figure 29: Run# 039, IJW120R100T1, C-131, $3.0e+05$ ions/cm², DUT 14, V_{DS}= 750.0 V, V_{GS}= -14.5 V

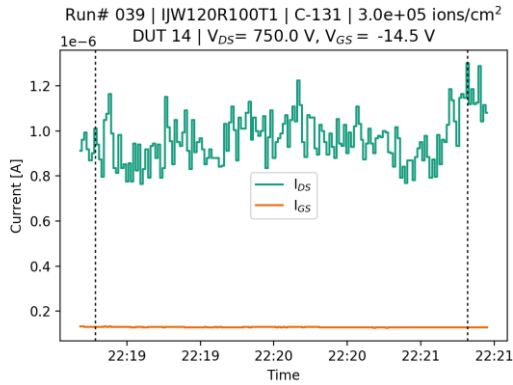


Figure 30: Run# 040, IJW120R100T1, C-131, $3.0e+05$ ions/cm², DUT 14, V_{DS}= 900.0 V, V_{GS}= -14.5 V

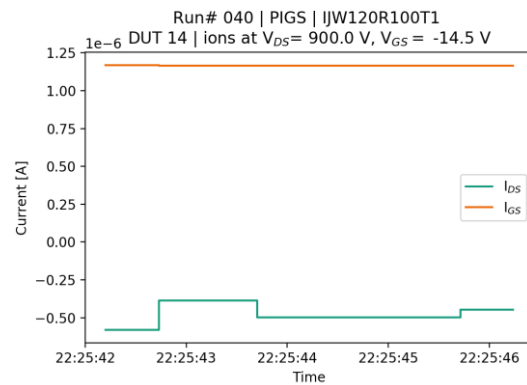
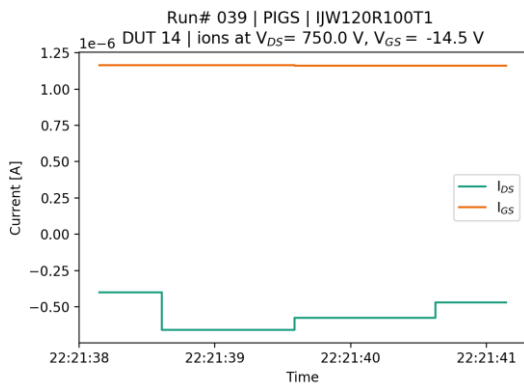
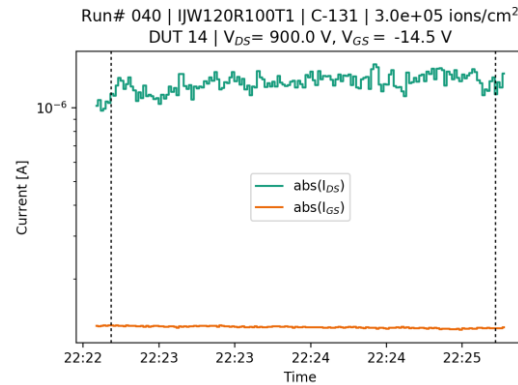
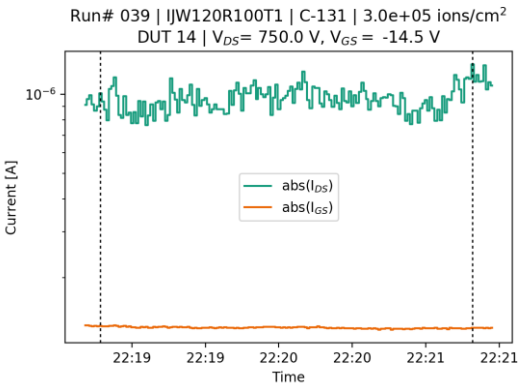
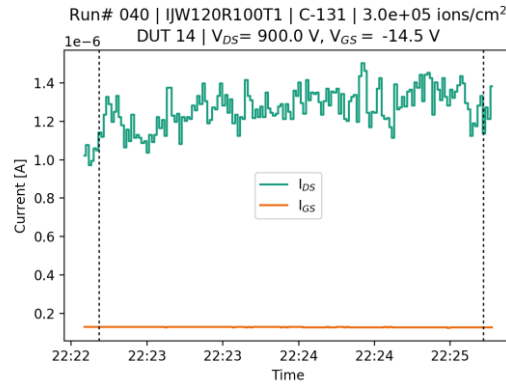


Figure 31: Run# 041, IJW120R100T1, C-131, $5.5e+04$ ions/cm², DUT 14, VDS= 1050.0 V, VGS= -14.5 V

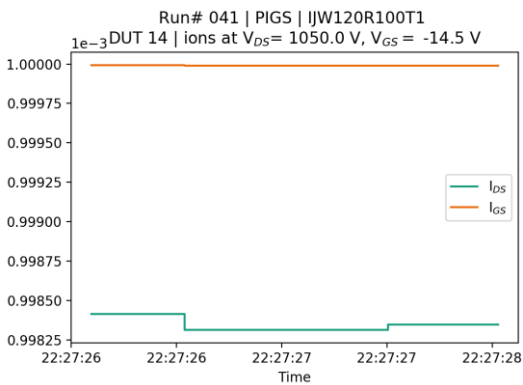
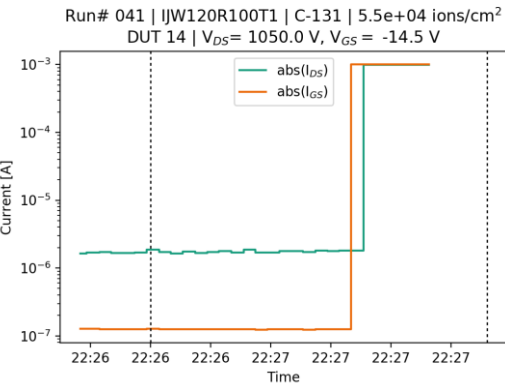
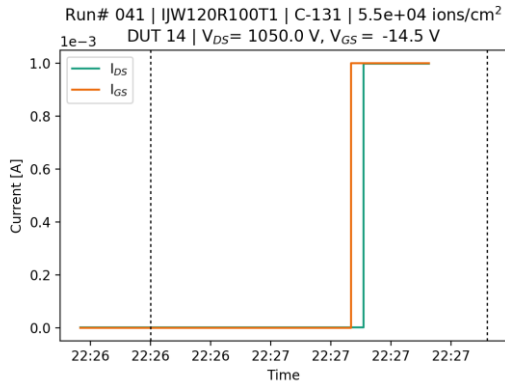


Figure 32: Run# 042, IJW120R100T1, C-131, $3.0e+05$ ions/cm², DUT 15, VDS= 900.0 V, VGS= -14.5 V

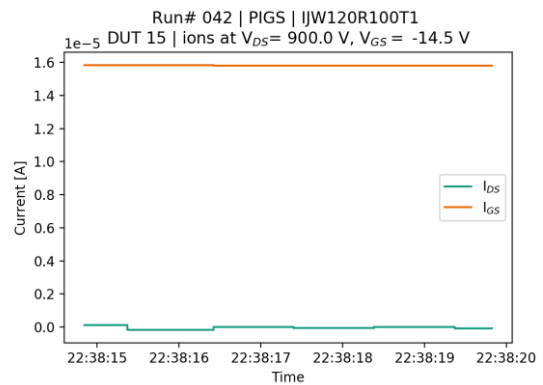
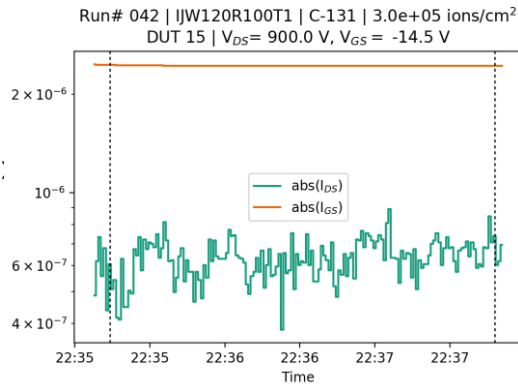
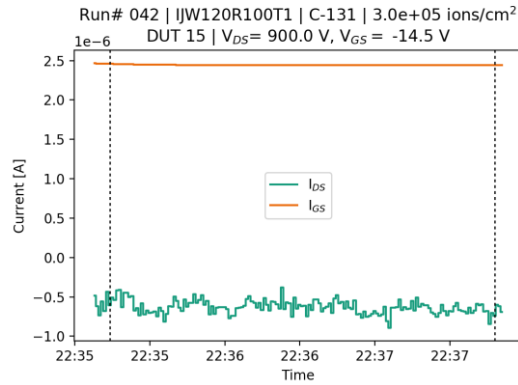


Figure 33: Run# 043, IJW120R100T1, C-131, $3.0e+05$ ions/cm², DUT 15, VDS= 900.0 V, VGS= -19.5 V

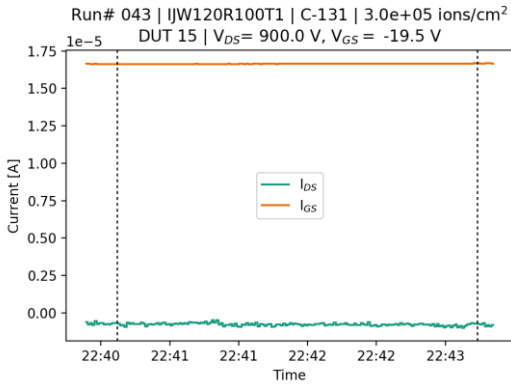


Figure 34: Run# 044, IJW120R100T1, C-131, $3.0e+05$ ions/cm², DUT 16, VDS= 900.0 V, VGS= -19.5 V

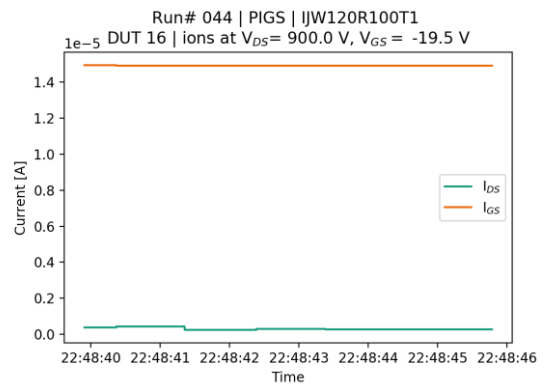
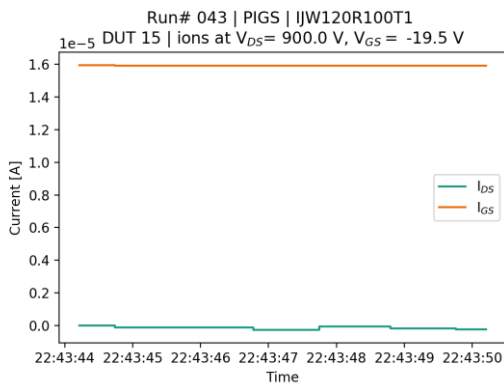
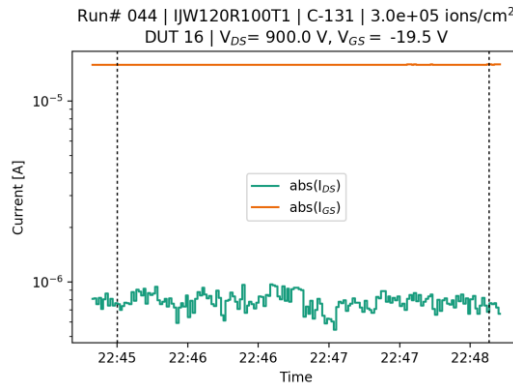
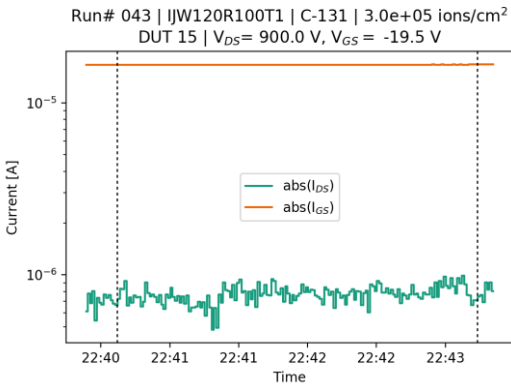
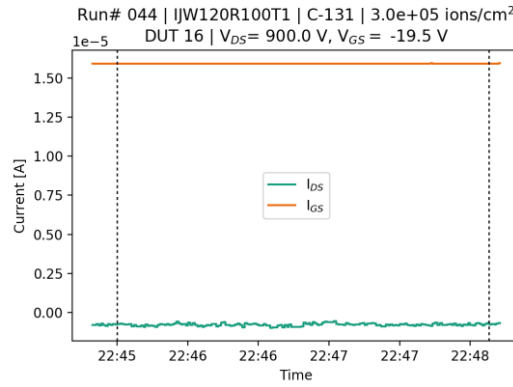


Figure 35: Run# 045, IJW120R100T1, Ne-238, $3.0e+05$ ions/cm², DUT 17, V_{DS}= 400.0 V, V_{GS}= -14.5 V

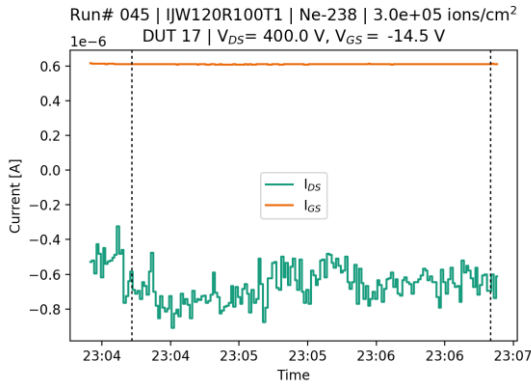


Figure 36: Run# 046, IJW120R100T1, Ne-238, $3.0e+05$ ions/cm², DUT 17, V_{DS}= 600.0 V, V_{GS}= -14.5 V

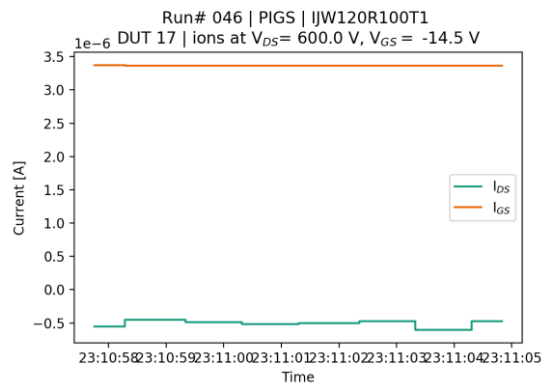
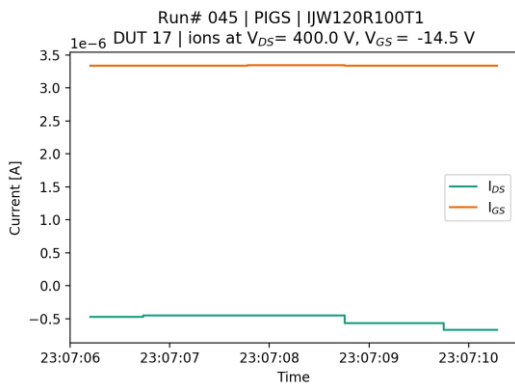
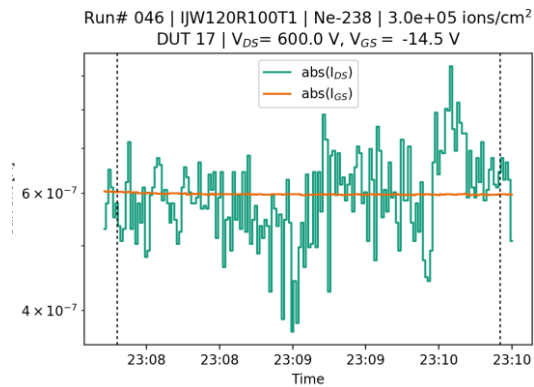
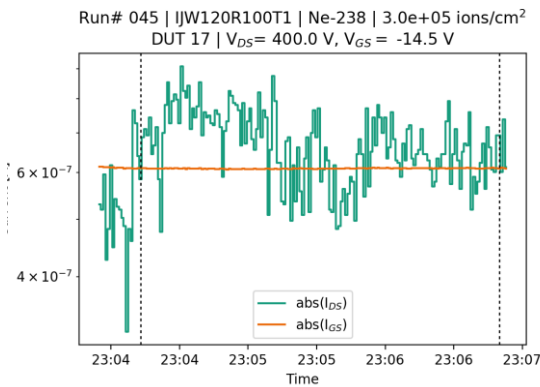
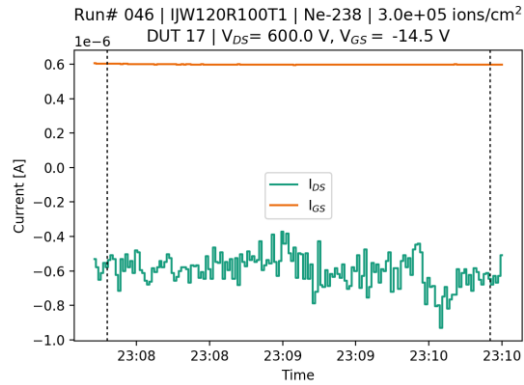


Figure 37: Run# 047, IJW120R100T1, Ne-238, $1.3e+04$ ions/cm², DUT 17, V_{DS}= 750.0 V, V_{GS}= -14.5 V

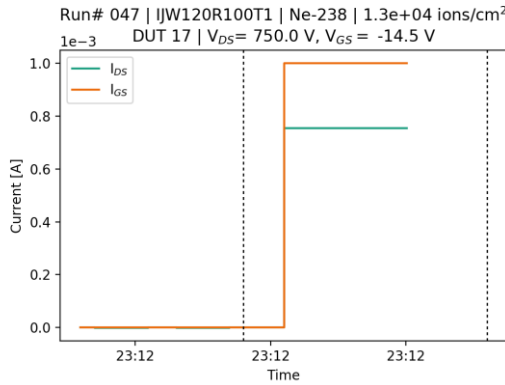


Figure 38: Run# 048, IJW120R100T1, Ne-238, $9.6e+04$ ions/cm², DUT 15, V_{DS}= 600.0 V, V_{GS}= -14.5 V

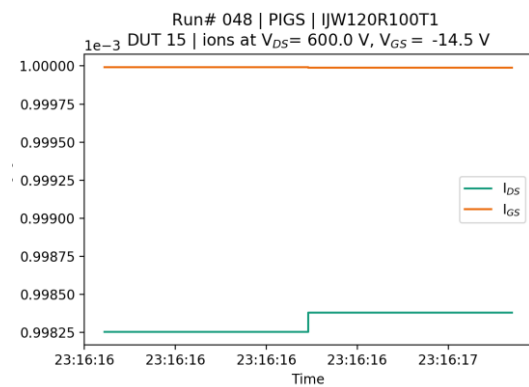
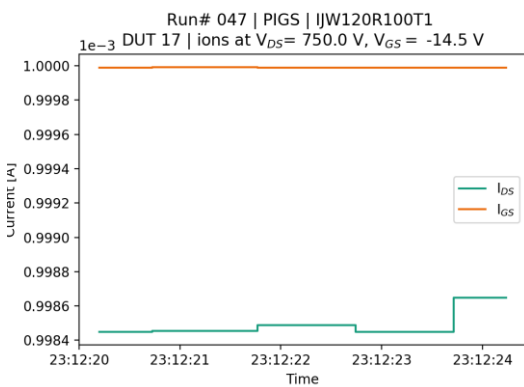
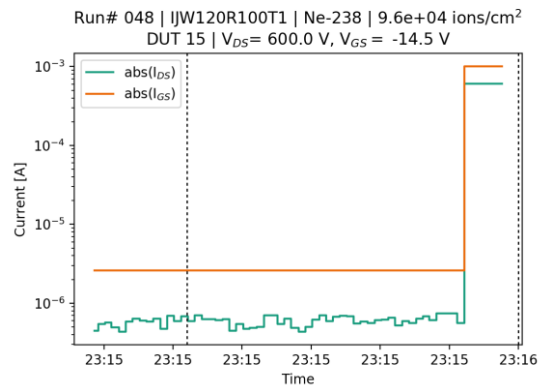
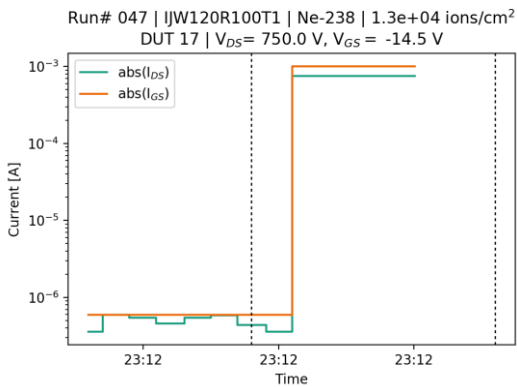
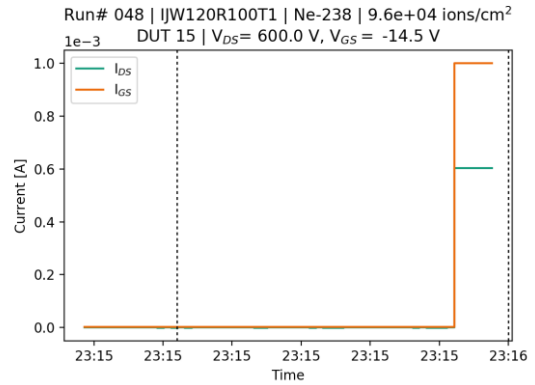


Figure 39: Run# 049, IJW120R100T1, Ne-238, $3.0e+05$ ions/cm², DUT 16, VDS= 500.0 V, VGS= -14.5 V

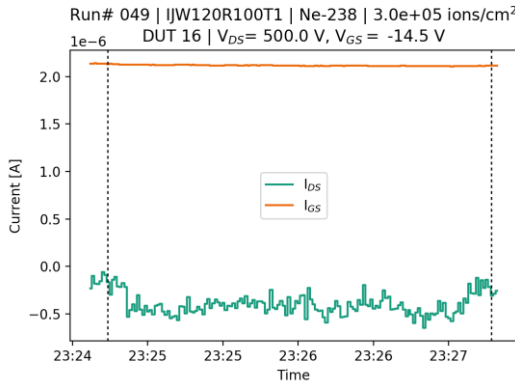


Figure 40: Run# 050, IJW120R100T1, Ne-238, $3.0e+05$ ions/cm², DUT 16, VDS= 550.0 V, VGS= -14.5 V

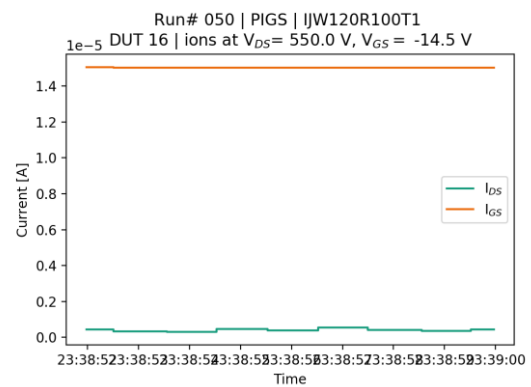
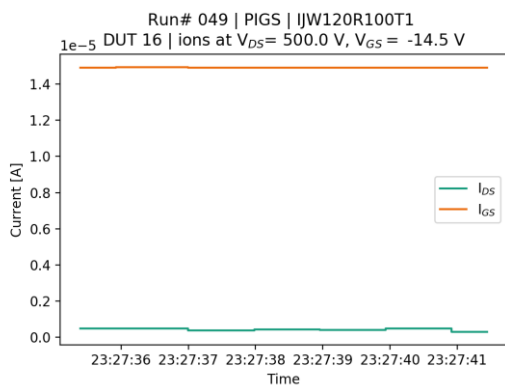
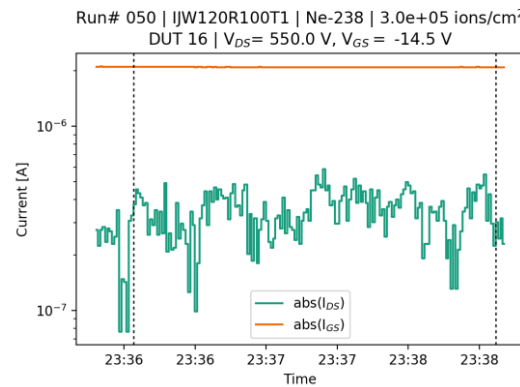
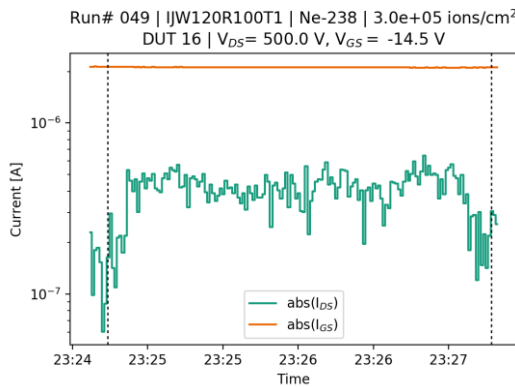
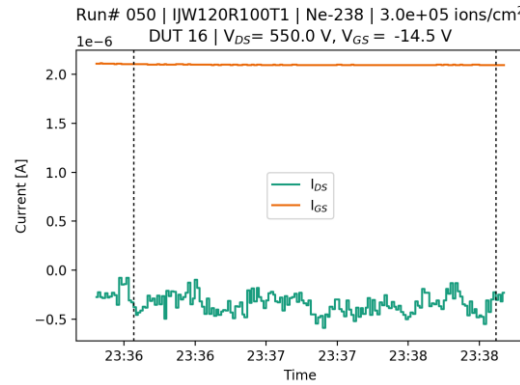


Figure 41: Run# 051, IJW120R100T1, Ne-238, $3.0e+05$ ions/cm², DUT 16, V_{DS}= 550.0 V, V_{GS}= -19.5 V

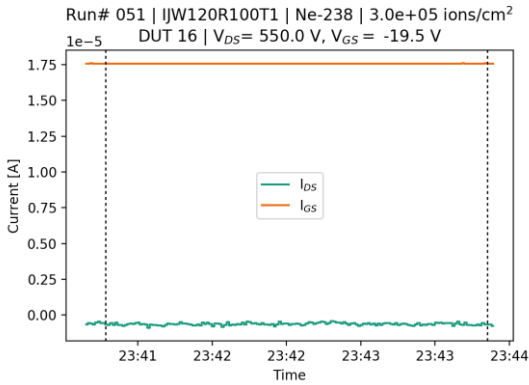


Figure 42: Run# 052, IJW120R100T1, Ne-238, $9.2e+04$ ions/cm², DUT 16, V_{DS}= 600.0 V, V_{GS}= -14.5 V

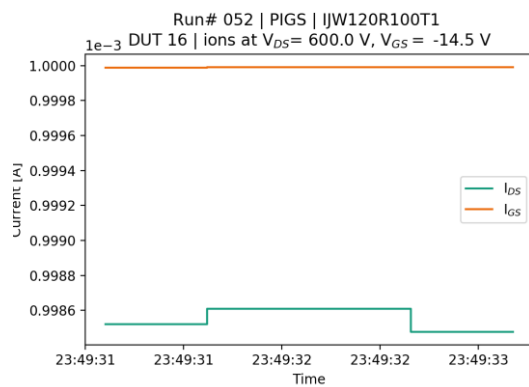
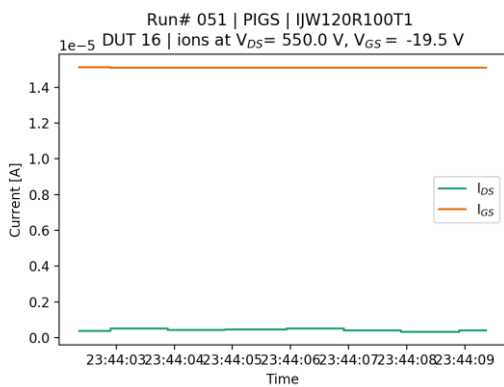
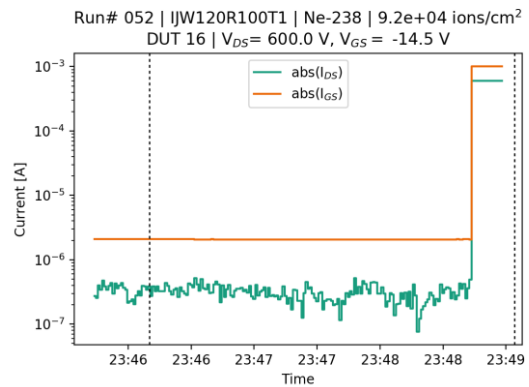
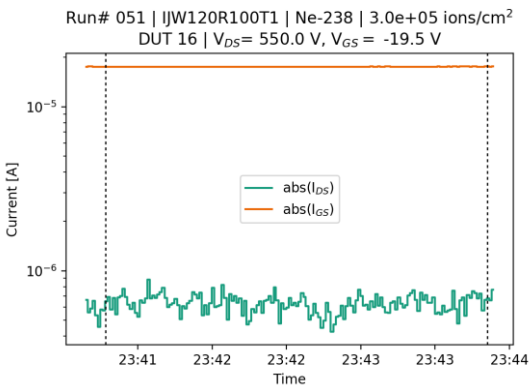
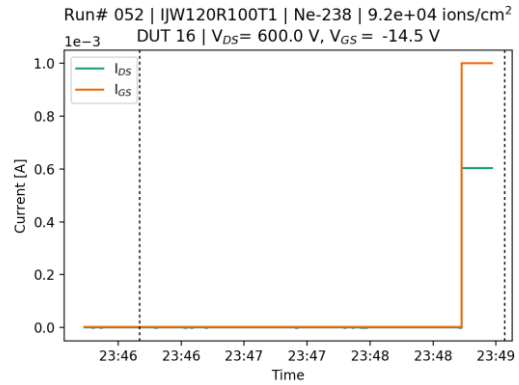


Figure 43: Run# 053, IJW120R100T1, Al-250, 3.0e+05 ions/cm², DUT 18, V_{DS}= 400.0 V, V_{GS}= -14.5 V

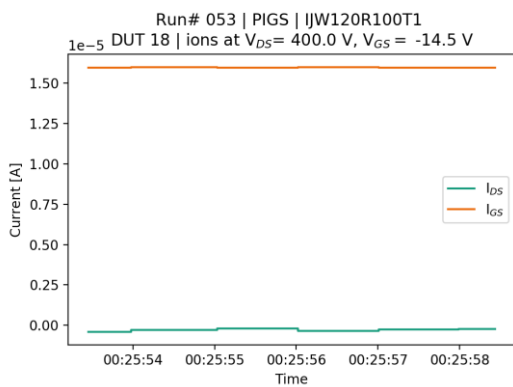
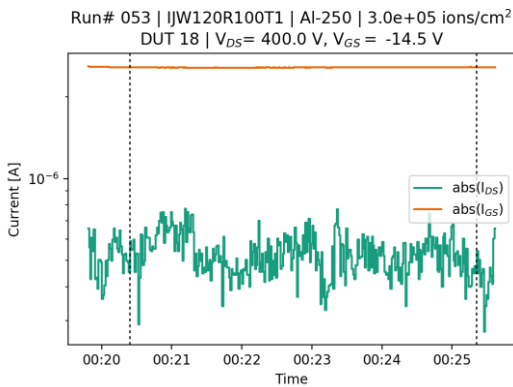
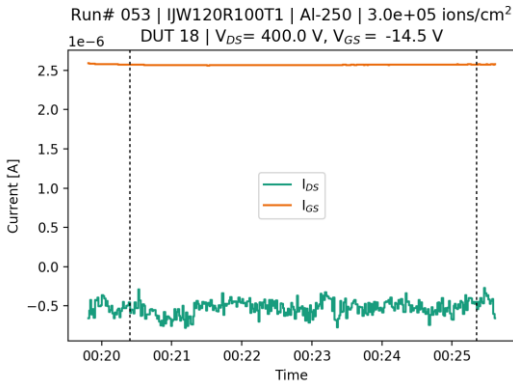


Figure 44: Run# 054, IJW120R100T1, Al-250, 3.0e+05 ions/cm², DUT 20, V_{DS}= 500.0 V, V_{GS}= -14.5 V

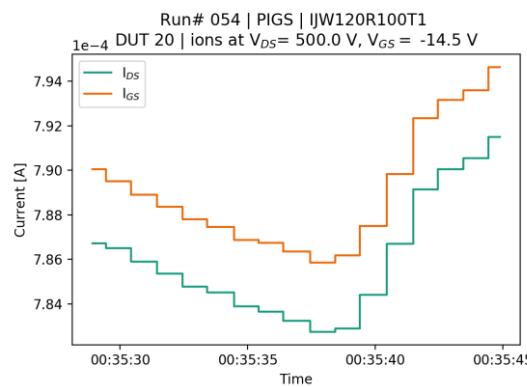
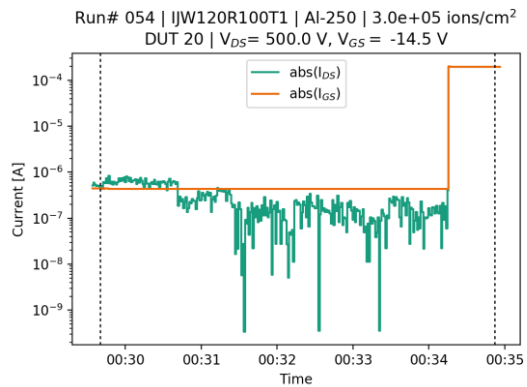
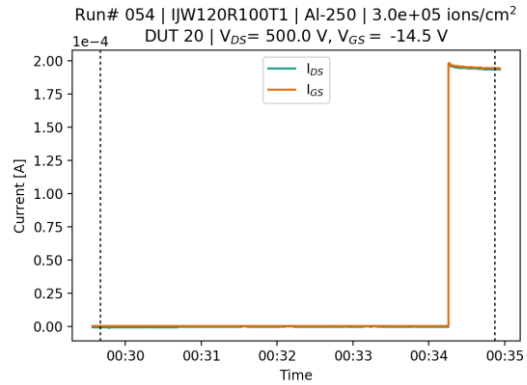


Figure 45: Run# 055, IJW120R100T1, Al-250, $1.3e+05$ ions/cm², DUT 18, VDS= 500.0 V, VGS= -14.5 V

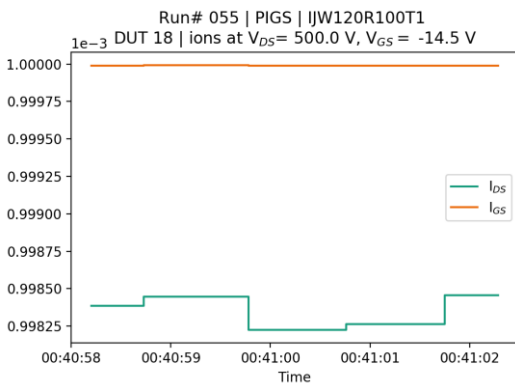
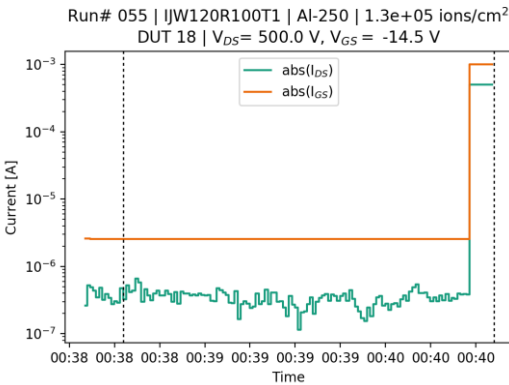
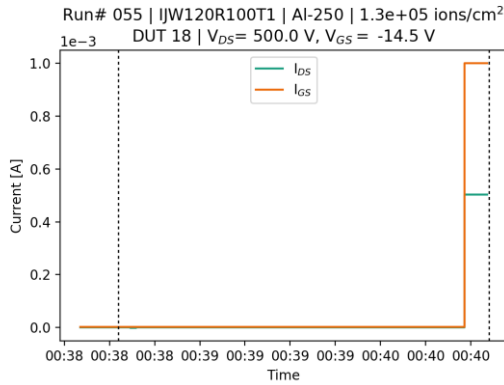


Figure 46: Run# 056, IJW120R100T1, Al-250, $3.0e+05$ ions/cm², DUT 22, VDS= 400.0 V, VGS= -14.5 V

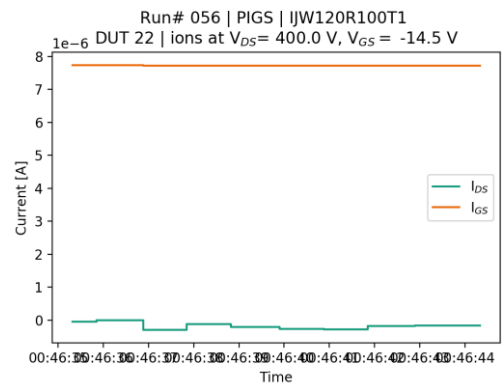
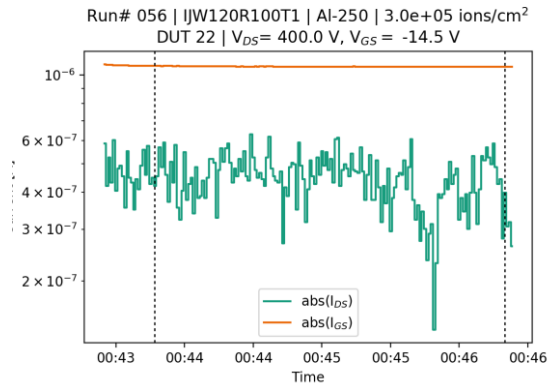
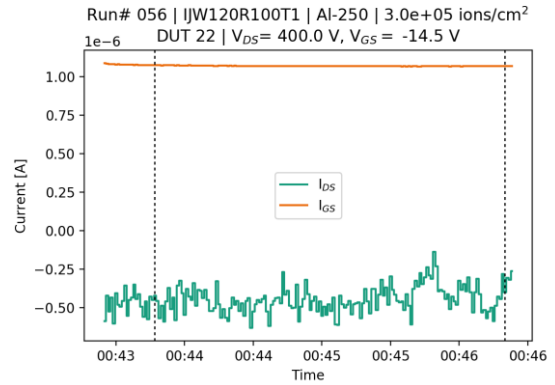
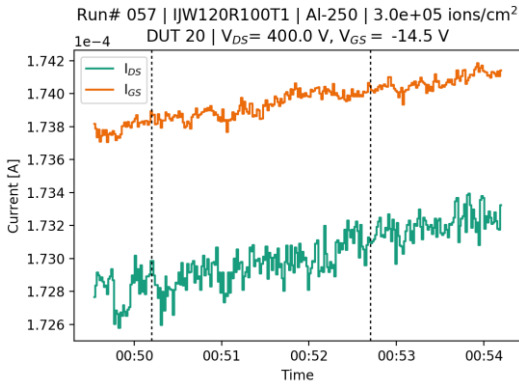


Figure 47: Run# 057, IJW120R100T1, Al-250, 3.0e+05 ions/cm², DUT 20, V_{DS}= 400.0 V, V_{GS}= -14.5 V



Run# 057 | IJW120R100T1 | Al-250 | 3.0e+05 ions/cm²
DUT 20 | V_{DS}= 400.0 V, V_{GS}= -14.5 V

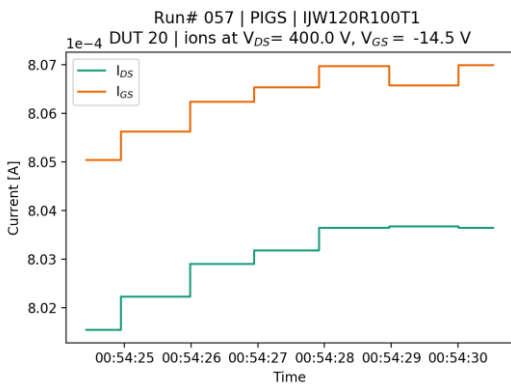
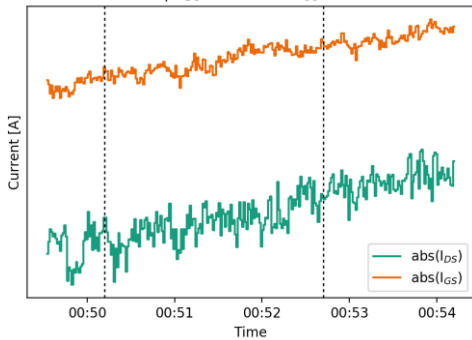
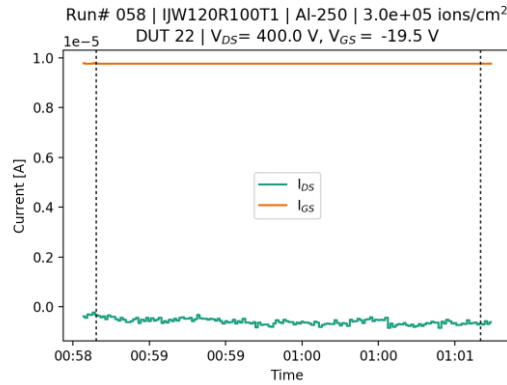


Figure 48: Run# 058, IJW120R100T1, Al-250, 3.0e+05 ions/cm², DUT 22, V_{DS}= 400.0 V, V_{GS}= -19.5 V



Run# 058 | IJW120R100T1 | Al-250 | 3.0e+05 ions/cm²
DUT 22 | V_{DS}= 400.0 V, V_{GS}= -19.5 V

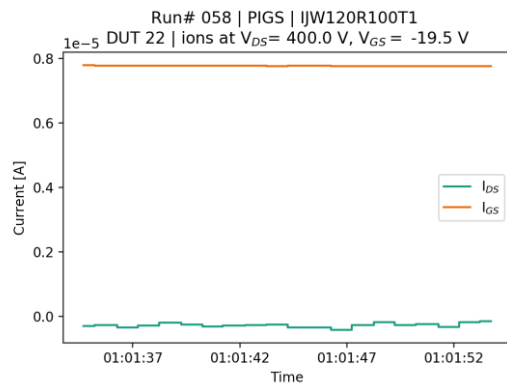
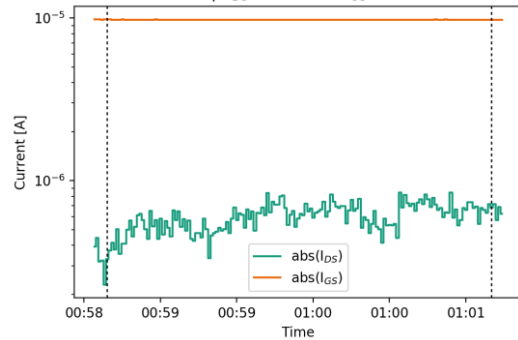


Figure 49: Run# 059, IJW120R100T1, Al-250, $3.0e+05$ ions/cm², DUT 22, V_{DS}= 450.0 V, V_{GS}= -14.5 V

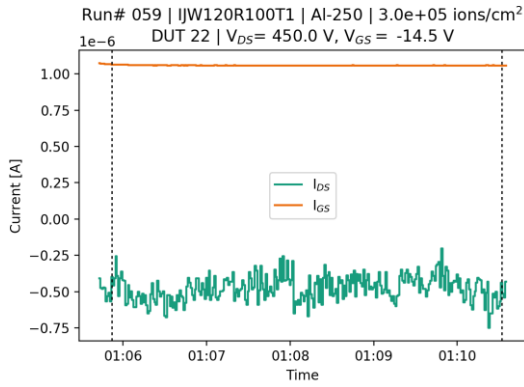
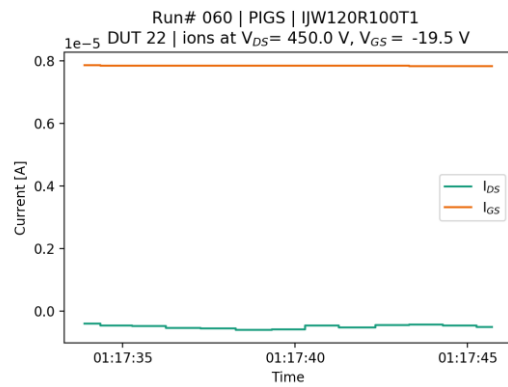
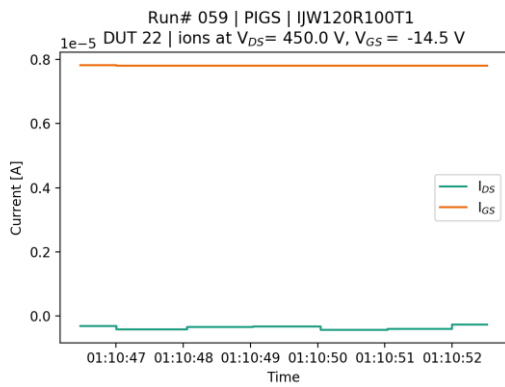
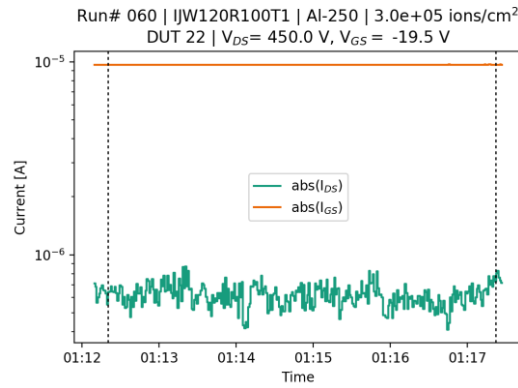
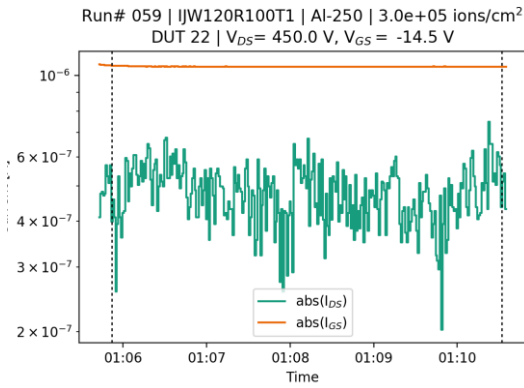
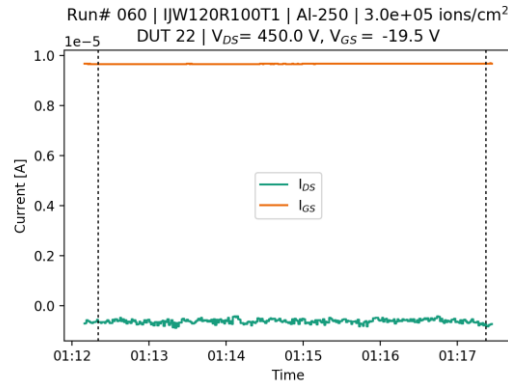


Figure 50: Run# 060, IJW120R100T1, Al-250, $3.0e+05$ ions/cm², DUT 22, V_{DS}= 450.0 V, V_{GS}= -19.5 V



C Appendix: Tests at JULIC

C.1. LET estimation

To receive the impact in terms of proton energy and LET on the Silicon Carbide die with packaged DUTs, radiation transport simulations have to be made:

- 1) The setup (beam exit window, air gap, package, die) were simulated with GRAS in standalone version 3.03 for $1E7$ protons. The average LET at the layer boundary from the package to the silicon carbide was evaluated by GRAS. This gives the average LET in MeV/cm. Rare events e.g. maximum recoil energy transfer, are few in these simulations. For the results in Table 14, this was then divided by the density $\rho = 3210 \text{ mg/cm}^3$ to give the LET in units of MeV cm^2/mg .
- 2) The setup (beam exit window, air gap, package, die) were simulated with MULASSIS in standalone version 1.26 for $1E7$ protons. The proton energy at the layer boundary from the package to the silicon carbide was evaluated by MULASSIS. With this proton energy, the maximum recoil energy to Silicon and Carbon atoms in SiC were calculated with $E_{ion}(E_p) = \frac{4 m_p m_{ion}}{(m_p + m_{ion})^2} \cdot E_p$. SRIM 2013 [10] simulations were then performed with the respective particles and maximum kinetic energy in Silicon Carbide. From the SRIM ionization curve the LET can then be calculated. This LET gives information on the recoils happening inside the SiC layer and is not restricted to the layer "surface" (although only extreme values were considered).

For these simulations, the 1 mm Aluminum exit window and 1.8 m of air were taken into account, such that the spread of the proton energy on the DUT package and the transport simulations through the package in the LET calculations is included. Package thickness for all materials was taken as 0.5, 1, 2 and 3 mm. The 3 mm was not simulated for Aluminum package (which was on the scale of 0.5 mm).

Alternatively the above geometry could be simulated only with SRIM. This has however some major drawbacks, when looking at a $100 \mu\text{m}$ layer at the end of the target of length $>1.8 \text{ m}$ as then only particles incident on $\pm 50 \mu\text{m}$ around the center are evaluated.

Information on the plastic package of the materials was not readily available for the use in SRIM or GRAS, as both require the atomic stoichiometry of the materials. For the sake of the Monte Carlo simulations this does not have to be chemically exact, but has to reflect the likelihood of interacting e.g. with a Silicon, if an interaction with a random nucleus takes place.

For some devices in this project, information was given in the Material Content Data Sheet. A value of 2.37 g/cm^3 was assumed for the density of the plastic mold and the stoichiometry for the example of SiC MOSFET C2M0080120D was estimated to be around Si:O:C:H = 1.6 : 3.6 : 1.2 : 1, thus the estimate for the chemical sum formula to be used in the simulations to be $\text{Si}_3\text{-O}_7\text{-C}_2\text{-H}_2$.

Table 22: Mold material of example C2M0080120D. Values indicated with * are estimates.

Name	CAS	Stoichiometry	Density [g/cm ³]	Molar mass [u]	Mass in Mold [mg]
Silicon Dioxide	7631-86-9	SiO ₂	2.6	60.0843	1640.71
Epoxy Resin	29690-82-2	C ₃₃ H ₄₂ O ₉ X ₂	1.12 *	582.68 *	189.62
Anhydride	2421-28-5	C ₁₇ H ₆ O ₇	1.57 *	322.23 *	159.68
Carbon Black	1333-86-4	C	1.7	12.01	5.99

Table 23: Results of GRAS simulations of the LET with package thickness. The GRAS results are the average "surface" LETs on the layer boundary from the package to SiC and would include error information. Error estimates are not given but are < 0.001 MeV cm²/mg in any case).

Name	LET _{GRAS} [MeV cm ² /mg]			
	0.5 mm	1 mm	2 mm	3 mm
Al	0.012	0.008	0.004	--
Si1-O2-C1-H1	0.012	0.008	0.005	0.003
Si3-O7-C2-H2	0.012	0.008	0.005	0.003
Si545-O1220-C512-H597-P3-B1	0.013	0.009	0.005	0.004

Table 24: Intermediate results of MULASSIS simulations of the proton energy with package thickness. Little variation is seen based on the package material.

Name	E(p) [MeV] at boundary Package → SiC			
	0.5 mm	1 mm	2 mm	3 mm
Al	37.72	36.08	32.64	---
Si1-O2-C1-H1	37.77	36.18	32.85	29.17
Si3-O7-C2-H2	37.80	36.24	32.97	29.38
Si545-O1220-C512-H597-P3-B1	37.77	35.75	32.83	29.15
Average	37.76	36.06	32.82	29.23
LETSRIM [MeV cm ² /mg]	0.013	--	--	0.016

Table 25: Results of SRIM simulations of the LET with package thickness. The SRIM results are the maximum LETs of the Silicon or Carbon recoil nuclei. The values given are the peak values, i.e. not necessarily at the beginning of the track, in the material. The average energies from Table 24 were taken for the recoil energies.

	Silicon				Oxygen			
	0.5 mm	1 mm	2 mm	3 mm	0.5 mm	1 mm	2 mm	3 mm
Max. Energy of Recoil Atom (180°) [MeV]	5.05	4.82	4.39	3.91	10.79	10.30	9.38	8.35
Peak LET _{SRIM} [MeV cm ² /mg] at max. recoil	12.30	12.16	11.86	11.31	5.81	5.81	5.80	5.80
Peak at track length [μm]	0	0	0	0	4.5	4.1	3.3	2.8
Range [μm]	2.01	1.96	1.84	1.72	6.6	6.3	5.7	5.1

C.2. Logfile / Test steps

In case of device failure the fluences in this table indicate the fluence provided by the facility not the fluence until failure which may differ by some additional seconds of beam.

#	Date	Time	Ion	Device Type	Device	DUT #	V_DS, V	V_GS	beam time [s]	fluence [cm ⁻²]
18	19.09.	16:50	p	JFET	IJW120RT100T1	#1	600	-14.5	152	2.0e10
19	19.09.	16:54	p	JFET	IJW120RT100T1	#1	750	-14.5	147	2.0e10
20	19.09.	16:58	p	JFET	IJW120RT100T1	#1	900	-14.5	148	2.0e10
21	19.09.	17:01	p	JFET	IJW120RT100T1	#1	1050	-14.5	150	2.0e10
22	19.09.	17:05	p	JFET	IJW120RT100T1	#1	1200	-14.5	149	2.0e10
23	19.09.	17:10	p	JFET	IJW120RT100T1	#1	600	-17	146	2.0e10
24	19.09.	17:13	p	JFET	IJW120RT100T1	#1	900	-17	149	2.0e10
25	19.09.	17:16	p	JFET	IJW120RT100T1	#1	1200	-17	148	2.0e10
26	19.09.	17:21	p	JFET	IJW120RT100T1	#1	600	-19.5	150	2.0e10
27	19.09.	17:24	p	JFET	IJW120RT100T1	#1	900	-19.5	151	2.0e10
28	19.09.	17:27	p	JFET	IJW120RT100T1	#2	1200	-19.5	151	2.0e10
29	19.09.	17:39	p	JFET	IJW120RT100T1	#2	1200	-14.5	152	2.0e10
30	19.09.	17:42	p	JFET	IJW120RT100T1	#2	1200	-17	142	1.9e10
31	19.09.	17:45	p	JFET	IJW120RT100T1	#2	1200	-19.5	473	6.3e10
32	19.09.	17:58	p	JFET	IJW120RT100T1	#3	1200	-14.5	152	2.0e10

C.3. Measurements

Figure 51: Run# 018, IJW120R100T1, p, 2.0e+10 ions/cm², DUT 1, V_{DS}= 600.0 V, V_{GS}= -14.5 V

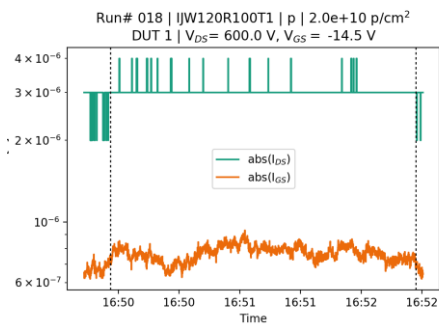
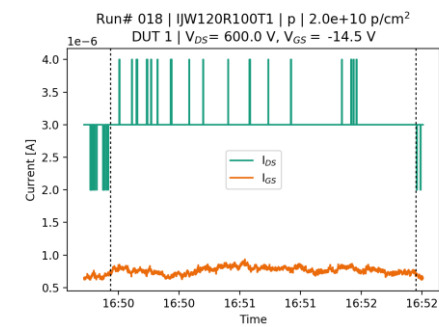
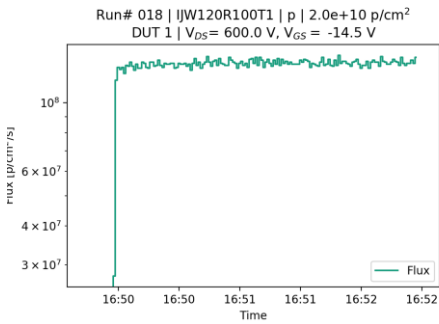


Figure 52: Run# 019, IJW120R100T1, p, 2.0e+10 ions/cm², DUT 1, V_{DS}= 750.0 V, V_{GS}= -14.5 V

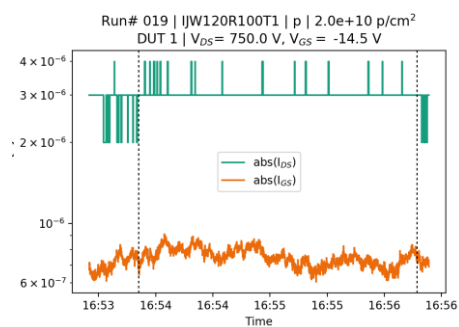
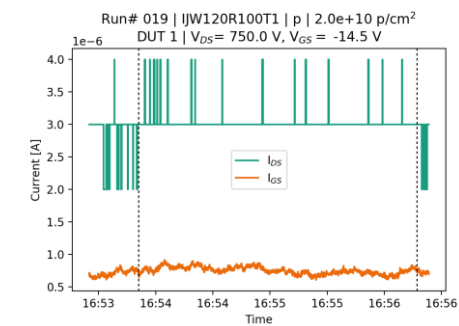
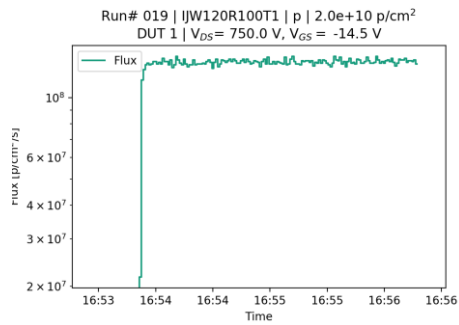


Figure 53: Run# 020, IJW120R100T1, p, 2.0e+10 ions/cm², DUT 1, V_{DS}= 900.0 V, V_{GS}= -14.5 V

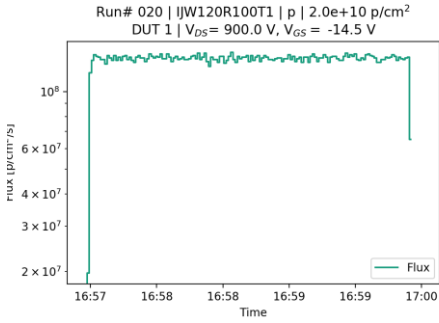


Figure 54: Run# 021, IJW120R100T1, p, 2.0e+10 ions/cm², DUT 1, V_{DS}= 1050.0 V, V_{GS}= -14.5 V

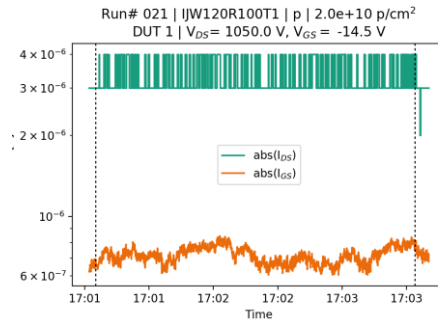
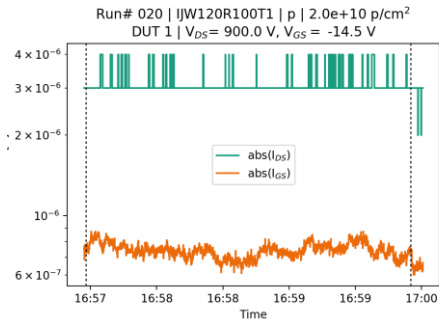
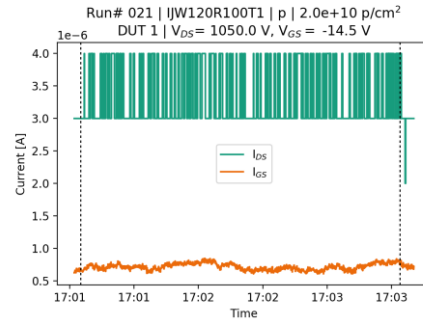
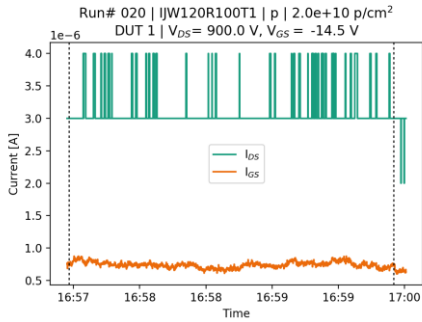
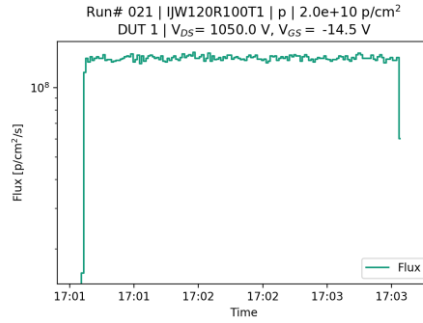


Figure 55: Run# 022, IJW120R100T1, p, 2.0e+10 ions/cm², DUT 1, V_{DS}= 1200.0 V, V_{GS}= -14.5 V

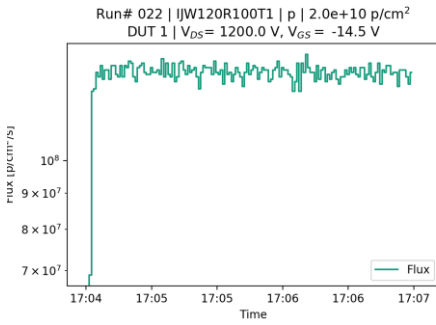


Figure 56: Run# 023, IJW120R100T1, p, 2.0e+10 ions/cm², DUT 1, V_{DS}= 600.0 V, V_{GS}= -17.0 V

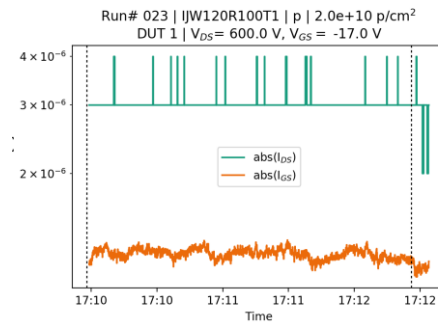
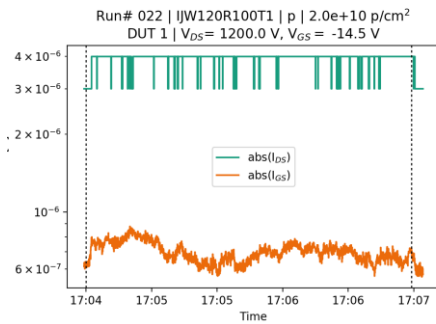
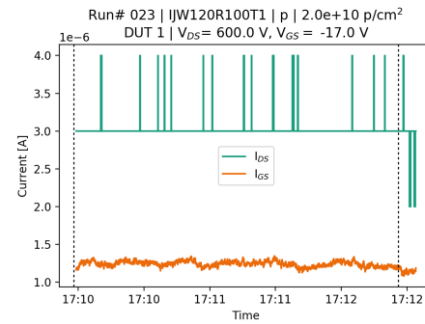
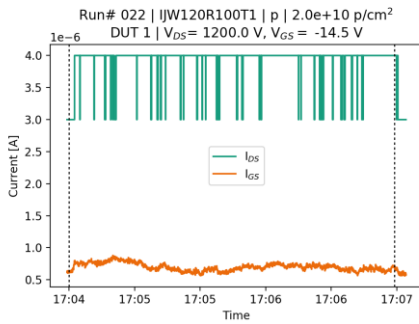
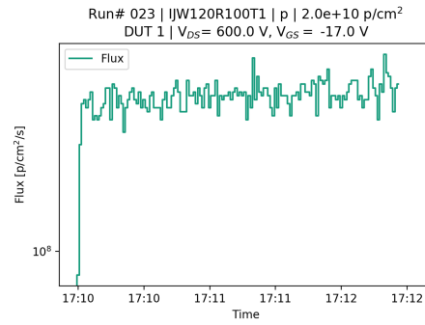


Figure 57: Run# 024, IJW120R100T1, p, 2.0e+10 ions/cm², DUT 1, V_{DS}= 900.0 V, V_{GS}= -17.0 V

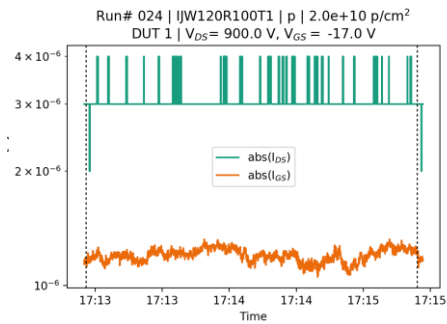
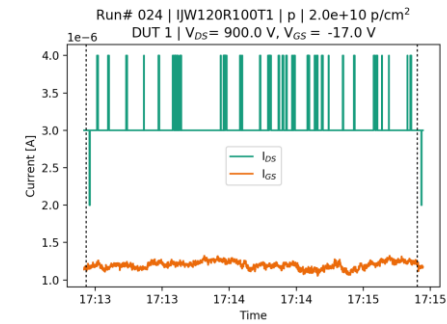
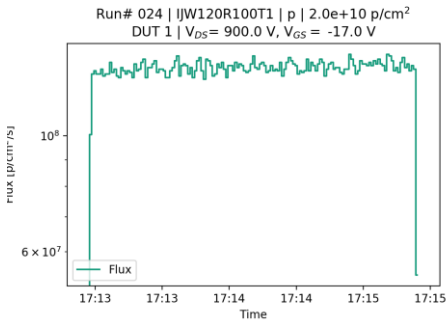


Figure 58: Run# 025, IJW120R100T1, p, 2.0e+10 ions/cm², DUT 1, V_{DS}= 1200.0 V, V_{GS}= -17.0 V

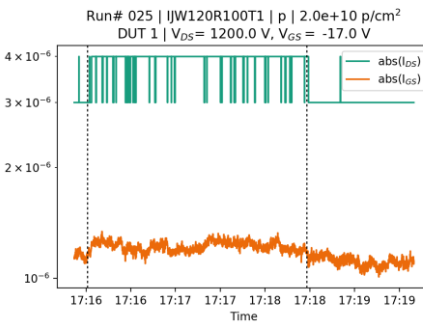
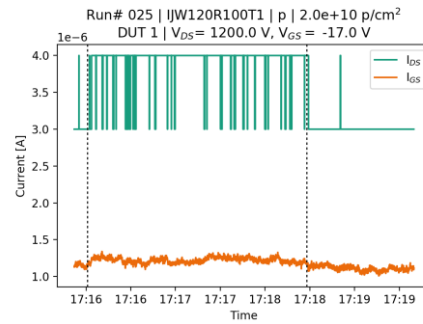
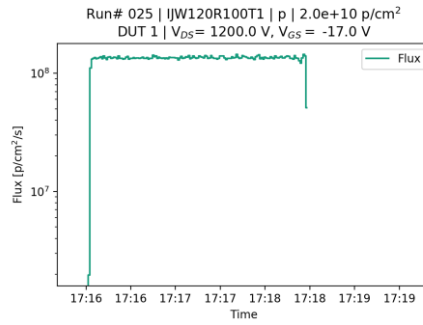


Figure 59: Run# 026, IJW120R100T1, p, 2.0e+10 ions/cm², DUT 1, V_{DS}= 600.0 V, V_{GS}= -19.5 V

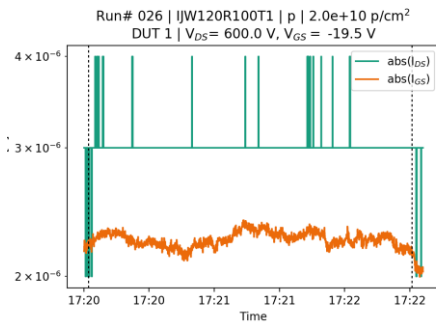
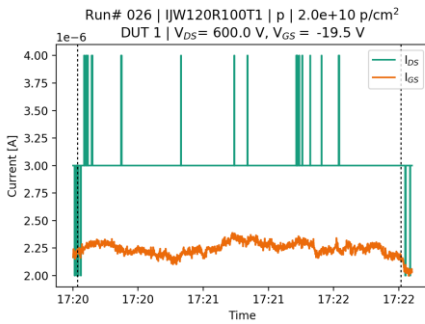
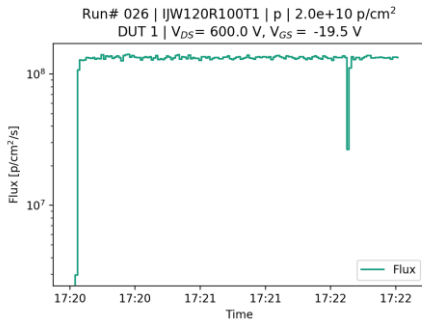


Figure 60: Run# 027, IJW120R100T1, p, 2.0e+10 ions/cm², DUT 1, V_{DS}= 900.0 V, V_{GS}= -19.5 V

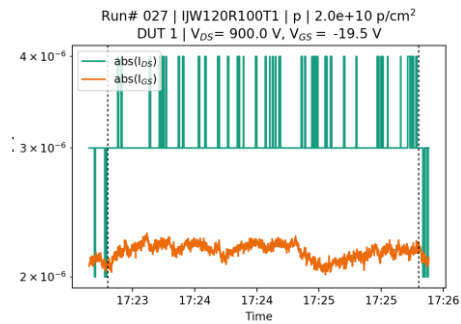
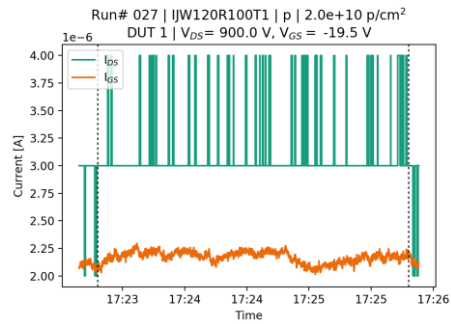
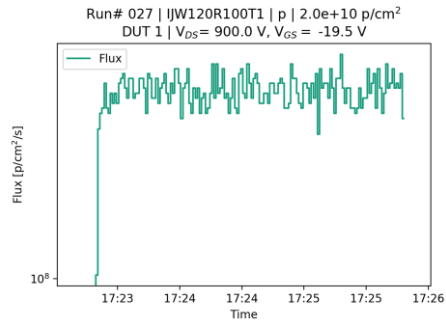


Figure 61: Run# 028, IJW120R100T1, p, 2.0e+10 ions/cm², DUT 2, VDS= 1200.0 V, VGS= -19.5 V

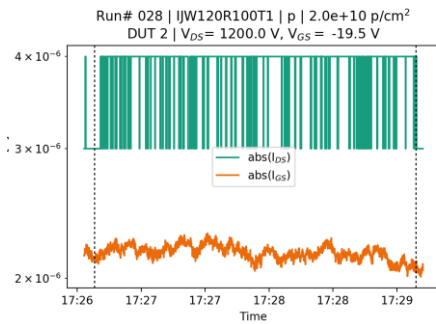
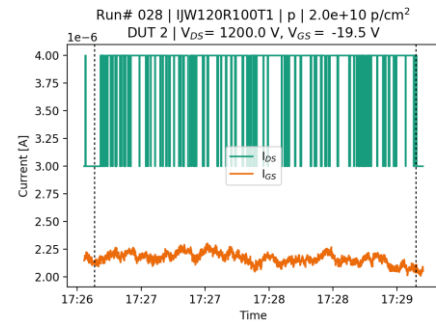
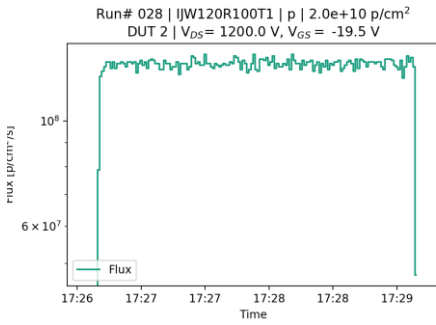


Figure 62: Run# 029, IJW120R100T1, p, 2.0e+10 ions/cm², DUT 2, VDS= 1200.0 V, VGS= -14.5 V

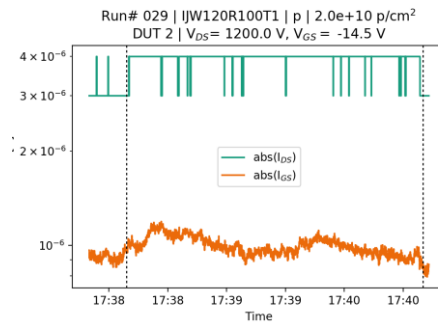
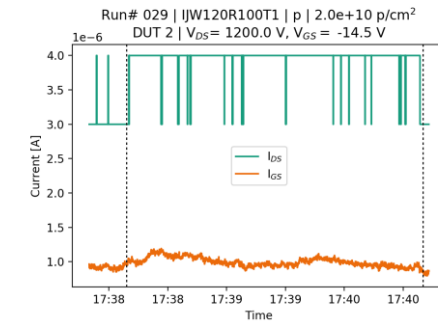
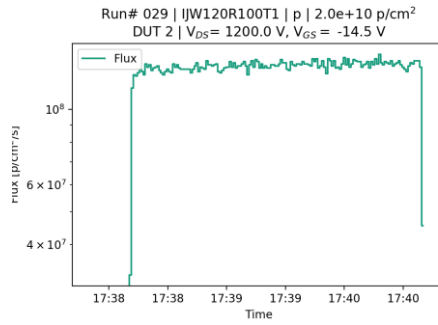


Figure 63: Run# 030, IJW120R100T1, p, $1.9e+10$ ions/cm², DUT 2, VDS= 1200.0 V, VGS= -17.0 V

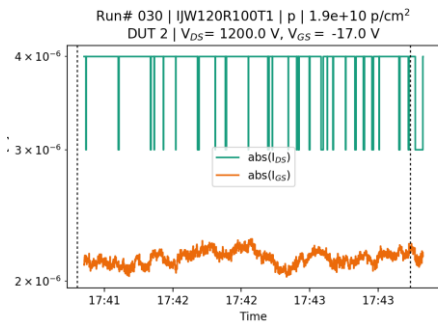
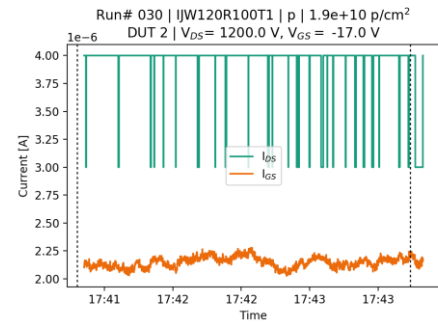
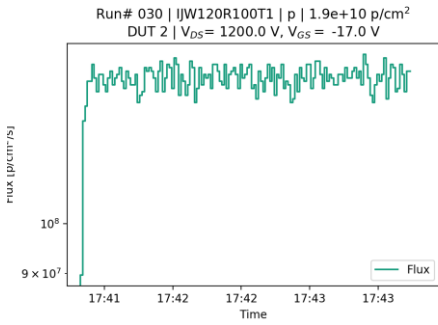


Figure 64: Run# 031, IJW120R100T1, p, $6.3e+10$ ions/cm², DUT 2, VDS= 1200.0 V, VGS= -19.5 V

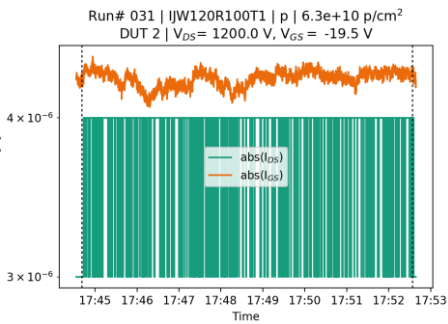
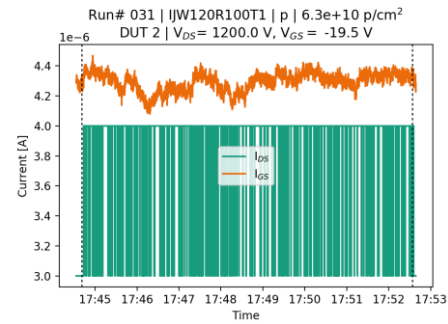
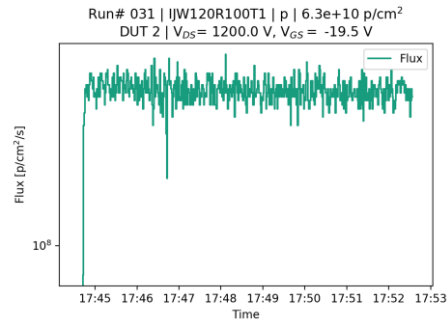
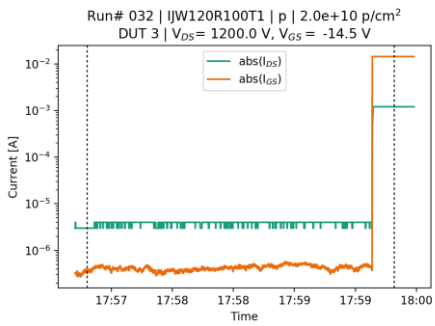
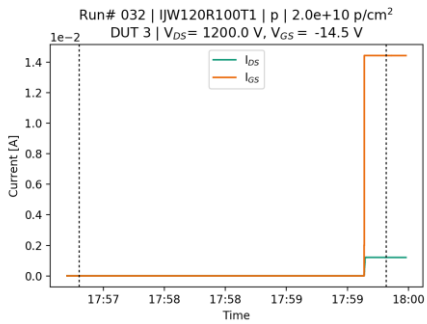
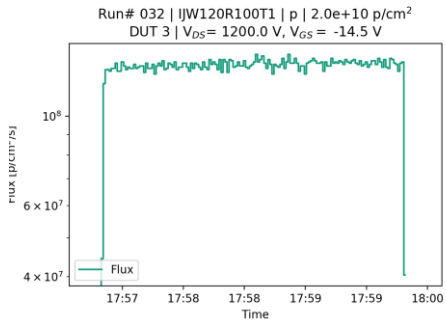


Figure 65: Run# 032, IJW120R100T1, p, 2.0e+10 ions/cm², DUT 3, VDS= 1200.0 V, VGS= -14.5 V



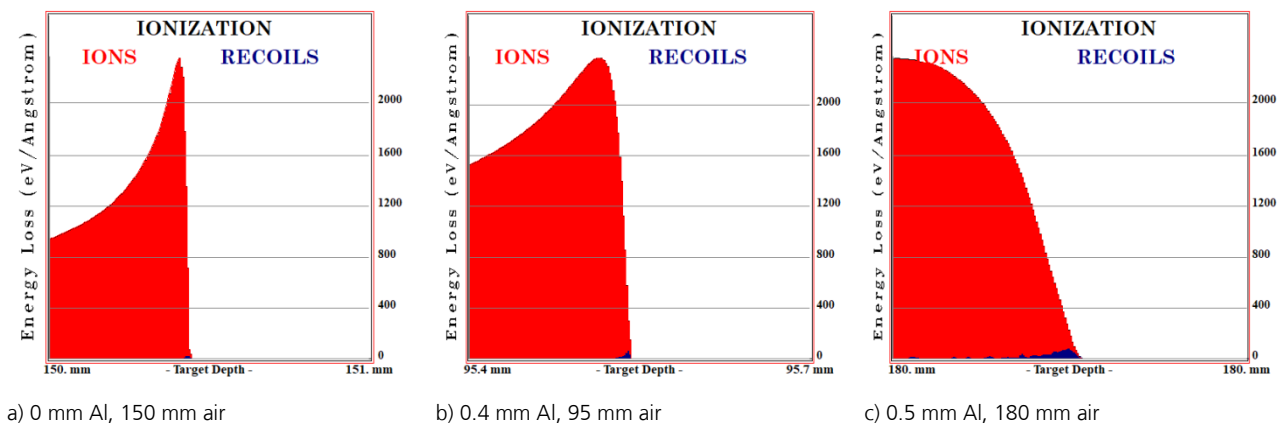
D Appendix: Tests at GANIL

D.1. LET estimation

To receive the impact in terms of LET on the Silicon Carbide die, radiation transport simulations have to be made. A major difference to the proton LET estimations, is that the tests were performed on decapsulated devices, so the package is not taken into account.

For these simulations, the 10 μm stainless steel exit window, a variable amount of air gap, and if applicable an Aluminium degrader were included in simulations with SRIM2013. The incident particles were 49.1 MeV/n Xenon ions (isotope mass = 136 u).

Figure 66: SRIM2013 simulations of the Ganil Xenon tests on SiC



The views of the ionization curves in Figure 66 start at the surface of the silicon carbide layer, so e.g. at 95.410 mm in Figure 66 b), although only one digit is displayed.

The LET in $\text{MeV cm}^2/\text{mg}$ can be directly calculated from the Energy loss in $\text{eV}/\text{\AA}$ by unit conversion ($1 \text{ eV}/\text{\AA} = 100 \text{ MeV}/\text{cm}$) and division by the SiC density of $3.21 \text{ g}/\text{cm}^3 = 3210 \text{ mg}/\text{cm}^3$.

Table 26: GANIL: Beam characteristics. Values in Silicon are provided by GANIL [13], Values in SiC are calculated by INT and given with one digit

Degrader [mm Al]	Air gap [mm]	LET (Si) ($\text{MeV}\cdot\text{cm}^2/\text{mg}$)	Range (Si) [μm]	LET _{SURF} (SiC) [$\text{MeV}\cdot\text{cm}^2/\text{mg}$]	Range (SiC) [μm]
0	150	27.76	640.33	29.2	430
0.4	95	42.03	226.23	47.2	141
0.5	180	60.12	65.68	72.9	30

D.2. Logfile / Test steps

#	Date	Time	Ion	Al [μm]	Air [mm]	Device Type	Device	Position on board	DUT #	V_DS, V	V_GS	beam time [s]	fluence [cm-2]
147	06.06.	13:45	Xe	0	150	JFET	IJW120R100T1	#2	25	300	-14.5	139	6.00E+05
148	06.06.	13:48	Xe	0	150	JFET	IJW120R100T1	#2	25	400	-14.5	145	6.00E+05

D.3. Measurements

Figure 67: Run# 147, IJW120R100T1, Xe 0 mmAl, 150 mm Air, 6.0e+05 ions/cm², DUT 25, V_{DS}= 300.0 V, V_{GS}= -14.5 V

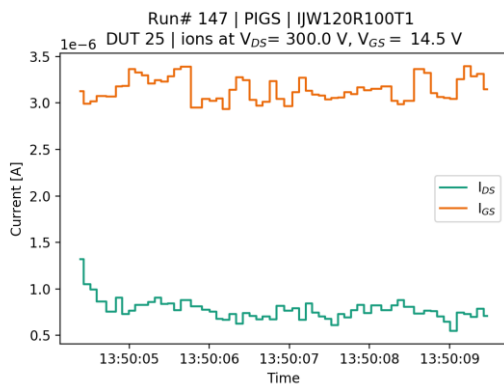
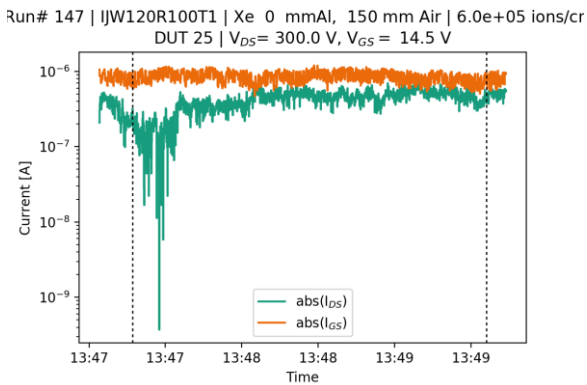
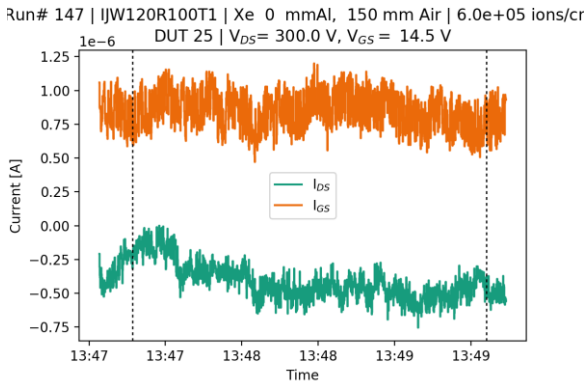
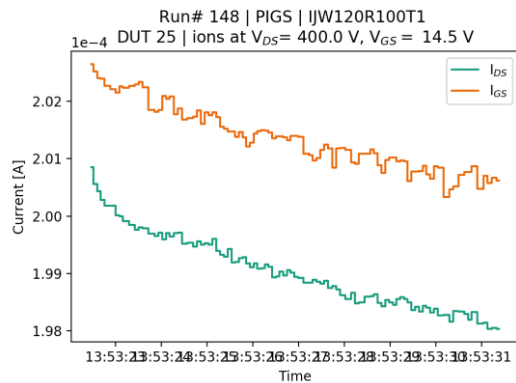
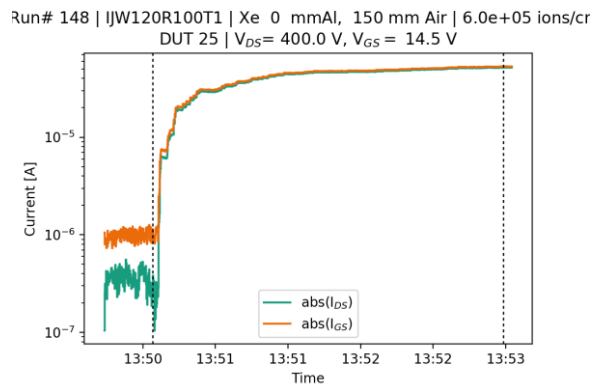
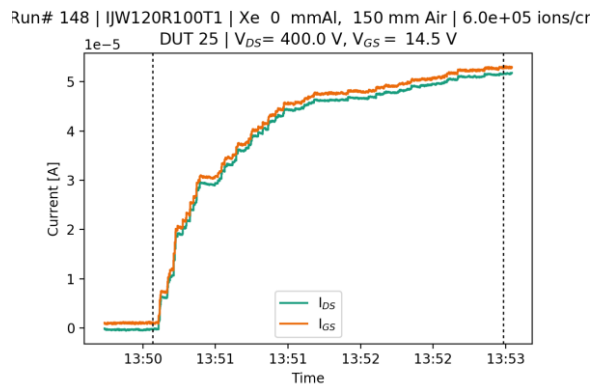


Figure 68: Run# 148, IJW120R100T1, Xe 0 mmAl, 150 mm Air, 6.0e+05 ions/cm², DUT 25, V_{DS}= 400.0 V, V_{GS}= -14.5 V



E Appendix: Tests at CERN

E.1. LET estimation

During the experiments (2017-11-30 – 2017-12-01) at the H8 beam line at CERN, the beam energy was set to 40 GeV/n. The calculation of the LET for particles of the energies cannot be done easily e.g. with SRIM. SRIM does not cover all interactions with matter at these energies and has a built-in limitation to ion energies of 10 GeV/n. Thus a realistic LET cannot be determined using SRIM.

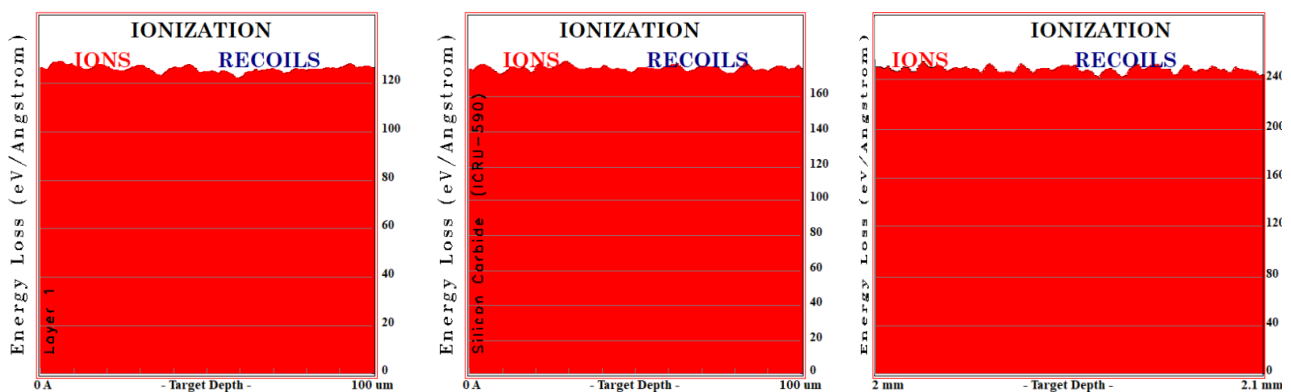
The LET values for silicon were simulated with FLUKA up to energies > 100 GeV/n and with SRIM up to 10 GeV/n by Rubén García Alía et al. and reported in [15]. There different LET values were considered, one unrestricted value taking into account all ionization caused by the beam (approx. 6.3 MeV cm²/mg) and a volume-restricted value covering the area of a 9.3 MeV/n Silicon particle track (approx. 3.7 MeV cm²/mg).

Up to energies of 10 GeV/n, the SRIM results closely follow the volume-unrestricted simulations in FLUKA. However, comparisons with the ESA SEU monitor in [15] indicate that the volume-restricted LET is a more proper expression for the particle LET in Silicon.

We will give only an approximation of the LET in SiC by looking at the similarity of results in Si and SiC with SRIM at 10 GeV/n energy. After that we compare simulations with and without a plastic package at that energy. Any air gap or beam exit window is ignored in these simulations, so the particles enter either the target material or a package immediately.

Figure 69 shows a constant ionization profile in a 100 μm layer of Si (left side) and SiC (right side). Taking the target density and the statistical fluctuations into account, the LETs amount to (5.43 ± 0.06) MeV cm²/mg for Si and (5.47 ± 0.05) MeV cm²/mg for SiC. Introducing a 2 mm plastic package (Si1-O2-C1-H1 as defined in Appendix C.1) in front of the SiC does not alter the LET at all and again gives (5.47 ± 0.05) MeV cm²/mg (image not shown).

Figure 69: SRIM2013 simulations of Xenon ions of 10 GeV/n energy on Si and SiC



a) 10 GeV/n energy Xenon on Si

b) 10 GeV/n energy Xenon on SiC

c) 10 GeV/n energy Xenon on SiC at 45° angle

The Silicon LETs are in the same range as the SRIM-simulated ones from [15] and the unrestricted LETs simulated with FLUKA.

Finally we make two assumptions, both of which cannot be validated here:

1. If Si and SiC still yield the same results at 40 GeV/n, the LET would then be approx. 6.3 MeV cm²/mg.
2. As mentioned above, measurements in Silicon showed that the volume-restricted LET is more representative for the particle LET in Silicon, however we have no indication about that in SiC. Assuming similar behaviour, then the more proper LET of the 40 GeV/n in SiC would still be identical to the value of approx. 3.7 MeV cm²/mg in Silicon.

Thus in the end we assume the 40 GeV/m Xenon LET in SiC to be identical with the LET in Si based on the SRIM simulation results with Si and SiC at 10 GeV/n energy and assuming similarity at higher energies.

Additional simulations were performed with the ion beam directed under 45° angle to the SiC (tests were done at 42°). The SRIM results give an LET of (7.72 ± 0.07) MeV cm²/mg, which follows the rule of effective LET proportional to 1/cos(Θ). However in general the concept of effective LET is not valid for power devices [3] and all data collected at these settings further implicate that assuming a larger LET is invalid.

E.2. Logfile / Test steps

#	Date	Time	Ion	Tilt [°]	Device Type	Device	DUT #	V_DS, V	V_GS	beam time [s]	fluence [cm-2]
012	01.12.	10:29	Xe	0	JFET	IJW120R100T1	1	1200	-14.5	2.77E+02	1.85E+03
013	01.12.	10:34	Xe	0	JFET	IJW120R100T1	1	1200	-19.5	8.46E+02	5.64E+03
014	01.12.	10:55	Xe	0	JFET	IJW120R100T1	1	1200	-19.5	1.80E+03	1.20E+05
015	01.12.	11:26	Xe	0	JFET	IJW120R100T1	1	1250	-19.5	3.00E+02	2.00E+04
016	01.12.	11:33	Xe	0	JFET	IJW120R100T1	1	1300	-19.5	2.10E+01	1.40E+03

E.3. Measurement

Figure 70: Run# 012, IJW120R100T1, Xe 0°, 1.8e+03 ions/cm², DUT 1, V_{DS}= 1200.0 V, V_{GS}= -14.5 V

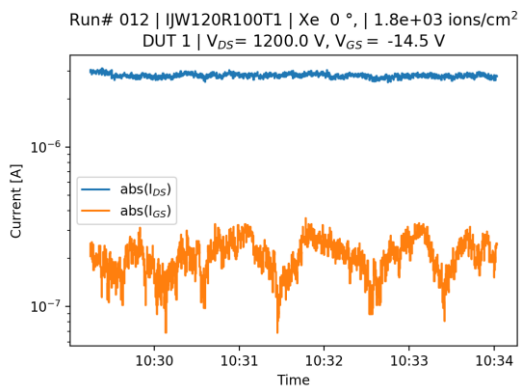
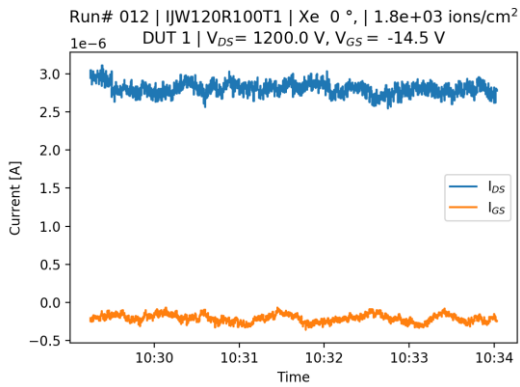


Figure 71: Run# 013, IJW120R100T1, Xe 0°, 5.6e+03 ions/cm², DUT 1, V_{DS}= 1200.0 V, V_{GS}= -19.5 V

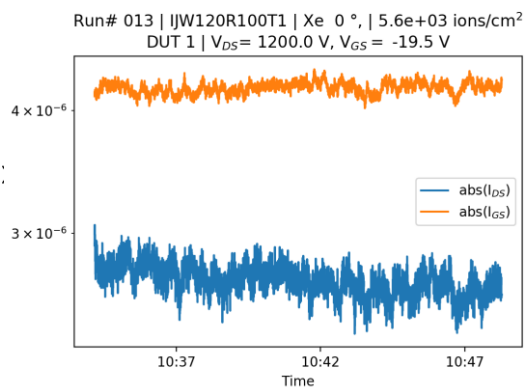
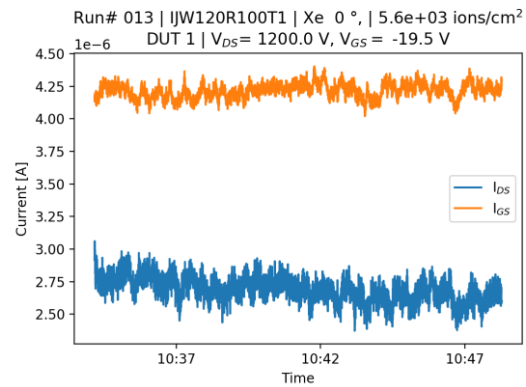


Figure 72: Run# 014, IJW120R100T1, Xe 0°, 1.2e+05 ions/cm², DUT 1, V_{DS}= 1200.0 V, V_{GS}= -19.5 V

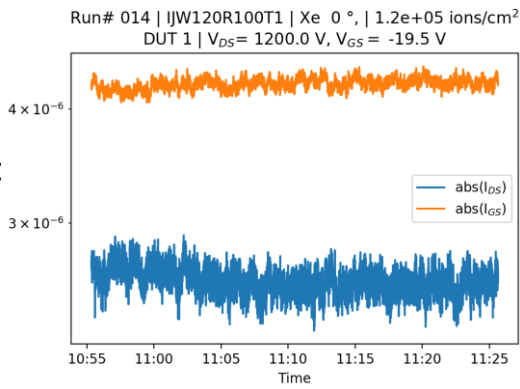
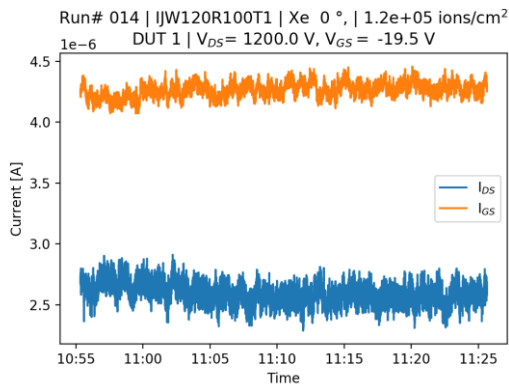


Figure 73: Run# 015, IJW120R100T1, Xe 0°, 2.0e+04 ions/cm², DUT 1, V_{DS}= 1250.0 V, V_{GS}= -19.5 V

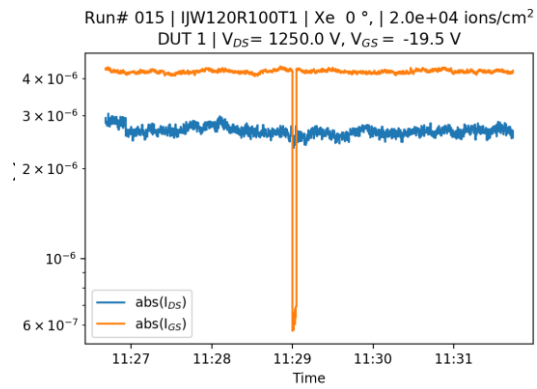
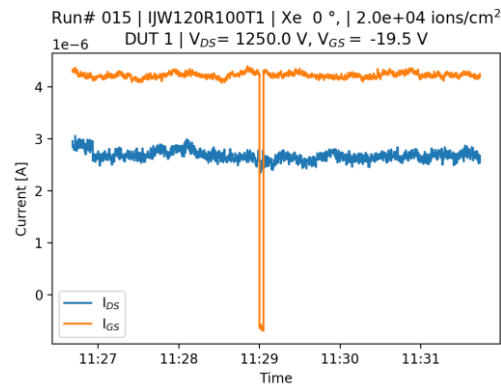


Figure 74: Run# 016, IJW120R100T1, Xe 0°, 1.4e+03 ions/cm², DUT 1, V_{DS}= 1300.0 V, V_{GS}= -19.5 V

